Department of Forest Products Technology

Adsorption studies on cellulose surfaces by combinations of interfacial techniques

Paula Eronen

Aalto University

DOCTORAL DISSERTATIONS

Aalto University publication series
DOCTORAL DISSERTATIONS 108/2011

Adsorption studies on cellulose surfaces by combinations of interfacial techniques

Paula Eronen

Doctoral dissertation for the degree of Doctor of Science in Technology to be presented with due permission of the School of Chemical Technology for public examination and debate in Auditorium Puu2 at the Aalto University School of Chemical Technology (Espoo, Finland) on the 4th of November 2011 at 12 noon.

Aalto University
School of Chemical Technology
Department of Forest Products Technology

Supervisor
Professor Janne Laine

Instructor
Docent Monika Österberg

Preliminary examiners
Professor Sirkka-Liisa Maunu, Helsinki University, Finland
Docent Eva Blomberg, KTH, Sweden

Opponent
Professor Lars Wågberg, KTH, Sweden

Aalto University publication series
DOCTORAL DISSERTATIONS 108/2011

© Paula Eronen

ISBN 978-952-60-4341-8 (pdf)
ISBN 978-952-60-4340-1 (printed)
ISSN-L 1799-4934
ISSN 1799-4942 (pdf)
ISSN 1799-4934 (printed)

Unigrafia Oy
Helsinki 2011

Finland

The dissertation can be read at http://lib.tkk.fi/Diss/

Author
Paula Eronen

Name of the doctoral dissertation
Adsorption studies on cellulose surfaces by combinations of interfacial techniques

Publisher School of Chemical Technology

Unit Department of Forest Products Technology

Series Aalto University publication series DOCTORAL DISSERTATIONS 108/2011

Field of research Forest Products Chemistry

Manuscript submitted 15 June 2011 **Manuscript revised** 7 September 2011

Date of the defence 4 November 2011 **Language** English

☐ **Monograph** ☒ **Article dissertation (summary + original articles)**

Abstract

In this work, the adsorption of various polymers on cellulose surfaces was studied in detail at molecular level. Special attention was paid on the interactions between renewable polysaccharides and different nanofibrillated cellulose (NFC) grades. Polymer or nanoparticle adsorption in aqueous medium was explored as a strategy to functionalize NFC. The role of pulp raw material and chemical pre-treatment on the NFC properties was clarified via indirect adsorption studies with ultrathin NFC films. Atomic force microscopy (AFM) -in different imaging and force detection modes-, quartz crystal microbalance with dissipation (QCM-D), Raman spectroscopy and surface plasmon resonance (SPR) were combined to carry out this research.

The similar backbone having polysaccharides had natural affinity on NFC substrates. Comparison between NFC from different origin (hardwood vs. softwood), although of similar morphology, revealed differences in the conformation of adsorbed polysaccharide layer. The polysaccharide structure rather than NFC origin had more notable effect on adsorbed polysaccharide amount and layer properties. The attachment of the very thin (only few nm thick) polysaccharide layer was uniform without aggregates. They nevertheless were able to change the surface properties of cellulosic materials. One example was the lowered friction co-efficient with one polysaccharide (chitosan) determined for regenerated cellulose spheres in low pH aqueous solution.

In addition, NFCs prepared after chemical pre-treatments were compared to unmodified NFC. Increasing the anionicity prevented the interfibril association by electrostatic repulsion. As a consequence the fibrillation efficiency was enhanced and very thin nanofibrils were achieved. The surface interactions were systematically probed and compared with different cationic counterparts using layer-by-layer (LbL)-technique. The high charged, chemically modified NFC behaved differently compared to low charged, unmodified NFC: they bound more water and the layer formation and stabilization was faster; and the adsorbed amount increased as the function of layer number. Nevertheless, multilayers could also be formed with the lower charged NFCs to some extent. Non-electrostatic interactions were significant between oppositely charged all-cellulosic materials. A considerable increase in adhesive forces during multilayer build-up due to high compressibility of the high charged NFC was also detected. The information obtained in this study for the interactions of emerging, renewable, bio-based materials can be used to create more sustainable material applications in the future.

Keywords nanocellulose, surface forces, polymer adsorption, polysaccharides, AFM

ISBN (printed) 978-952-60-4340-1 **ISBN (pdf)** 978-952-60-4341-8

ISSN-L 1799-4934 **ISSN (printed)** 1799-4934 **ISSN (pdf)** 1799-4942

Location of publisher Espoo **Location of printing** Helsinki **Year** 2011

Pages 175 **The dissertation can be read at** http://lib.tkk.fi/Diss/

Aalto-yliopisto

Tiivistelmä

Aalto-yliopisto, PL 11000, 00076 Aalto www.aalto.fi

Tekijä
Paula Eronen

Väitöskirjan nimi
Adsorption tutkiminen selluloosapinnoilla pintavuorovaikutustekniikoiden yhdistelmillä

Julkaisija Kemian tekniikan korkeakoulu

Yksikkö Puunjalostustekniikan laitos

Sarja Aalto University publication series DOCTORAL DISSERTATIONS 108/2011

Tutkimusala Puunjalostuksen kemia

Käsikirjoituksen pvm 15.06.2011 **Korjatun käsikirjoituksen pvm** 07.09.2011

Väitöspäivä 04.11.2011 **Kieli** Englanti

☐ **Monografia** ☒ **Yhdistelmäväitöskirja (yhteenveto-osa + erillisartikkelit)**

Tiivistelmä

Erilaisten polymeerien adsorptiota selluloosapinnoille tutkittiin molekyylitasolla. Erityisesti työssä keskityttiin tutkimaan uusiutuvien luonnonpolymeerien (polysakkaridien) ja nanoselluloosafibrillien vuorovaikutuksia. Polymeerien tai nanopartikkeleiden adsorptiota nanoselluloosan funktionalisointimenetelmänä tutkittiin vesiympäristössä. Nanoselluloosan valmistukseen käytetyn raaka-aineen alkuperän ja kemiallisten esikäsittelyjen vaikutusta fibrillien ominaisuuksiin tutkittiin epäsuorasti adsorptiokokeilla ultraohuille fibrillipinnoille. Tutkimusmenetelminä olivat kvartsikidemikrovaaka dissipaatiolla (QCM-D), atomivoimamikroskopia (AFM) kuvantamis- ja voimamittaussovellutuksissa, Raman -spektroskopia sekä pintaplasmaresonassi-mittaukset eri yhdistelminä.

Selluloosan kanssa samantapaisesti sitoutuneen pääketjun omaavat polysakkaridit adsorboituivat luontaisesti nanofibrillipinnoille. Havu- ja lehtipuuselluloosasta valmistettujen, mutta morfologialtaan hyvin samanlaisten, nanofibrillipintojen vertailu paljasti eroja polysakkaridikerroksen kiinnittymistavassa. Polysakkaridin rakenteella havaittiin olevan suurempi vaikutus adsorboituneeseen määrään ja kerrosominaisuuksiin. Adsorboitunut polysakkaridikerros oli hyvin ohut eikä aggregoituneita rakenteita havaittu. Kuitenkin ohuellakin polysakkaridikerroksella selluloosan pintaominaisuudet muuttuivat, esimerkiksi kitosanin adsorptio regeneroitujen selluloosapallojen pinnalle pienensi huomattavasti kitkakerrointa alhaisessa pH:ssa. Esikäsitellyistä ja muokkaamattomista massoista valmistettuja nanofibrillejä vertailtiin pintavoimamittauksilla. Anionisen varauksen kasvu esti fibrillien yhteenliittymistä elektrostaattisen repulsion johdosta. Näin ollen hyvin ohuiden fibrillien erottumistehokkuus parani.

Pintavuorovaikutuksia tutkittiin systemaattisesti, ja kerroksittaisia rakenteita muodostettiin eri nanofibrillien ja vastakkaisesti varautuneiden polymeeristen materiaalien välille. Fibrillit, joilla oli korkea negatiivinen varaus sitoivat enemmän vettä rakenteeseensa muokkaamattomiin verrattuna. Niillä myös muodostuneen kerroksen stabilisointi oli nopeampaa ja adsorboitunut määrä kasvoi kerrosnumeron funktiona. Kuitenkin myös muokkaamattomien fibrillien avulla monikerrosrakenteita pystyttiin muodostamaan. Muillakin kuin elektrostaattisilla vuorovaikutuksilla oli merkitystä vastakkaisesti varautuneiden nanofibrillien vuorovaikutukiessa.

Pintavoimamittauksissa havaittiin merkittävä adheesion kasvu kerrosrakenteissa, kun uloimpana oli korkeasti varautuneita nanofibrillejä. Työstä saadulla lisätiedolla voi tulevaisuudessa olla hyötyä kehittyvien selluloosa- ja bioperäisten materiaalien laajamittakaavaisemmassa soveltamisessa.

Avainsanat nanoselluloosa, pintavoimat, polymeerien adsorptio, polysakkaridit, AFM

ISBN (painettu) 978-952-60-4340-1 **ISBN (pdf)** 978-952-60-4341-8

ISSN-L 1799-4934 **ISSN (painettu)** 1799-4934 **ISSN (pdf)** 1799-4942

Julkaisupaikka Espoo **Painopaikka** Helsinki **Vuosi** 2011

Sivumäärä 175 **Luettavissa verkossa osoitteessa** http://lib.tkk.fi/Diss/

PREFACE

This work was carried out in the Department of Forest Products Chemistry, Aalto University School of Chemical Technology, formerly known as Helsinki University of Technology during the years 2007-2011. The work was funded and performed within "Innoforest" and "Naseva"- projects funded by the National Agency for Technology and Innovation (TEKES) and industrial partners. The Finnish Centre for Nanocellulosic Technology is thanked for providing the NFC samples.

I'm most grateful for the opportunity to do (and faith in finishing) a PhD- thesis for my supervisor, Professor Janne Laine. My instructor, Docent Monika Österberg is also thanked for the day-to-day guidance and improvements to both my scientific knowledge and writing.

Besides, there are quite a few people I have to acknowledge for their contribution:

All my co-authors: Anna-Stiina Jääskeläinen, Prof. Mark Rutland, Niklas Nordgren, Prof. Maija Tenkanen, Susanna Heikkinen, Karoliina Junka, Prof. Janne Ruokolainen, Isabel Diez, Markus Linder, Prof. Olli Ikkala and Robin Ras. I appreciate the opportunity to work with you and the pleasant co-operation.

All the past and present colleagues of my research group. It has been a pleasure working with you. Special mention to few but most useful (and fun) meetings on Friday-afternoons to Ania, Tiina and Karoliina!

My group of PUU-friends. Thanks that after all these years and memorable activities including travelling, sport-, TTT- and PI-events you still patiently stand me and my moods.

My family. My parents are thanked for their continuous support and encouragement for my studies from primary school days to these post-graduate studies. I owe a lot to my sister Anna for putting up of being my personal help-desk for various matters especially during the recent year.

Last but not least, my husband-to-be, Juanjo. To me personally, meeting you was the best result of this work. Thank you for your understanding, selfless scientific help, and love… you know, just a little.

Barcelona, October 7th, 2011

Paula Eronen

LIST OF PUBLICATIONS

This thesis is mainly based on the results presented in six publications which are referred as Roman numerals in the text. Some additional unpublished data related to the work is also discussed.

Paper I Eronen P., Österberg M., and Jääskeläinen A-S. (2009) Effect of alkaline treatment on cellulose supramolecular structure studied with combined confocal Raman spectroscopy and atomic force microscopy. *Cellulose* 16 (2), 167-178.

Paper II Eronen P., Österberg M., Heikkinen S., Tenkanen M. and Laine J. (2011) Interactions of structurally different hemicelluloses with cellulose nanofibrillar films *Carbohydrate Polymers*, 86 (3) 1281-1290.

Paper III Eronen P., Junka K., Laine, J. and Österberg, M. (2011) Interaction between water soluble polysaccharides and native nanofibrillar cellulose thin films. *Bioresources*, 6 (4), 4200-4217.

Paper IV Nordgren N., Eronen P., Österberg M., Laine J. and Rutland M.W. (2009) Mediation of the Nanotribological properties of Cellulose by Chitosan Adsorption. *Biomacromolecules* 10 (3), 645-650.

Paper V Eronen, P., Laine J., Ruokolainen, J., Österberg M. (2011) Comparison of multilayer formation between different cellulose nanofibrils and cationic polymers *Journal of Colloidal and Interface Science*, accepted, doi: 10.1016/j.jcis.2011.09.028.

Paper VI Diez. I., Eronen P., Österberg M., Linder M.B, Ikkala O., Ras R.H. (2011) Functionalization of nanofibrillated cellulose with few-atom silver nanoclusters: Fluorescence and antibacterial activity *Macromolecular Biosciences*, 11 (9) , 1185-1191.

Author's contribution to the appended joint publications:

I-III,V Paula Eronen was responsible for the experimental design, performed the main part of the experimental work, analysed the corresponding results, and wrote the manuscripts.

IV,VI Paula Eronen participated in defining the research plan, analysing the results and writing the manuscript with the co-authors.

LIST OF MAIN ABBREVIATIONS

AFM	atomic force microscopy
AgNC	silver nanoparticles
cat NFC	cationic nanofibrillar cellulose
CD	charge density
CNC	cellulose nanocrystals
COF	co-efficient of friction
CPM	colloidal probe microscopy
cryo-TEM	cryogenic transmission electron microscopy
DPFM	digital pulsed force mode
DLVO	Derjaguin, Landeau, Verway and Overbeek
DS	degree of substitution
DP	degree of polymerization
LbL	layer-by-layer
LS	Langmuir-Schäefer
MFC	microfibrillated cellulose
M_w	molecular weight
NFC	nanofibrillated cellulose
PDADMAC	poly(diallyldimethylammonium chloride)
PEI	polyethylenimine
QCM-D	quartz crystal microbalance with dissipation
RAX	rye arabinoxylan
RMS	root mean square
SFA	surface force apparatus
SPR	surface plasmon resonance
TEMPO	2,2,6,6-tetramethylpiperidine-1-oxyl radical
TMSC	trimethylsilyl cellulose

TABLE OF CONTENTS

1 INTRODUCTION AND OUTLINE OF THE STUDY

In the past, cellulose fibres used traditionally for papermaking purposes have been extensively studied related to e.g. their strength properties. During the past decades however, with the aid of well-defined cellulose model films suitable for modern, high-precision applications, more detailed information of cellulose molecular level properties have been obtained. Within the last decade, also cellulose based nanomaterials have emerged as materials with interesting properties along with the interest in nanomaterials in general. This improves the potential for new applications of cellulose based materials. Following this trend, the nanofibrillated cellulose (NFC), specially prepared as ultrathin substrate, was the most utilized cellulosic substrate in this work. Also other, pure cellulose substrates were used for comparison and supporting purposes. Many different, already prominent techniques were combined to find out the most feasible ways to characterize the nanosized cellulosic materials and their interactions. In **Paper I**, as a preliminary study, the relationship between cellulose chemistry and morphology was compared. This was done by combining Raman spectroscopy and atomic force microscopy (AFM)-imaging, two convenient and popular high-precision techniques. The effect of chemical treatment (alkaline mercerization, which is also of technical importance especially in the textile industry) on the microfibril structure was evidenced from combined measurements same sample positions. In addition, the spectra obtained could be used when nanofibrillated cellulose materials were characterized by Raman spectroscopy before and after chemical pre-treatments.

The main focus of this work was to study the effect of adsorption of polymers from various origins on surface properties of cellulosic materials. All the work was performed in aqueous phase. This environmentally friendly approach preserves better the fine nano-or microfibrillar structure of cellulose fibrils, which facilitates their use in enhancing the material properties. However, modifications are necessary to improve for example the poor moisture resistance of NFC based materials, in order for them to have real commercial potential. In this work, most of the studies were still focusing on the fundamental interactions and properties level, but in **Paper VI** a more practical result from modification by adsorption was quantified.

Both electrostatic and nonelectrostatic interactions were compared, and some conclusions about the effect of NFC surface chemical composition and charge properties could be attributed in this indirect way. The strong affinity of polysaccharides towards cellulosic material, known to originate from the close cell-wall composition and similar backbone structure, was studied in two papers. In **Paper II** various, structurally well-characterized water-soluble polysaccharides with different degrees of side-groups substitution were adsorbed on unmodified NFC substrate to study the interactions in detail. Adsorbed amount, layer structure and layer property estimations were performed by measurements and analysis with quartz crystal microbalance with dissipation (QCM-D). In second part of this study NFC prepared from different wood raw material (hardwood vs. softwood pulp) was systematically compared with selected hemicelluloses. The composition of the nanofibrillar cellulose was found to affect the adsorption of hemicellulose, but only slightly. The study was continued in **Paper III** with adsorption of a number of commercially available, only roughly characterized water-soluble polysaccharides. These included gums and cellulose derivatives. Similar, unmodified NFC substrates as in previous study were used. Some polysaccharides also had charged moieties. They were tested in order to find the most suitable both structure and price-wise for future modification studies. With a special digital pulsed force mode (DPFM) of AFM-imaging, the adsorbed hemicellulose layer could be identified on top of NFC substrate in a preliminary way. For selected polysaccharides, a comparison of the adsorbed amount in dry state was performed by measuring the adsorption with surface plasmon resonance (SPR). The calculated adsorbed amounts from QCM-D and SPR were compared to estimate the water content of the polysaccharide layer, which was found to be very high with all of the polysaccharides. In addition, one of the polysaccharides, chitosan, has markedly different properties and behaviour. It is a renewable based cationic polysaccharide with very similar structure to cellulose (originating from the similar reinforcing role of chitin, where it is derived, in fungi, insects and marine crustaceans shells). Therefore it was studied more in detail in **Paper IV** by both direct surface force and nanotribology measurements on a molecular level. Measurements were performed by AFM colloidal probe microscopy (CPM) at different pH-conditions.

To conclude, surface force studies with CPM in normal force mode in combination with QCM-D adsorption studies were performed to estimate the effect of different charge properties of NFC ultrathin film in **Paper V**. Chemically pre-treated vs. unmodified NFC prepared from similar raw material were systematically compared. Multilayer build-up using layer-by-layer (LbL) deposition with charged polyelectrolytes and different cationic counterparts was implemented. In this way, fundamental interaction study could be combined with more practical way, as LbL is a widely applied method also in commercial applications. The results verified the marked effect of charge properties on layer formation and structure, but also revealed that a nonelectrostatic contribution is significant between the cellulosic interactions. From this study, implication of practical advantages of using highly charged cellulose nanofibrils was also obtained, as the multilayer approach was able to increase the adhesive forces significantly. In addition, extensive AFM-imaging was applied in each study to verify that no dramatic morphological changes to the important micro- or nanofibrillar structure had occurred. In general, in this work indirect information of different cellulose nanofibril surfaces and their interactions by combined interaction measurements was obtained. This could be useful in future in optimizing the NFC preparation and selection of NFC grade for different applications.

2 BACKGROUND

2.1 Cellulosic fibres

Forests cover about 30 % of world's land area (4 billion hectares) and thus they make up a renewable option to supply raw material for various processes. Wood, pulp and paper products have until now dominated the large-scale commercial utilization. One area predicted to heavily increase is the share of wood as energy resource, either by direct burning or through new concept biorefineries (Carroll and Somerville, 2009). Interest to exploit wood and other cellulosic (non-wood) materials and by-products in new applications has been strong in recent years (Eichhorn et al. 2010, Ebringerová, 2005, Hansen and Plackett, 2008), not the least because fine paper consumption is predicted to decline in the coming years in the developed countries. Another contributing factor is the global concern for more sustainable future. However, basic and fundamental understanding of the properties and interfacial behaviour of the material is essential to efficiently and in an economically feasible way achieve the desired new material applications. A viable option for raw material supply is to extend the value-chain of pulp fibres. They are produced in large-scale in modern, existing production facilities. In addition, their fundamental chemistry and properties are quite well-known and understood from research over past century. The chemistry and properties of cellulosic fibres are presented briefly in the following.

2.1.1 Chemistry of cellulose

Carbohydrate polymers containing periodically repeating sugar units linked together mainly by O-glycosidic bonds are known as polysaccharides. They are usually divided into structural and matrix polysaccharides groups according to their function (Aspinall, 1982). Cellulose is the main constituent of the first group with highly regular, linear structure. It is formed as a result of glucose photosynthesis and forms the structural skeleton for plants from simple seaweeds to large trees with complex native nanocomposites-structures. In wood, cellulose constitutes about 40-45

w- % of dry mass depending on wood species. Therefore it is by far the most abundant biopolymer. More precisely, cellulose is a linear homopolysaccharide consisting of (1→4)-linked β-D glucopyranose units (in chair conformation). The repeating unit is cellobiose, with estimated length of 1.03 nm consisting of two anhydroglucopyranose units (AGU)s (Sjöström, 1993; Fengel and Wegener, 1984). This structure is illustrated in Figure 1. Notable is that it has non-equivalent end-groups, as one end contains an alcoholic OH group at C4, while on the other end the C1-OH is as aldehyde group a reducing end group. The degree of polymerization (DP) of native wood cellulose is very high, around 5000-10 000 depending on the plant species.

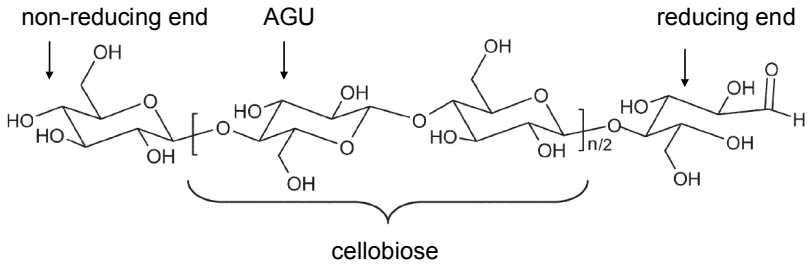

Figure 1. Structure of cellulose (adapted from Kontturi et al. 2006.)

The structure of cellulose is responsible for the unique, almost non-dissolving properties of cellulose, although the fundamental reason behind this remains still ambiguous (e.g. Lindman et al. 2010). The strong tendency of cellulose to form both intra- and intermolecular hydrogen (H)-bonds is explained by the availability of three hydroxyl moieties in each AGU. The H-bonding pattern in native cellulose consists of intrachain associations at O3-H···O5 and interchain bonding at O6-H··· O3. The former H-bond is responsible for the characteristic rigidity via co-crystallization of multiple chains into parallel stacked structures forming first elementary fibrils, which in turn form microfibrils with high aspect ratio. (Fengel and Wegener; 1984, Kontturi et al. 2006; Gandini, 2011; Moon et al. 2011). The main function of cellulose is to provide mechanical strength to trees and plants. This is achieved via precise ordering in highly hierarchical structures. However, there is an alternating pattern of highly crystalline regions and less ordered amorphous regions, the formation of which is not yet completely understood. Figure 2 illustrates the formation of wood microfibrils, starting from the terminal enzyme complexes. The formed cellulose chains are held

together by van der Waals forces. An elementary fibril is suggested to consist of rectangular, 6x6 cellulose I lattice, with dimensions estimated to vary between 3 and 5 nm. These further form the microfibrils, in which the amorphous and crystal regions alternate (Nishiyama, 2009; Moon et al. 2011).

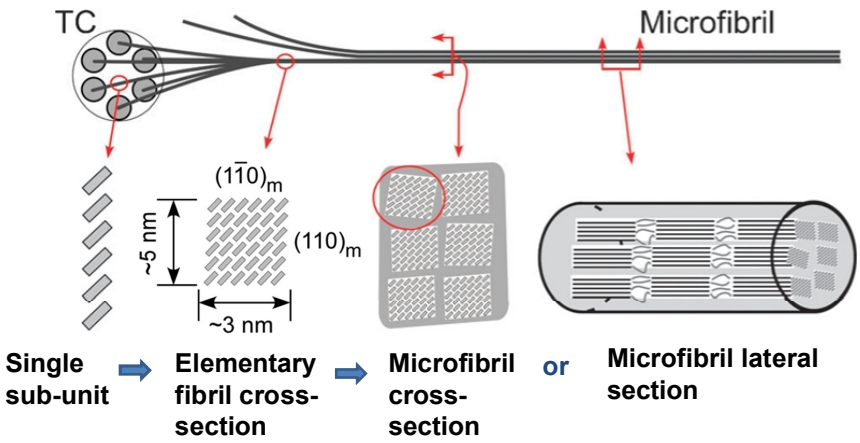

Figure 2. Schematic formation of cellulose microfibrils from wood (adapted from Moon et al. 2011).

2.1.2 Hemicelluloses

Hemicelluloses belong to the matrix group of polysaccharides. There are differences in grouping and classification of hemicelluloses, but usually they comprise the equatorial β-(1→4)-linked backbone consisting of glucose, mannose or xylose (Scheller and Ulvskov, 2010). In plant primary and secondary cell walls, they form a complex embedding network together with pectins around the cellulose microfibrils, as illustrated for example for the primary cell wall in Figure 3. The chemical composition of this network depends on the plant species and the cell wall layer. In both softwood and hardwood the major part of cellulose and hemicelluloses are located in the secondary cell wall (divided further into three sub-layers of S1, S2 and S3, of which the S2 is clearly the largest). Both the compositions and relative percentages of different hemicelluloses vary to a great extent between different wood species and morphological location. (Fengel and Wegener, 1984; Sjöström, 1993).

Hemicelluloses contribute to the strength formation of cell wall in association with cellulose microfibrils. Other main function of hemicelluloses is to cross-link or bring flexibility to the structural assembly of cell wall components. Small pores within the cell wall enable the transfer for nutritive (mainly salts and water) but prevent the diffusion out of partly water-soluble hemicelluloses. (Cosgrove, 1997; Vuorinen and Alén, 1999; Burton et al. 2010; Scheller and Ulvskov 2010). Compared to cellulose, common features for hemicelluloses include larger degree of heterogeneity both on molecular and tissue level (varying according to both species and cytological location), lower molecular weight (DP usually max. 200), higher degree of branching and lower degree of crystallinity. The backbone of hemicelluloses can resemble to a great extent a homopolymer structure. The heterogeneity is imposed from the complex side group substituent patterns. The mono-or oligosaccharide side groups prevent the formation of aggregated, fibrillar structure and instead a more gel-like structure is formed (Burton et al. 2010). Higher degree of side-group substitution yields to higher solubility but consequently less tight binding to cellulose (Lawther et al. 1995). An implication of the tailor made nature of hemicelluloses is the strong dependency of even minor changes on the structure to physical properties of hemicelluloses, such as the solubility (Aspinall 1982). Hemicelluloses are also more susceptible to chemical and enzymatic degradation compared to cellulose, e.g. in chemical pulping.

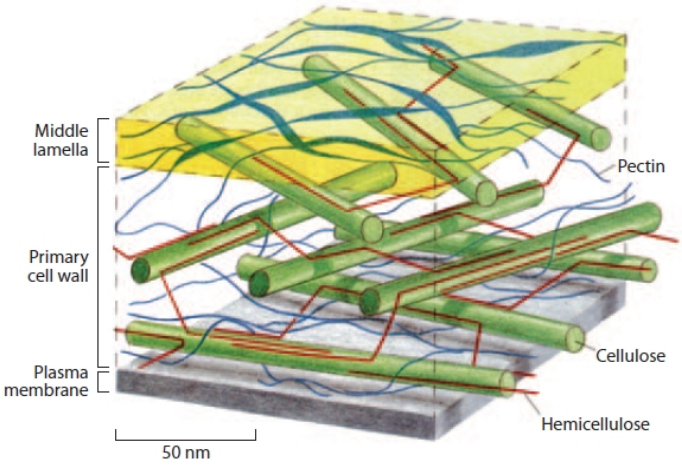

Figure 3. A schematic representation of the network structure of primary cell wall. (McCann and Roberts, 1991).

The composition and relative amount of hemicelluloses in the cell wall depend on both species and cytological location (Joseleau et al. 1992). Xylans, a diverse and common group built up from (1→4) linked β-D-xylopyranosyl units in all plants differ from the side-group substitution pattern. The xylan in hardwood trees is known as glucuronoxylan ((1→2)-linked 4-O-methyl-α-D-glucopyranosyl uronic acid and acetyl groups). It is the main hemicellulose component, about 25 -% of relative mass proportion of wood depending of the species. In softwood trees the xylan is arabinoglucuronoxylan (both (1→3)-linked α-L-arabinofuranosyl and (1→2)-linked 4-O-methyl-α-D-glucopyranosyl uronic acid substituents) and it is present in lesser weight percentage. In non-tree plant cell walls, such as those of cereal origin, the xylan is arabinoglucuronoxylan (main substituents are 1→3) - and /or (1→2)-linked α -L-arabinofuranosyl units). Most notable difference compared to wood originating xylans is the absence of uronic acid groups, meaning that cereal origin xylans are neutral polysaccharides unlike negative charge bearing wood originating xylans. (Ebringerova 2005). Mannans on the other hand have a backbone which consists of both mannose and glucose units, referred as glucomannans. Mannans are only scarcely present in hardwoods, but in softwoods contain they constitute a significant proportion (20-25 % relative mass). Known as O-acetyl-galactoglucomannans, they are formed from a backbone with (1→4)-linked β-D-mannopyranosyl and β-D-glucopyranosyl units substituted with (1→6)-linked α-D-galactopyranosyl and acetyl groups. (Whitney et al. 1998; Salmén and Olsson 1998). Xyloglucans are present in almost all land plants primary walls, and they have a heterogeneous branched structure depending on the origin. They have a more specific role in bringing flexibility to the primary cell wall layer by crosslinking the spaces between cellulose microfibrils (Zhou et al. 2007). In general, hemicelluloses are associated with cellulose microfibrils via hydrogen bonding and with other cell wall constituents via covalent linkages, e.g. ether linkages with lignin (Sun et al. 2004). Hemicelluloses interact with different cell wall components according to their structure. It has been speculated for example that different mannans with 2-fold structure are involved more in interactions with cellulose whereas xylans with 3-fold, screw-like structure are involved in hydrophobic interactions with lignin (Joseleau et al. 1992; Salmén and Olsson, 1998; Whitney et al. 1998; Almond and Sheehan 2003; Picout et al. 2003;, Scheller and Ulvskov 2010).

Cell walls are surrounded by lignin, which increases both the mechanical resistance of cell walls and as amorphous, branched high M_w biopolymer also acts as a binder (Alén 2000; Burton et al. 2010). The purpose of chemical pulping is to selectively remove lignin in order to liberate the fibres from the tight cell wall composition, but due to complex lignin-hemicellulose (or carbohydrate) complexes, this is never achieved. After the chemical pulping and following treatments such as bleaching, the cellulose and hemicelluloses are partly depolymerised, and also contain residual lignin to a varying degree depending on wood species and pulping method (Treimanis 1996). These can strongly affect the properties of the fibres (kraft pulp) produced and therefore all the way to the manufactured end-products. Characterization methods for pulp fibres have been established to relate the desired end-product properties to the chemical and morphological properties of fibres.

2.1.3 Surface characterization of cellulosic materials

Traditionally, the cellulose fibres have been liberated for paper manufacturing. Therefore many of the routine standard analyses developed (ISO, SCAN or TAPPI standards) have served for this purpose (brightness, kappa number, fibre length classifications etc.). The surface potential arising from the acidic groups of hemicellulosic materials can be determined and located by different titration techniques; such as conductometric (Katz et al. 1984), potentiometric (Laine et al. 1994; Bygrave and Englezos, 1998) and polyelectrolyte titrations (Wågberg et al. 1989; Horvath and Lindström, 2007) to name a few. However, to properly characterize in detail the structural and chemical fibre surface properties more elaborate methods are needed. The chemical structure of fibres can be unravelled to the relative percentages of sugar components. This requires the cleavage of glycosidic bonds, most commonly with either acidic or enzymatic hydrolysis or methanolysis. The resulting monomers are often derivatized i.e. to volatile components for gas chromatography (GC). Also liquid chromatographic techniques, nowadays mainly high performance liquid chromatography (HPLC) for monosaccharide analysis and size-exclusion chromatography (HPSEC) are used to determine the molecular weight distributions of polydisperse hemicellulose or dissolved cellulose (Aspinall 1982;

Vuorinen and Alén 1999; Holmbom and Stenius 2000). Another, nondesctructive way is to use spectroscopic techniques, of which ^{1}H and ^{13}C nuclear magnetic resonance (NMR) spectroscopies and infrared (IR) and Raman spectroscopies are most informative for cellulosic samples. Especially the solid state (^{13}C) NMR with modern instrumentation enabling in-situ analysis of fibrous samples has revealed unique information about the complex chemical composition. Structure of pure oligosaccharides can be unravelled to individual sugar components with multidimensional total correlation spectroscopy (TOCSY). This has revealed important information of the composition in particular of lignin and hemicelluloses (Aspinall 1982; Vuorinen and Alén 1999; Holmbom and Stenius 2000). IR spectroscopy is based on different vibrational modes of chemical bonds. It is able to identify functional groups, although the spectra of complex molecules can be challenging to interpret. The Raman spectroscopy is a complementary technique to IR, able to distinguish double and triple carbon bonds and unlike IR, insensitive to water. Although IR in particular is a reliable and relatively fast method able to provide specific and fundamental information about chemical structure, it unfortunately is not very surface sensitive. This can to some extent be improved using a thin reflecting diamond in attenuated total reflection (ATR)-mode of Fourier Transformed IR microscopes (FTIR). Also modern confocal Raman spectroscopes can achieve quite high sensitivity. To characterize the chemical composition of the fibre surface, different spectroscopic methods have been successfully implemented. One of the first methods applied was electron spectroscopy for chemical analysis (ESCA) (Dorris and Gray, 1978a; Dorris and Gray, 1978b). It has since become a relatively popular technique applied to characterize the chemical composition of various pulp samples as it can distinguish between polysaccharides and aromatic compounds (e.g. Laine and Stenius 1994; Laine and Stenius 1996; Fardim et al. 2006; Gray et al., 2010). However, there are limitations in distinguishing either cellulose and hemicelluloses or lignin and extractives. Despite the extreme surface sensitivity, it cannot distinguish between the structural features of cellulose, hemicellulose and lignin and it requires a high vacuum. Another surface sensitive technique applied for fibres is time of flight secondary ion mass spectroscopy (ToF-SIMS) (Kleen, 2005; Fardim and Duran, 2003; Orblin and Fardim, 2010), most often as a compliment method to ESCA. In this work, Raman-spectroscopy was the applied spectroscopic technique for chemical characterization (introduced in more detail in Chapter 3.4).

Besides chemistry, the morphology of fibres was early on studied with different standardized fibre analytical techniques involving selective staining of aqueous fibre suspensions and optical microscopy. However, the rapid development of technology improved markedly the resolution of the visual fibre surface characterization. For example, the environmental scanning electron microscopy (ESEM) (Jähn et al. 2002), transmission electron microscopy (TEM) (Molin and Daniel, 2004), confocal laser scanning microscopy (CLSM) (Barsberg and Nielsen, 2003) and atomic force microscopy (AFM) (Hanley et al. 1992; Kuutti et al. 1995; Baker et al. 1997) have all been applied in fundamental cellulosic studies. However, to get comprehensive, reliable and useful information of the heterogeneous cellulosic fibres in applied systems, none of the characterization techniques alone can provide sufficient information. The combinations of different techniques have proven to be most successful to extract new information. Possibilities for combinations are numerous. In the past, for example ESCA for chemical surface analysis and AFM/SEM for visualization have frequently been combined for pulp samples. (Maximova et al. 2001; Gustafsson et al. 2002; Duchesne et al. 2003; Koljonen et al. 2003).

The relatively high roughness and heterogeneity of pulp fibres have prevented their use as such for precise adsorption, affinity, and interaction studies on molecular scale. In some studies, silica or mica has been used to model the behaviour cellulose due to the presence of hydroxyl groups (e.g. Bogdanovic et al. 2001; Lingström et al. 2007), but the mineral surfaces cannot be considered as very good representatives of cellulosic surfaces. Therefore various ultrathin films have instead been developed to represent more precisely surface of cellulosic fibres. They are introduced in detail in a review article (Kontturi et al. 2006) and have been applied in adsorption and swelling studies (e.g. Fält et al. 2003; Tammelin et al. 2006) or direct surface force measurements (e.g. Notley and Wågberg, 2005). Recently also cellulosic nanomaterials have found use as ultrathin cellulose films. In this work the focus will be on nanofibrillated cellulose (NFC), which will be introduced in the following chapter in greater detail. It is worth to mention that the cellulose nanocrystals (CNC), or whiskers, are also very important cellulosic nanomaterials. They contain only the crystalline part after the amorphous parts are hydrolyzed in the acidic preparation

method. Reviews by Aziz Samir et al. (2005) and recent one by Eichhorn (2011) provide more information related to CNCs.

2.2 Nanofibrillated cellulose (NFC)

2.2.1 Preparation and properties

The concept of nanofibrillated cellulose or cellulose nanofibrils, is somewhat nebulous, but in this work it is used to denote the long and thin (thickness of nanometre range), flexible fibrils containing both crystalline and amorphous regions (Fig. 2). The preparation using high-pressure fluidizer method and the properties of corresponding NFC are described and illustrated in detail by Pääkkö et al. (2007). Friction grinding is an alternative method to produce NFC (Abe et al. 2007). Pulp straight from the mill (preferably washed into its sodium-form) can be used to produce the fibril suspensions, but a further fractionization step is required to distinguish the truly nanosized fibrils. Often, the term microfibrillar cellulose (MFC) is also used to denote the fibril material also containing larger fibril aggregates (Hubbe et al. 2008). MFC was produced already in the 1980's (Turbak et al. 1983; Herrick et al. 1983), but it took over 20 years for this gel-like material to become a hot topic in cellulosic research. Various cellulosic materials including hardwood and softwood industrial pulps (Stelte and Sanadi, 2009; Zimmermann et al. 2010; Spence et al. 2010; Syverud et al. 2011) have been compared as potential raw material for the cellulosic nanomaterials. Also cellulose fibrils from non-wood plant origin outside the traditional industrial pulp manufacture, for example sugar beet pulp (Dufresne et al. 1997), sisal (Morán et al. 2008) and even banana rachis (Zuluaga et al. 2007) have been studied as a result of the grown interest in global utilization of renewable materials. In general there are as many potential raw materials for NFC as there are cellulosic materials. As cost is still the ruling factor for commercial applications, large-scale produced industrial pulps have an advantage. An interesting alternative is combining the biorefineries with nanofibrillated cellulose production via cellulase treatment of kraft pulp (Zhu et al. 2011).

The main reason for interest in cellulosic nanomaterials, and NFC more specific, are their unique properties. These include abundant availability, high aspect ratio (~100-150), high strength properties combined with low density and renewability. This yields to possibility of producing sustainable light weight high strength composites and various other, novel materials beyond traditional scope of wood based materials. Envisaged products include use of NFC as supporting material in medical and pharmaceutical applications, as packaging, papermaking and filtration aid and use even in electronic devices such as flexible displays or template materials (Siró and Plackett 2010, Moon et al. 2011). Before these are realized, there is still a lot of work related to two main challenges of NFC: the production cost from high energy consumption and the properties of unmodified NFC. As only disintegration method, mechanical treatments to disintegrate the cellulose fibres into nanoscale dimensions are considered too expensive for large-scale production. However, different pre-treatments prior to fibrillation can reduce the energy consumption considerably. These include enzymatic pre-treatment by endoglucanase (Pääkkö et al. 2007), carboxymethylation (CM) (Wågberg et al. 2008; Eyeholzer et al. 2010) and selective oxidation with a primary oxidant (e.g. hypochlorite) and 2,2,6,6-tetramethyl-piperidinyl-1-oxyl (TEMPO) radical as catalyst (Saito et al. 2007). The latter two treatments induce the polyelectrolyte behaviour of NFC via increased charge properties, thus facilitating the separation of individual nanofibrils. Recently, also cationization used already in chemical modification of starches by 2,3-epoxypropyltrimethylammonium chloride (e.g. Rutenberg et al. 1984) has been applied to produce cationic NFC (Aulin et al. 2010b). The properties of individual nanofibrils affect the behaviour of NFC all the way to final end-use applications.

One of the most utilized property of NFC is its excellent film forming ability due to presence of –OH groups at the fibril surfaces, sometimes referred as nanopaper (Henriksson et al. 2008; Syverud and Stenius, 2009; Aulin et al. 2010a; Sehaqui et al. 2010; Fujisawa et al. 2011). Figure 4 illustrates how the fibril morphology affects the appearance of films produced from different fibrillation levels. The smaller TEMPO-fibrils form a completely transparent film whereas the larger fibril aggregates containing unmodified fibrils forms a less transparent, but high-strength durable film.

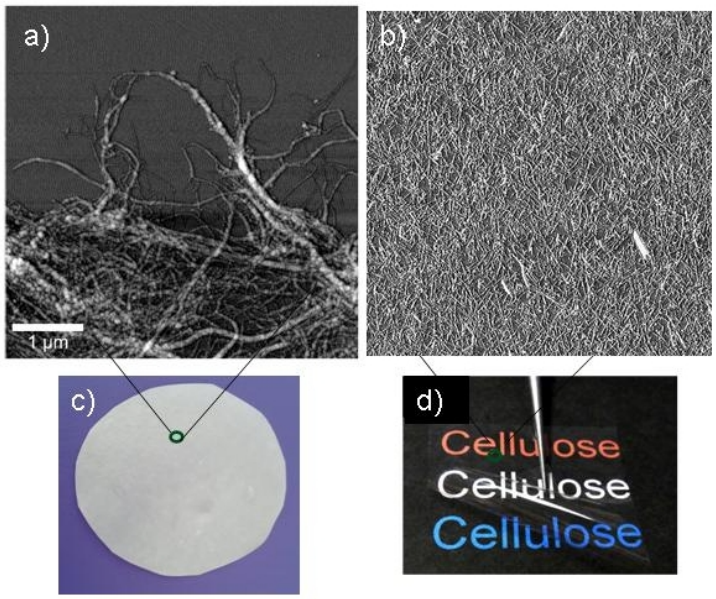

Figure 4. Examples of cellulose fibril grades and films produced.: AFM phase contrast images (5x5 µm²) of a) friction grind, unmodified fibrils (MFC) and b) TEMPO-oxidized fibrils, spincoated on silica surface.(unpublished results.) In c) and d) the appearance of films produced from MFC (Österberg et al. unpublished results and TEMPO-fibrils (adapted from Fujisawa et al. 2011), respectively, are shown.

Although the films have excellent strength and barrier properties, unfortunately the hydrophilic nature of cellulose prevents the direct utilization of them in replacing oil-based materials e.g. in packaging. The previously mentioned pre-treatments do not change the hydrophilic nature of NFC, which in addition to poor moisture resistivity prevents also their direct compatibilization with non-polar composite matrixes. For possible chemical modifications acetylation (with bacterial cellulose; Kim et al. 2002; Nogi et al. 2006), silanation (Andresen et al. 2006; Andresen and Stenius 2007) and surface grafting (Stenstad et al. 2008; Littunen et al. 2011) have been suggested. However, in these modifications, the ultrastructure of individual fibrils is almost always irreversibly changed to more aggregated and less tightly bound network, which causes lower strength properties.

Incorporation of NFC into various nanocomposites is another of the main studied NFC applications (Nakagaito and Yano, 2005; Nogi and Yano, 2008; Wang et al. 2011) including more specific biodegradable nanocomposites, e.g. with

poly(lactic) acid (PLA) (Nakagaito et al. 2009; Tingaut et al. 2009; Suryanegara et al. 2010; Lönnberg et al. 2011). As was the case with NFC films, modifications are needed to distribute the fibrils evenly in composite to convert the high strength properties of individual nanofibrils into composite materials. Recent review articles provide background information about the modifications needed in these applications (Hubbe and Rojas, 2008; Eichhorn et al. 2010; Siró and Plackett, 2010; Moon et al. 2011). In this work, the focus was on using adsorption in NFC modifications. Therefore the following chapter introduces the concept of adsorption and use in previous NFC modifications.

2.2.2 Modification by adsorption

The surface of the individual fibril contains always –OH groups to different extent depending on the manufacturing method. This enables possibilities for modification and functionalization. Adsorption is a general concept denoting both the process by which substances are concentrated from the adsorbent to the adsorbing surface and the amount of accumulated adsorbent. Based on the formed bonds, adsorption can be irreversible if covalent chemical bonds are formed (chemisorption) or reversible via formation of only physical attachment (physisorption). Polymer adsorption on cellulose surfaces, including NFC, belongs to the latter one. It has been utilized in papermaking for years as cellulosic materials in aqueous solutions have negative charge. Thus the most common way is to use cationic polyelectrolytes to achieve either flocculation or dispersion of the system in a quite precisely controlled way, utilized for example in the wet-end of the paper machine. Numerous factors contribute to the adsorption, which depends on ionic strength, medium, and polyelectrolyte dosage, charge density (CD) and molecular weight (Fleer et al. 1993; Wågberg 2000). However, adsorption of also nonelectrostatic origin, namely interactions of various polysaccharides with cellulose kraft fibers have been observed. (Swanson 1950; Laleg and Pikulik 1991; Laine et al. 2000; Hannuksela et al. 2002; Christiernin et al. 2003; Westbye et al. 2006; Ren et al. 2009). The mechanisms behind the interactions have been partly unravelled, but they are more divergent when compared to synthetic polyelectrolytes. Mechanism for this most likely arises from hydrogen bonding, seen especially with other similar backbone having

polysaccharides or cellulose derivatives (Swanson 1950; Ishimaru and Lindström 1984; Mishima et al. 1998). The polysaccharides can also carry a charge, such as chitosan and in these cases the interactions are speculated to be combinations of electrostatic and nonelectrostatic interactions. Fundamental basis behind polymer adsorption at interfaces has been thoroughly presented (Fleer et al. 1993). In addition, extensive reviews related to the use of polyelectrolytes and polysaccharides in papermaking have also been written (e.g. Wågberg 2000; van der Ven 2000; Hubbe and Rojas 2008).

For fine structured NFC, functionalization via physisorption could be an especially suitable alternative. The fibrillar ultrastructure of NFC is preserved in physisorption, which is turn can be modified to achieve the desired modifications (Teeri et al. 2007). In addition, there has been fundamental research on the interactions of pulp fibres and different polymers for decades, giving sufficient background information about the type and mechanisms of interactions. Quite a number of adsorption studies have already been performed utilizing both the electrostatic and nonelectrostatic interactions either in single-or multilayer adsorption studies. The polyelectrolyte multilayer (PEM)-technique (Decher et al. 1992) is suitable in particular for the chemically pre-treated NFCs with increased charge. In cellulosic materials, it has been first applied to CNCs with different cationic or non-ionic counterparts (e.g. Cranston et al. 2006; Jean et al. 2009; Cerclier et al. 2010). With NFC, Wågberg et al. (2008) compared the effect of different cationic polyelectrolytes and their interactions in building layer-by-layer (LbL)-structures with CM NFC on supporting silica wafer. The ionic strength and cationic counterpart M_w and CD were found to influence the thickness of the formed layers the most. Later, the PEMs consisting of polyethyleneimine (PEI) and NFC have been studied in more detail using combinations of different techniques (Aulin et al. 2008; Aulin et al. 2010b). Ahola et al. (2008c) investigated the adsorption of cationic poly(amideamine) epichlorohydrin (PAE) in both bilayer and complex addition on NFC ultrathin film and the properties of handsheets with similar NFC-PAE additions. Results showed that the amount adsorbed was independent of the addition strategy, but that bilayer adsorption resulted in more uniform distribution of components. In another study by the same authors (Ahola et al. 2008a) the adsorption estimated as dry-and wet amounts was determined for two polysaccharides, xyloglucan (XG) and

carboxymethyl cellulose (CMC). CMC adsorption was reversible due to too high electrostatic repulsion in the experimental conditions used but XG adsorbed irreversibly. Utsel et al. (2010) used NFC in building LbL thermoresponsive PEM with atom transfer radical polymerized (ATRP) cationic component.

Salmi et al. (2009) combined in their LbL and complex studies both cationic polyelectrolyte and as anionic component either CM NFC or silica nanoparticles. The incorporation of charged nanoparticles, acting as binding sites between polymers, was verified to yield excellent reflocculation properties, useful in papermaking applications. However, nanoparticles can also be used in functionalization of material properties. For example, previous studies have shown how the known antimicrobial effect of silver nanoparticles (Rai et al. 2009) can be templated into cellulosic materials, maintaining the antibacterial properties (Cai et al. 2008; Maneerung et al. 2008; Dong et al. 2008; Ifuku et al. 2009; Sureshkumar 2010). In freestanding NFC film applications, improvements in moisture resistivity using adsorption of cationic surfactants (Xhanari et al. 2011) have also been reported.

2.2.3 NFC characterization

The (routine) characterization methods of pulp are not directly applicable to NFC. However, the ultrastructure and morphology of NFC can be determined by using different high-end precise microscopic techniques used to characterize nanomaterials in general. Successfully implemented techniques to characterize the morphology include the electron microscopy techniques: different scanning electron microscopies, e.g. field emission (FE-SEM), transmission electron microscopy, TEM, also in cryo-freezed mode (cryo-TEM) to estimate dimensions of wet fibrils, and atomic force microscopy (AFM). In addition, crystallinity has been estimated using wide-angle X-ray scattering (WAXS) and structure using solid state ^{13}C NMR in cross-polarized magic angle spinning (CPMAS) mode and ESCA. The properties of the pulp used for NFC production correlate quite well with the properties of nanosized suspensions, e.g. related to charge properties or carbohydrate composition (at least in bulk NFC suspension). Cellulose fibril films have more or less the cellulose I structure with equal crystallinity percentages detected compared to pulp fibres as

determined by X-ray diffraction (XRD) measurements (Aulin et al. 2009). The morphological characterizations can be used to indirectly estimate the degree of fibrillation, either solely by visual observations or by using special software to obtain numerical information. Other, also indirect possibilities to do this include application of degree of polymerization measurements, as DP is noted to decrease as the fibril length (fibrillation) decreases (Henriksson et al. 2007). In addition, water retention or viscosity measurements can be used; they are related to the surface area which also increases as the fibrillation proceeds.

The main challenges include morphological quantification of NFC fibril lengths, as the flexible fibrils readily form interpenetrated networks. Also the exact surface chemical composition is difficult to determine due to extremely low amounts of material present. In this work, the surface composition of NFC was probed via indirect adsorption studies. AFM-imaging was the main morphological characterization technique due to fast sample preparation and possibility to characterize samples also in their native, wet-state. In composite NFC studies, important feature is to estimate the mechanical and thermal properties of the composites. For NFC, the estimation of the strength properties of individual nanofibrils have not been determined, unlike for many other cellulosic nanoparticles, including CNC and bacterial cellulose (Iwamoto et al. 2010; Guhados et al. 2005). It has been estimated to be of the order of at least 2 GPa (Siro and Plackett 2010). Also the swelling and surface force measurements, previously done with regenerated cellulose films have been performed with NCC or NFC (e.g. Notley et al. 2006; Stiernstedt et al. 2006b; Ahola et al. 2008a; Ahola et al. 2008b; Aulin et al. 2009; Salmi et al. 2009; Cranston et al. 2010) to name a few. A recent review presents interactions at cellulose model surfaces (Wågberg et al. 2010) and the studies were continued in this work.

2.3 Forces in cellulosic systems

Cellulosic materials, especially the nanosized fibrils belong to colloids (particles with at least one dimension in the nm to μm range). One implication of this is the large area/unit, giving significant importance to interfacial phenomena. In the case of

charged surfaces in liquid medium, a classical theory developed independently by Derjaguin & Landeau (1941) and Verway & Overbeek (1948). It is known as DLVO-theory and often used to describe the combined interaction forces arising from van der Waals attraction and electrostatic repulsion of similar particles. The additive components will be shortly introduced.

2.3.1 van der Waals forces

The origin of the van der Waals (vdW) forces is in the fluctuations of the electron clouds of the atoms (polarization) creating permanent or temporary dipoles. This occurs in all molecules and thus vdW forces are universal. According to Hamaker (1937), the vdW interactions between two particles is assumed to be additive, and thus the total interaction energy can be estimated by integrating the energy of all atoms in the interacting particles. For two flat surfaces, the interactions energy (W_{vdW}) as the function of distance (D) is:

$$W_{vdW}(D) = -\frac{A_H}{12\pi D^2}, \qquad (2.1)$$

where A_H is the Hamaker constant specific for each material and medium.

Except for the calculation of Hamaker-constant, this additive approach is still considered valid. To accurately estimate the Hamaker-constant, a theory based on calculations of Lifshitz (1956) takes better into account both the surrounding medium and neighbouring atoms. vdW interaction between similar particles is always attractive and quite significant at short distances related to colloidal systems.

2.3.2 Electrostatic forces

Most surfaces, including cellulosic substrates, are charged when in contact with aqueous solutions. This results that the ions in the surrounding solution carry an opposite charge of same magnitude and net charge thus forming the electrical double

layer, which as whole is neutral. The counter-ion concentration in the freely mobile, diffuse layer in the solution (a.k.a. Guoy-Chapman layer), increases toward the surface. For a flat surface with uniform charge density this equation can be written as complex Poisson-Bolzmann equation (derived from the fundamental electrostatic relationship of charge and potential):

$$\frac{d^2\psi(x)}{dx^2} = -\frac{e}{\varepsilon\varepsilon_0}\sum z_i n_{i\infty} \exp\left(-\frac{z_i e\psi(z)}{kT}\right), \qquad (2.2)$$

where $\psi(x)$ is the electrostatic potential at distance x from surface, z_i is the valency of the counterions e is the elementary charge, $n_{i\infty}$ is the number density of ions in the bulk solution, ε_0 is the permittivity of vacuum ε is dielectric constant of water k is the Bolzmann constant and T is the temperature. The solutions to the Eq. 2.2 are usually obtained by approximations using algorithms (e.g. Ninham and Parsegian 1971). The algorithms assume either constant charge or constant potential, which give the lower and upper limits of the interactions, respectively.

Surfaces with similar charge sense a repulsive force arising from the overlap of double-layer forces as they approach each other. The thickness of the electrical double layer can be estimated by the Debye length (independent of the properties of the surface):

$$\kappa^{-1} = \sqrt{\frac{\varepsilon\varepsilon_0 kT}{\sum_i e^2 z_i^2 n_{i\infty}}}, \qquad (2.3)$$

Assuming additive nature, the total interactions of charged (ideal) colloidal particles in solution have been calculated and compared to experimental findings with real systems. Double layer interactions (assumed solely responsible for the electrostatic interactions) are non-specific. The magnitude of the force depends on charge of surface but the Debye length is solely dependent on ionic strength. According to the theory, attraction dominates at short distances and electrostatic repulsion at longer. DLVO-theory has been able to describe many phenomena related to colloidal stability. Increasing electrolyte concentration and counter-ion valence

always decrease the stability (e.g. promote coagulation of the system) whereas increase of surface charge density improves the stability. In the complex world of surface interactions, other than DLVO forces of course exist. These include additional repulsive component, due to organization of the solvent around particles or effects of water molecules, known as hydration force. On certain materials, this force has noted to increase as the electrolyte concentration increases, opposite to electrostatic double layer behaviour. (Israelachvili and Wennerström, 1996). Repulsive steric forces affect large polymer molecules, when mingling of tails from opposing surfaces reduce the configurational entropy, as depicted in Figure 5. They are considered to have a major impact on cellulosic interaction forces, as will be discussed more in the further chapters focusing on cellulose interactions before and after modifications. For comprehensive theoretical background, books by Israelachvili (1992) and Evans and Wennerström (1999) are recommended.

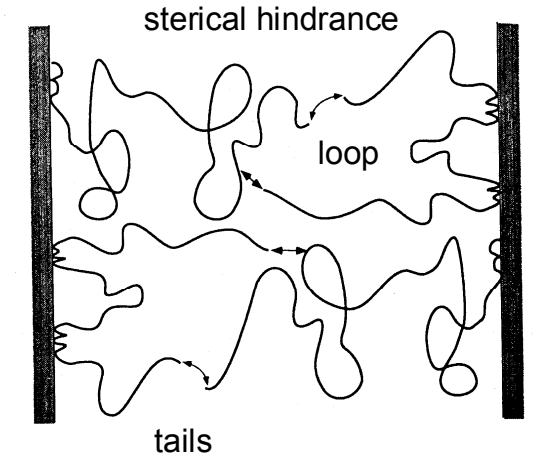

Figure 5. Effect of polymer chains. Adapted from Evans and Wennerström (1999).

2.3.3 Frictional forces

Frictional forces can still be relatively well characterized by classical Amonton's law:

$$F_f = \mu L \qquad (2.4)$$

where F_f is the friction force and L the applied load and μ the friction coefficient. It can be determined as the slope of friction force versus load graphs. Macroscopic, wet friction measurements are difficult to perform, but recent advances in AFM nanotribology have provided an alternative way to probe molecular scale frictional forces, sometimes noted as lateral force microscopy. (Perry et al. 1995; Heim et al. 1999; Feiler et al. 2000; Butt et al. 2005). However, for fibres and AFM frictional measurements an additional parameter, F_0, independent of normal force has to be added (Lord 1955; Carpick et al. 1996):

$$F_f = F_0 + \mu L \qquad (2.5)$$

It is also known that microscale friction is affected by the contact area (surface roughness), which in molecular scale measurements is never considered smooth (e.g. Berman et al. 1996; Rabinovich et al. 2000). Therefore to compare friction force microscopy results topographical features should also be taken into account.

2.3.4 Cellulose-cellulose interactions

Direct surface force measurements between cellulosic surfaces have revealed interesting details of the interactions of cellulose at molecular scale. DLVO-theory has been found to be applicable at larger separations, but deviations at short separations have been observed between differently prepared cellulose surfaces. The surface force apparatus (SFA) was first applied to measure interaction forces between trifluoroacetic acid dissolved microcrystalline cellulose films (thickness 30-40 nm) spincoated on mica (Neuman et al. 1993). The characteristic, soft, swollen and viscoelastic gel-like nature cellulose surface was evident. It complicates the analysis and fitting of the recorded data to the DLVO-theory and estimation of surface potential. Nevertheless, the basic interaction forces were already observed, namely the monotonically repulsive forces on approach decreasing as the function of ionic strength. The repulsive forces were extending to separations on the order of 100 nm. In subsequent SFA and colloidal probe microscopy (CPM) measurements with various regenerated cellulose surfaces similar observations have been made, although

the range of the repulsion has usually been of the orders of tens nanometres (e.g. Holmberg 1997; Rutland et al. 1997; Carambassis and Rutland 1999; Zauscher and Klingenberg 2000a) due to the more robust cellulose substrates used in these studies.

The repulsive forces have been divided into three or two different regimes according to electrostatic and steric repulsion regimes. The forces at intermediate separations follow the predictions of the DLVO-theory relatively well and have thus been interpreted to originate from electrostatic repulsion. The deviations from DLVO-theory observed at short separations have been assigned first to steric (or alternatively electrosteric) forces or deformation of the soft cellulose substrates (e.g. Carambassis and Rutland, 1997; Zauscher and Klingenberg 2000a; Stiernstedt et al. 2006b). The attractive van der Waals forces has also been detected at low pH, where the adjoined carboxylic groups are protonated, thus dispelling the electrostatic contribution to surface forces (Notley et al. 2004). Increasing pH leads to increase in repulsion, due to the increased charge of the film via the dissociation of carboxyl groups of residual uronic acid groups (–COOH $\rightarrow COO^- + H^+$) (Carambassis and Rutland 1997; Österberg and Claesson 2000; Notley and Wågberg 2005). The divalent ion (Ca^{2+}) on the other hand was found to reduce the magnitude and range of the repulsion, either by reduced repulsion or bridging of the carboxylic groups by calcium ions (Carambassis and Rutland 1997). The adhesive forces increase as the function of compression rate and ionic strength but are nevertheless low between neat cellulosic surfaces (Zauscher and Klingenberg 2000; Carambassis and Rutland 1997; Salmi 2007). The forces between NFC ultrathin films and regenerated cellulose spheres using CPM have also been studied as the function of NFC charge and pH (Ahola et al. 2008b). Increasing charge of NFC increased the range and magnitude of repulsive forces, as seen also with carboxymethylated cellulose model films (Notley et al. 2006; Notley 2008). Besides increasing the carboxyl group content via chemical treatment of cellulose, adsorption of polyelectrolytes is also used to increase the charge properties of cellulosic surfaces.

The co-efficient of friction (COF) between different wet cellulose surfaces have been determined to vary between 0.6 and 1. Taking into account the varying roughness for differently prepared films (Zauscher and Klingenberg 2000b; Zauscher and Klingenberg 2000c; Stiernstedt et al. 2006b; Theander et al. 2005), these values

are relatively constant. They are also of the same range than the value determined for kraft pulp fibres in aqueous conditions (Andresson et al. 2000). Friction between a cellulose sphere and various (model) surfaces has also been compared (Bogdanovic et al. 2001). Factors that influence especially CPM friction measurements are the surface roughness (asperities of interacting cellulosic surfaces), and the scan-size (relative to sliding in single and multiple topographical domains). Typical stick-slip behaviour in conformation with the topographical features is observed at low applied loads. As the applied force is increased the friction force is more constant when asperities are flattened under increased load. (Zauscher and Klingenberg, 2000c). As novel approaches, AFM-tip modified with a piece of fibre and a single pulp fibre configuration has been applied in frictional studies (Huang et al. 2009), and recently friction measurements between human hair fibres was achieved (Mizuno et al. 2010). Therefore interesting possible future developments include friction force measurements directly between cellulosic nanomaterials.

2.3.5 Effect of polymer adsorption on cellulose interaction forces

Polymer adsorption induces changes at the molecular scale between cellulosic surfaces, as observed using polyelectrolytes (Holmberg et al. 1997b; Zauscher and Klingenberg 2000a; Poptoshev et al. 2002; Salmi et al. 2007). Attraction has been observed at charge neutralization point. Below repulsive forces are decreasing and above they are increasing. The polymer M_w and CD affect the interaction via adsorption conformation. Higher CD results in more compact attachment, which causes lower increase in detected repulsion compared to lower CD. Together with high M_w it promotes the formation of loops and tails, which increases the repulsion via steric hindrances, extending over considerable separations, estimated for example to be 1-2 times the radius of gyration (R_g)/surface (Zauscher and Klingenberg, 2000b). The addition of non-ionic polysaccharide, xyloglucan (XG) also increased the range and magnitude of repulsive forces (Stiernstedt et al. 2006a). Formation of extended loops and tails from non-binding parts of the XG backbone are believed to be responsible for this repulsion. The cross-linking nature of XG is evident from the increases observed also in time-dependent adhesive force, seen also with e.g.

PDADMAC (Salmi et al. 2007). The saw-tooth pattern with multiple steps indicates presence of multiple contact bonds with different contour lengths.

As was the case with normal forces, polymer adsorption changes also the frictional forces between cellulosic surfaces, depending on added polymer concentration and properties, in analogy of normal force induced changes. Addition of polymers lowers the COF. At low polymer concentration, the frictional force increases with the applied load, before reaching the maximum usually at charge neutralization point. At high polymer concentration on the other hand, it becomes nonlinear of the applied load. The change between these regions is found to coincide with the leveling off of the polymer adsorption, i.e. reaching approximately monolayer coverage (Zauscher and Klingenberg, 2000c). The studied polymers have mainly been different polyelectrolytes, such as CMC or cationic polyacrylamides (C-PAMs), but also the effect of surfactants (Theander et al. 2005) and neutral polysaccharides, such the already mentioned XG (Stiernstedt 2006a) has been studied. The XG for example reduced COF while improving also the adhesive forces. In addition, the effect of LbL-modification on interaction forces of NFC or CNC have been studied (Salmi et al. 2009; Aulin et al. 2010b; Cranston et al. 2010), further elucidating the mechanisms and interplay of different layer in the LbL buildup.

3 EXPERIMENTAL

The main cellulosic and polymeric materials used in this work are presented in the Materials section. The main applied characterization techniques and some theory behind them are presented in the Methods section. Detailed descriptions of materials and methods are available in Papers I-VI.

3.1 Materials

3.1.1 Cellulose nanofibrils

All the cellulose fibril samples used were prepared in the Finnish Centre for Nanocellulosic Research from industrial, never-dried kraft pulps obtained from Finnish pulp mills. Unmodified hardwood (birch) pulp was the most used raw material for the NFC substrates (Papers II, III and V). It was washed into sodium form according to Swerin et al. (1990) The carbohydrate composition of the pulp was 73 % glucose and 25 % xylan and 1 % mannose. Also unmodified softwood (spruce) pulp with higher glucose (84 %) and respectively smaller hemicellulose proportion (~9% arabinoxylan, 6 % mannan 0.6 % arabinose and 0.2 % galactose) was used to compare the effects of different hemicellulose composition on interactions (Paper II). Also chemical pre-treatments, namely TEMPO-catalyzed selective oxidation (Saito et al. 2007) and cationization via covalent attachment of 2,3-epoxypropyltrimethylammonium chloride (EPTAC) (Aulin et al. 2010b) were applied prior to disintegration (Paper V). Fibrillation for all samples was performed via extensive fluidization (Microfluidics M-110 or M700, Microfluidics Intl. Corp, Newton, MA, USA.) or friction grinding (Masuko Sangyo Co Ltd, Japan). Detailed information describing the fibrillation procedures can be found from recent publication (Taipale et al. 2010). The disintegration method, charge density and zeta potential (ζ) values of the NFC samples used are collected in Table 1. In order to use the cellulose fibril suspension in interfacial studies, ultrathin films were prepared following the procedure developed previously (Ahola et al. 2008b) with minor modifications. PEI was used as cationic anchoring agent and for the chemically

treated fibrils the centrifugation step (to remove the large fibril aggregations) was not necessary.

Table 1. Preparation and properties of the cellulose fibrils.

Referred as	Kraft pulp	Chem. mod.	Disint. method	Passes	CD (μeq/g)	ζ -pot (mV)
HW/ref	birch	-	F	~30	-65 [a]	- 3
SW	spruce	-	F	~15	-50 [a]	nd
TEMPO	birch	TEMPO-oxidation	F	2	-800 [a]	-39
CAT	birch	cationatization	M	3	+1200 [b]	+35

F= fluidization, M= Masuko friction grinding, nd= not determined
[a] determined by conductometric titration (Katz et al. 1984)
[b] determined by polyelectrolyte titration (Wågberg et al. 1989)

3.1.2 Other cellulose materials

Cellulose filter paper (Whatman 40, Whatman Ltd. England) prepared from cotton linters and consisting of mainly pure cellulose I (Piantanida et al. 2005) was used to study the transformation of the cellulose crystalline structure by alkali treatment (Paper I). Regenerated cellulose spheres (Kanebo Co., Japan) were applied in colloidal probe atomic force microscopy (AFM)-studies (Paper IV and V). The spheres were precipitated from viscous process and are mostly amorphous containing 5-35 % crystalline cellulose II areas. They are described in detail elsewhere (Rutland et al. 1997). Regenerated, ultrathin trimethylsilylcellulose (TMSC) films were prepared by Langmuir-Schäefer (LS)-deposition in KSV Mini Through with horizontal dipping system (KSV Instruments LTD, Helsinki Finland). They have well defined surface chemistry and morphological structure, and they were used as a reference for NFC ultrathin films (Paper VI). More details of the technique and properties can be found from Tammelin et al. (2006).

3.1.3 Additives

In Table 2, the abbreviations, preparation method and basic properties of the different additives used in this study are briefly described. The different polyelectrolytes used in papermaking were also studied in Paper V. They were used as

received and their properties are also included in Table 2. Chemical structures of selected hemicelluloses and polymers are introduced in Figure 6.

Table 2. Preparation and basic properties of the polysaccharides. (Papers II-V)

Name	Abbr.	Supplier (product no)	Solution preparation	M_w (kDa)	charge (n, +, -)
Xyloglucan	XG	Megazyme	dissolving in 80 ºC H_2O, mixing 3 h (Parikka et al. 2010)	190[a] 470[b]	n
Guar gum	GG	Sigma-Aldrich (G4129)	magnetic stirring overnight, centrifugation (10 kG, 20 ºC	2100[a] 2000[b]	n
Locust bean gum	LBG	Sigma-Aldrich (G0753)	30 min) to remove undissolved fractions	1900[a] 1060[b]	n
GG degraded	GG_{deg}		acid hydrolysis (Cheng et al., 2002) , repeated 3x	250[a] 460[b]	n
Spruce galactogluco mannan	GGM	ÅA	filtration (Xu et al. 2007)	60[b] 20[c]	n
Birch xylan	XYL	Fluka (95588)	-	9[a]	-
Oat spelt arabinoxylan	OAX	Sigma-Aldrich (X0627)	filtration (Mikkonen et al., 2009)	58[c]	n
Rye arabinoxylan	RAX	Megazyme	filtration (Pitkänen et al., 2009)	290[b] 250[c]	n
Wheat arabinoxylan	WAX	Megazyme	filtration (Virkki et al., 2008, Pitkänen et al., 2009)	340[b] 320[c]	n
WAX degraded	WAX_e	Megazyme	enzymatic degradation	90[b] 80[c]	n
Chitosan, low M_w	CHI	Sigma-Aldrich (448869)	dissolving in 1 % acetic acid, filtration	230[a]	+
Chitosan, medium M_w		Fluka		400[c]	+
Carboxymethylcellulose	CMC	CP Kelco (BW)	-	370[a]	-
Methyl cellulose	MC	Sigma-Aldrich (M7140)	dissolving in cold water	20[a]	n

Name	Abbr.	Supplier	Solution preparation	M_w (kDa)	Charge
Polyethylen eimine	PEI	Polysciences	-	~50[d]	+(15.5)[e]
Polydimethyl diammoniu mchloride	PDAD MAC	Sigma-Aldrich	-	<14[d]	+(6.2)[e]
Cationic starch	CS	Ciba	gelationazation at elevated pressure	200[a]	+(0.8)[e]

n= neutral, += cationic and -= anionic charge

[a] determined by intrinsic viscosity according to Mark-Houwink equation (3.6)

[b] determined by HPSEC in water and [c] determined by HPSEC in DMSO

[d] manufacturer's specification

[e] charge density, determined by polyelectrolyte titration

a) GGM

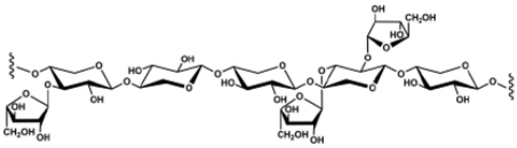

b) WAX

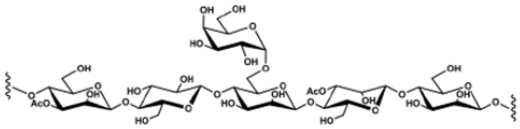

c) XG

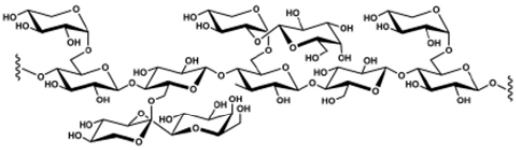

d) PEI

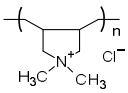

e) cat NFC

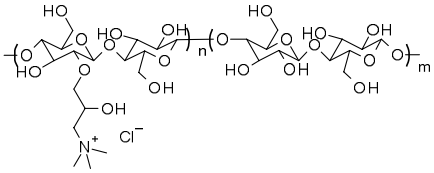

f) CS

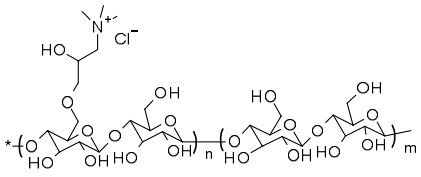

Figure 6. Selected examples for schematic polymer structures used in this work.

3.2 Methods

3.2.1 Raman spectroscopy

Raman spectroscopy has been widely used to characterize chemical structure of cellulosic samples, including pure cellulose fibrils extracted from algae and various wood fibres. First it was a complementary method to infrared spectroscopy (IR) (Blackwell et al. 1970, Blackwell and Marchessault, 1971). Later it became an established technique of its own (Agarwal, 2008), especially due to the recent improvements in the instrumentation of Raman microspectroscopy. It has been used to characterize crystallinity of cellulose (Schenzel 2001), the residual lignin distribution (Halttunen et al. 2001) and micromechanical deformation (Kong and Eichhorn, 2005). Its main advantage is the insensitivity towards water. The technique is based on detected so called Raman scattered photons, which have an increased or decreased scattering wavelength to elastically scattered photons. (Fig. 7) The relative scattering intensities can be attributed to the molecular vibrations. In this work the Raman spectra was acquired with confocal Raman configuration (WITec alpha 300R, WITec GmbH, Ulm, Germany) in ambient conditions (c.a. 25 ºC). A frequency doubled Nd: YAG green laser (wavelength 532.14 nm, power ~30 mW) for the photon excitation and Nikon 100X (NA=0.90) air objective for collection of the Raman scattered electrons from the sample surface. The optical fibre used to collecting the scattered photons had a diameter of 50 µm and grating of the spectrogram was 600 grooves/mm. The excitation light was polarized horizontally in x-direction. As detector, a sensitive electron multiplying (EM) CDD camera (Andor Newton DU970-BV, Andor Technology Belfast, U.K) was used. Integration times varied from 0.1 s to 2s, depending on how much laser intensity the sample could take. In the case of low integration time (easily burning materials) spectra were averaged over several hundred individual spectra to improve their quality. The spectra were only baseline corrected after measurements.

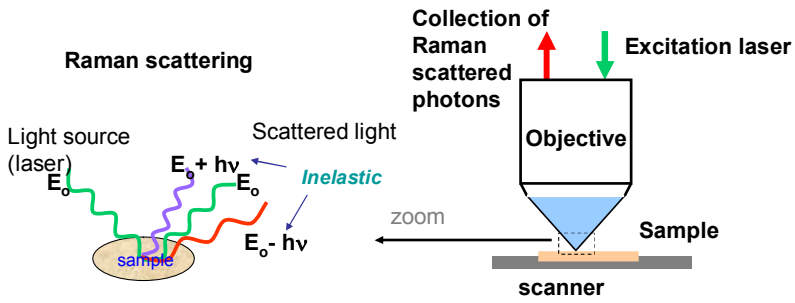

Figure 7. Principle and configuration of confocal Raman-microspectroscopy.

3.2.2 AFM-imaging

Atomic force microscopy (AFM) is one of the most popular techniques in surface science. Since its invention 25 years ago (Binnig et al. 1986), it has been one of the most influential factors in the rapid development of nanoscience- and technology. It is relatively inexpensive and easy to use, and does not require extensive sample preparation procedures. Nearly everything is possible to image, either in air or in liquid. In addition, it produces relatively fast high precision information up to atomic scale resolution. The method principle is relatively simple, and in fact has nothing to do with microscopy in the traditional sense. Imaging is done via a sharp tip (radius of curvature 5-10 nm), which is brought into either contact or oscillated closely above sample surface, as illustrated in Figure 8. In contact mode, a selected set point deflection is maintained constant via feedback loop and piezoelectric scanner, and the image is built up from the movement of the scanner. Laser directed at the end of the cantilever is reflected via a mirror to a quadruple photodetector, recording the movement for recreating precise height-images of topographical features of sample surface. Although most high precision images reaching atomistic resolution have been obtained using contact mode, the rather high force excreted on the sample surface can damage especially soft samples. An alternative is to oscillate the tip in close vicinity of the surface, known as tapping or alternating current (AC)-imaging. In this mode, the tip is oscillated at its resonance frequency, and it actually touches the sample surface only briefly during the oscillation cycle, making it more suitable for soft polymeric samples. The intensity of the oscillation is controlled with the ratio between set-point and free amplitude (known as damping ratio). The lower the damping ratio,

the “harder” is the force applied to the sample during the brief contact. In addition, material properties such as hardness and softness can be compared by recording the phase-shift between set and detected oscillation. AFM instruments record simultaneously these so called phase contrast images (Zhong et al. 1993; Magonov et al. 1997), which for especially rough cellulose fibre samples have been found more informative than height images (Niemi and Paulapuro, 2002).

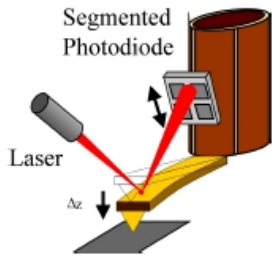

Figure 8. Simple principle of AFM-imaging.

Extensive review articles about AFM in surface characterization of deformable materials have been written (Magonov, 2000; Hansma et al., 1997). Quite early on, AFM has also been applied in cellulosic research (Hanley et al. 1992; Kuutti et al. 1995; Baker et al. 1997; Gustafsson et al. 2002; Koljonen et al. 2003). Also new cellulosic nanomaterials have been extensively characterized using AFM (e.g. Pääkkö et al. 2007; Kontturi et al. 2008; Ahola et al. 2008a-b; Li and Renneckar 2009). In this work, AFM-imaging was the main technique used to characterize the morphology of the cellulose surfaces. Two instruments were used in this work; a Multimode IIIa (Digital Instruments Inc. Santa Barbara, CA) and WiTEC Alpha 300R in AFM configuration (WiTEC GmbH, Ulm, Germany). Tapping or corresponding AC (alternating current) imaging modes were used. In the latter instrument, the digital pulsed force mode (DPFM) was also tested to compare the adhesive properties of cellulose fibril substrates. More information for this technique can be found from previous publication (Schmidt et al., 2005). Details for the settings and cantilevers used can be found from the attached articles (Papers I-VI).

3.2.3 Quartz crystal microbalance with dissipation (QCM-D)

QCM-D was the main technique to characterize the adsorbed amounts. It has become popular during the past decade in adsorption studies because it is a fast and reliable technique applicable to almost any thin surface. The principles are described more in detail in by (Rodahl et al. 1995). The set-up in this work is illustrated in Figure 9.

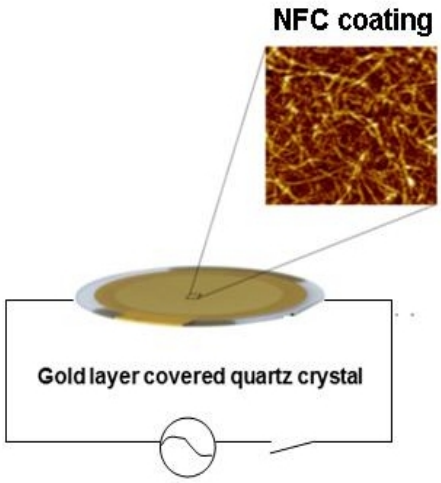

Figure 9. QCM-D crystal operating principle and modification by spincoating onto NFC substrate.

The main principle is that the change in frequency and dissipation are recorded at the fundamental resonance frequency (f) and its 13 overtones. The adsorbed mass per unit surface is proportional to the decrease in the resonance frequency according to Sauerbrey equation (1).

$$\Delta m = -\frac{C\Delta f}{n}\ , \qquad (3.1)$$

where C is the device sensitivity constant and n is the overtone number.

The simultaneously measured dissipation (D) factor gives information of the frictional losses due to the viscoelastic properties of the adsorbed layer. The

dissipation energy increases as a function of adsorption if viscoelastic layers are formed when adsorbing the polysaccharide on the cellulose model film. The dissipation factor is defined in Equation 3.2

$$D = \frac{E_{diss}}{2\pi E_{stored}} \quad , \tag{3.2}$$

where E_{diss} is the dissipated energy during one oscillation and E stored is the total energy stored in the oscillation system. More information for the calculation methods behind dissipation can be found from (Höök et al. 1998).

The QCM-D measurements were performed with the E4 instrument (Q-Sense AB, Västra Frölunda, Sweden) with controlled flow. The samples diluted at 100 mg/l were pumped at constant rate of 0.1 ml/min through the measurement chambers. Adsorption was started by adding the solutions after a stable baseline was acquired with buffer solution. Results are shown and calculated from the 3rd overtones. All the experiments were at least duplicated on separate days and using freshly prepared solutions to get representative results.

For swollen gel like films the Sauerbrey equation has been found to underestimate the adsorbed amount, as it is most suitable for rigid layers. Another model, based on calculations by Johannsmann et al. (1992) was used:

$$\hat{m}^* = m^0\left(1 + \hat{J}(f)\frac{\rho f^2 d^2}{3}\right) \tag{3.3}$$

where $\hat{m}^*$ is the equivalent mass, ρ is the density of the fluid, d is the thickness of the film and $\hat{J}(f)$ the complex shear assumed independent of the frequency and m^0 is the sensed mass. The latter was obtained from the intercept of plotting the equivalent mass as the function of frequency squared. This equation gives more accurate estimate of the true sensed mass for viscous films. The adsorption curves were also analyzed using Voigt-based model provided by Q-Tools data analysis program (Voinova and et

al. 1999). Similar fitting parameters as used in a recent work (Tammelin et al., 2009) were applied.

3.2.4 Colloidal probe microscopy (CPM)

The AFM instrument was also used in direct surface force measurements by applying the colloidal probe microscopy (CPM)-technique (Ducker and Senden, 1992). The principle of the technique is introduced in Figure 10. CPM is applied in the contact mode of AFM, and usually in liquid. Using the accurate piezo driven scanner, the surface and probe are brought into contact. The laser is again used to monitor the position of the cantilever. From the deflection of the cantilever recorded by the photodiode, surface interactions can be monitored, as shown in Figure 10.

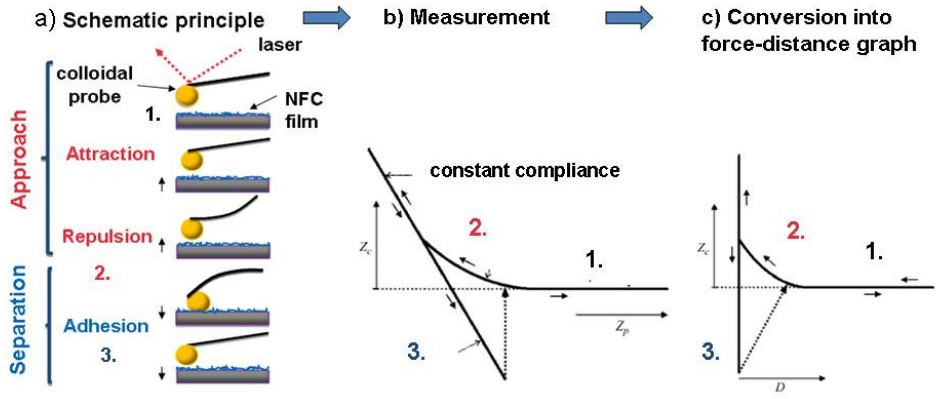

Figure 10. Illustration of the schematic principle of probe movement and illustration of raw data and conversion into force-distance graph of idealized material using the CPM technique. (Combined from illustrations by T. Nypelö and Butt et al. 2005).

When the cantilever is well above the sample and surface forces are not yet influencing, the cantilever remains at reference position. As the sample surface approaches, depending on the nature of the interactions the cantilever can either bend upwards (repulsion) or downwards (attraction). Eventually the spring constant of the cantilever is exceeded, and the sample and probe snap into contact and move together (denoted constant compliance region). After reaching the predefined distance of piezo extension, the cycle is reversed. When the probe and substrate are separated gradually,

they remain in contact until they snap apart. Usually there is a slight hysteresis between approach and retraction. Possible adhesive forces are recorder at close to zero contact force part, as shown in Figure 10, exceeding the forces on approach. Finally the probe is returned to the starting position. If the cantilever spring constant k is accurately know, simple Hooke's law

$$F = k\Delta z \tag{3.4}$$

forms the basis for quantification of raw data of volts recorded in photodetector (vertical) displacement into forces. The constant compliance region is utilized in conversion of the piezo movement into distance units; a so-called sensitivity value is determined by the slope of the linear region to estimate the zero contact position. Resulting force should ideally resemble that of Figure 10c. However, with soft, deformable cellulose surfaces this is usually not as straightforward, and usually the sensitivity value has to be determined and compared using relatively hard substrate for the cellulose sphere. In this work, the spring constants of commercial tipless AFM-probes were determined separately prior to attachment of the cellulose probe (Hutter and Bechhöfer 1993; Sader et al. 1999). Forces were divided by the radius of the sphere to facilitate comparison between measurements, and in the case when two spheres were used; they were normalized taking the geometry into account. When appropriate, the forces were fitted to the DLVO-theory to estimate the surface potentials. Hamaker-constant was used from previous estimations by ellipsometry (Bergström et al. 1999) and the nonlinear approximation according to algorithms for constant potential (Devereux and de Bruyn, 1963) was used. More detailed descriptions of basics and theory behind this technique can be found from literature (e.g. Butt et al. 2005; Butt et al. 2007; Ralston et al. 2005).

3.2.5 CPM friction measurements

Friction measurements were performed by the AFM in CPM configuration by moving the substrate laterally in controlled manner. Gradually increasing the applied load, so-called friction loops can be plotted as the function of lateral movement and lateral detected voltage displacement from the twisting of the AFM cantilever. The

difference in the lateral voltage response in derived from the difference in the advancing and retracting traces divided by two. Additional parameters needed for friction force calculation include lateral photodetector sensitivity (δ), height of probe and half of cantilever (effective height h) and the torsional spring constant (k_Φ) yielding:

$$F_{friction} = \frac{\Delta V_l}{2} \frac{k_\phi}{\delta} \frac{1}{h} \tag{3.5}$$

Determined friction force is usually shown as the function of applied load, which enables the extraction of friction co-efficient as the slope of fitted line. It showing lateral movement as the function of lateral photodetector displacement. The difference between the two traces divided by two gives the friction voltage. Although friction measurements itself are relatively straightforward to perform with AFM, the accurate calibration of torsional spring constant can be laborious. It is however necessary to perform in order to get reliable and reproducible results. In this work, calibration according to thermal vibration was used, described in more detail by (Pettersson et al., 2007). In this work, friction forces between two cellulose spheres were measured first with increasing and then decreasing loads, with a relative movement of 2 µm and scan rate of 1 Hz.

3.2.6 Additional techniques

Surface Plasmon Resonance (SPR) was used in combination with QCM-D in order to compare the dry amount of adsorbed polysaccharide mass to the aqueous mass detected by QCM-D. Both the NFC substrate and polysaccharide solution preparations were kept as similar as possible to the QCM-D measurements. A Biacore 1000 instrument (GE Healthcare, Uppsala, Sweden) with flow rate of 5 µl/min and injection volume of 300 µl was used in this study. More information about theory behind this technique is available in e.g. Green et al. (2000). In Papers II and III the parameters and equations used for calculating the dry mass are presented.

Intrinsic viscosity measurements were used to get an estimation of the M_w of the commercial polysaccharides. The Mark-Houwink equation:

$$[\eta] = KM^{\alpha} \tag{3.6}$$

where $[\eta]$ is the intrinsic viscosity, M the molecular weight and K and α the Mark-Houwink parameters used in estimations. The intrinsic viscosity was measured by capillary viscometer (Schott Geräte AVS 350, Hofheim, Germany) at 25 ±0.05 °C. The parameters K and α were taken from the literature values. More information about these measurements can be found in e.g. Cheng et al. (2002) and Picout and Ross-Murphy (2007).

High-performance Size Exclusion Chromatography (HPSEC) was used to characterize the M_w properties of selected polysaccharides in solutions. Measurements were performed as described in Pitkänen et al. (2009) in in DMSO eluent containing 0.01 M LiBr and in aqueous 0.1 M $NaNO_3$.

Cryogenic Transmission Electron Microscopy (cryo-TEM)-imaging was performed by to compare the morphology to AFM-images performed from dried fibrils. The measurement details are more thoroughly explained in Paper V.

4 RESULTS AND DISCUSSION

Combining different analytic techniques is one way to gain more information from heterogeneous cellulosic fibre structures. In the following, different cellulosic materials are characterized by combining different interfacial high-precision techniques, with the main focus in characterizing the interactions of NFC fibrils with adsorption of various polymers. Necessary background studies with pure cellulosic materials were also performed to facilitate the comparison.

4.1 Combined characterization of structure and morphology

There are still many questions related to interpretation of structure-chemistry properties of cellulosic fibres in both native wood and industrially processed fibrous products such as pulp and paper, not to mention in the new nanostructured materials. Before adsorption studies, basic characterizations of the cellulose structure and morphology were determined. The study was started with pure cellulose (model system), to which the cellulose nanofibrils used in further adsorption studies were compared.

4.1.1 Pure cellulose (filter paper)

First, the cellulose structure-morphology relation was studied by combining chemical characterization (Raman microspectroscopy) with high resolution morphological characterization (AFM-imaging). Detailed results are presented in Paper I. A simple system (filter paper) was chosen to get representative cellulose spectra from almost pure cellulose. Another reason was to ease the comparison to fundamental studies done on algae cellulose (Atalla 1976, Atalla 1983, Okano and Sarko 1985). Figure 11 shows the alkali-induced changes in the cellulose polymorphous structure detected by Raman-spectroscopy. The lattice change from cellulose I to cellulose II was confirmed from considerable relative decrease in band

intensity at the positions at 380, 519, 1120 and 1479 cm^{-1}. For example the change in the relative band height at 1120 has been associated to the mode of the glycosidic and ring-related COC linkage (Jähn et al. 2002). The simultaneous intensity increase observed at 896 cm^{-1} in turn has been associated with the bending mode of HCC and HCO at the C6 carbon of anhydroglucopyranose units of cellulose (Schenzel & Fischer 2001). The intermediate samples (10- and 15-% NaOH treated showed characteristic features from both lattice structures, but the 25 % NaOH treated was transformed into cellulose II. This was in good accordance with previous studies including cotton cellulose (e.g. Fengel et al 1995), where the transition occurred between 12-15 % NaOH-treatment.

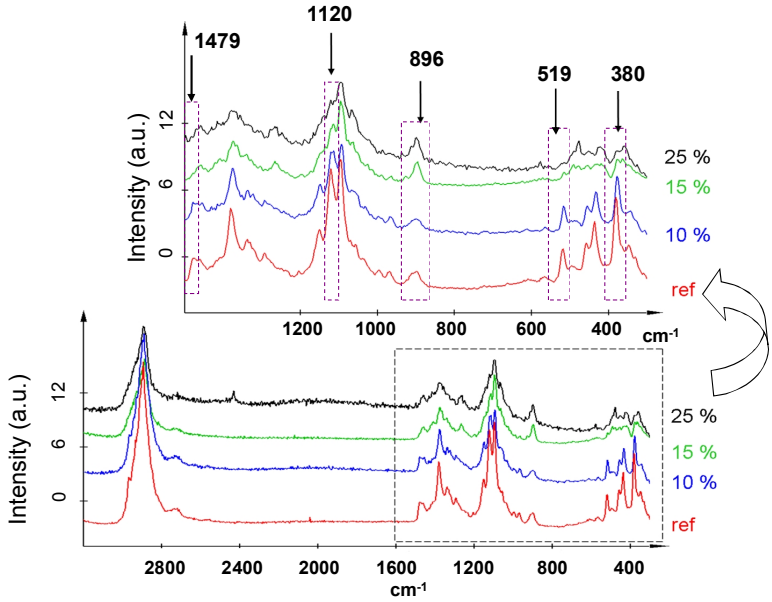

Figure 11. Raman-spectra of reference and samples treated with NaOH solution of varying concentration (10-25 %) (Paper I). The dashed rectangle indicates the magnification shown in the upper spectra, highlighting the main observed changes.

The AFM phase images (Fig. 12) recorded from the close vicinity of the Raman spectral collection positions revealed characteristic differences in the surface morphology. The reference and 10 % NaOH-treated surfaces preserved the microfibrillar fine structure, while the 15- and 25 % NaOH surfaces had granular and more swollen structures. Also the corresponding root mean square roughness (RMS)-values from height images were clearly higher for reference and 10 % NaOH sample

(180±60 nm and 130±50 nm, respectively) than for 15- and 25 % NaOH-treated samples (80±30 nm and 90±60 nm). This is in accordance with the Raman spectra where the transition between cellulose I and II lattices was found to occur between 10 and 15 % NaOH-treatment.

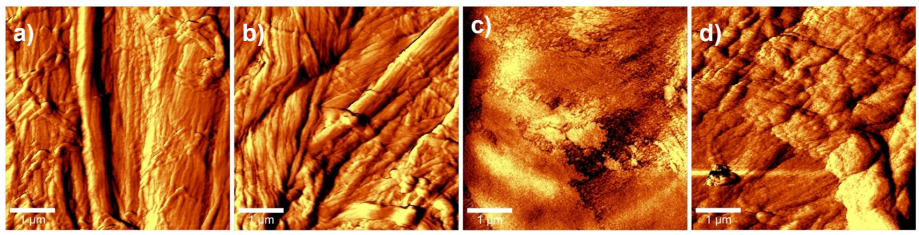

Figure 12. AFM-phase contrast images (5x5 µm²) for a) reference and b) 10 % c) 15 % d) 25 % NaOH treated samples (paper I). The z-scales a-d are 26°, 18°, 30° and 15°, respectively.

Although mercerization has been extensively studied, no directly comparable AFM-images of mercerized cotton fibres have been found. However, on a wider scale both optical microscopy- (Stana-Kleinscheck et al. 1999) and environmental scanning electron microscopy (ESEM) –images (Jähn et al. 2002) illustrate loosening of the fibre structure as the function of alkali treatment. Unbleached sulphate pulp fibres, which had been alkali-treated for delignification and imaged by AFM were found to have also more granules and smooth regions compared to reference fibres (Gustafsson 2004). Transmission electron microscopy (TEM)-imaging has revealed that alkali treatment of dilute fine structured, individual microfibril dispersions converts them into dispersed precipitates attached on remaining fibril bundles (Dinand et al. 2002). The change was attributed to the swelling of metastable extended chain crystals of cellulose microfibrils, which causes the cellulose chains to relax and adopt a more coiled conformation. The crystallinity of cellulose is also reduced by the alkali treatment (Fengel et al. 1995; Schenzel and Fischer 2005). In this work a decrease in crystallinity was also seen from the less resolved and broader Raman-bands for 15 % and especially 25 % NaOH-treated sample (Fig. 11). The Raman spectra obtained for cellulose I and II could be utilized in further work analysing cellulose substrates used in adsorption studies and was used also in the characterization of native and unmodified cellulose fibrils.

4.1.2 Nanofibrillated cellulose

The different nanofibrillated cellulose grades were compared to estimate if the disintegration and modifications had any effect on the lattice structure and crystallinity. The rather low spatial resolution (in micrometer order) of Raman spectroscopy in air however prevented the analysis of ultrathin nanocellulose films used in adsorption studies. Free-standing films were therefore prepared for spectroscopy. The optical images of the films are presented together with the spectra in Figure 13 (unpublished results). The unmodified NFC (reference) was used in the single layer adsorption studies (Papers II, III and VI) and the chemically modified NFC grades in multilayer build-up comparison (Paper V). The characteristic Raman bands (1095 and at 2895 cm^{-1}) for cellulose I structure can be seen for all NFC grades. A conversion to cellulose II would decrease the relative intensity of the band at 1120 cm^{-1} compared to 1095 cm^{-1}. The lower degree of crystallinity leads to broader and less defined peaks, which was not observed compared to references spectra obtained from cotton cellulose (Fig. 11).

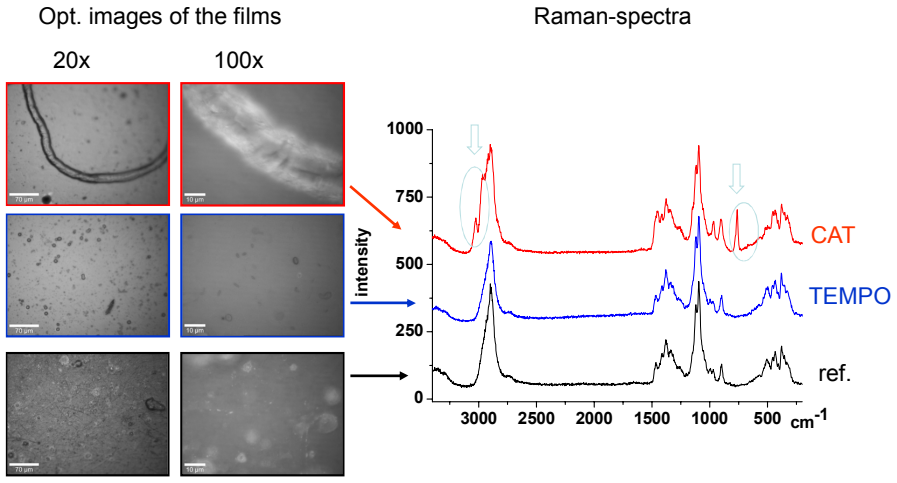

Figure 13. Optical microscope images of free-standing NFC films and the corresponding Raman-spectra (unpublished results).

Selective oxidation via TEMPO-catalyst or addition of cationic group to cellulose fibrils therefore did not alter the native cellulose I crystal lattice. This was also observed in a previous study with XRD for enzymatically modified and

carboxymethylated NFC samples (Aulin et al. 2009). The oxidation did not greatly affect the relative band positions. Li and Renneckar (2011) recently studied the effect of sonification on the TEMPO-oxidized structure of cellulose by also Raman spectroscopy, and their results were in good accordance with this work. The cationic modification also did not alter the cellulose spectra. However, it introduced the characteristic peaks from the covalently attached trimethyl ammonium group (Fig. 13). These are most notably seen at positions 761 (symmetric stretching of the $(CH_3)_3$-N^+), and 3030 (CH_3 antisymmetric stretching) (Phillips et al. 1999, Pigorsch 2009). The disintegrated industrial pulps used as raw material for NFC production also contained the similar percentage of hemicelluloses as the starting raw material (Ahola et al. 2008b, Paper II), mainly xylan. Due to the similar backbone of (1→4)-linked β-D-backbone structures of glucose and xylopyranose, the characteristic peaks were overlapping with cellulose. Nevertheless, Raman could be used to verify that cellulose maintains both the cellulose I lattice structure and crystallinity is not markedly reduced in the modifications.

AFM-imaging of the ultrathin NFC substrates was frequently performed to characterize the morphology both before and after adsorption studies. As an example, the AFM-images of differently prepared ultrathin NFC substrate are shown in Figure 14. The left image (Fig. 14a) is a height image of the spincoated cellulose substrate in air. The height profile from the middle of the image shows that nanosized fibrils form a network with uniform coverage. Both appearance and fibril dimension (similar roughness root mean square RMS-values) correspond to similarly prepared surfaces by Ahola from dissolving sulphite pulp (Ahola et al. 2008b). Figure 14b shows the same NFC fibril substrate imaged in water. The fibril network has a more swollen structure compared to imaging in air, clearly visible from the height profile. This result contradicts to recent findings of chemically modified NFC imaging AFM-imaging by Olszewska et al. (2011), who recorded smaller dimensions of never-dried cationized NFC fibrils produced from sulphite pulp imaged in water. One reason for the thicker appearance could be attachment of the fibril network via electrostatic adsorption of branched PEI, allowing water to penetrate between the voids in fibrillar structure, creating the thicker appearance of fibril bundles. Another possibility is that

related somehow drying and rewetting the fibril network. It is certain that more experiments should be performed to verify the results.

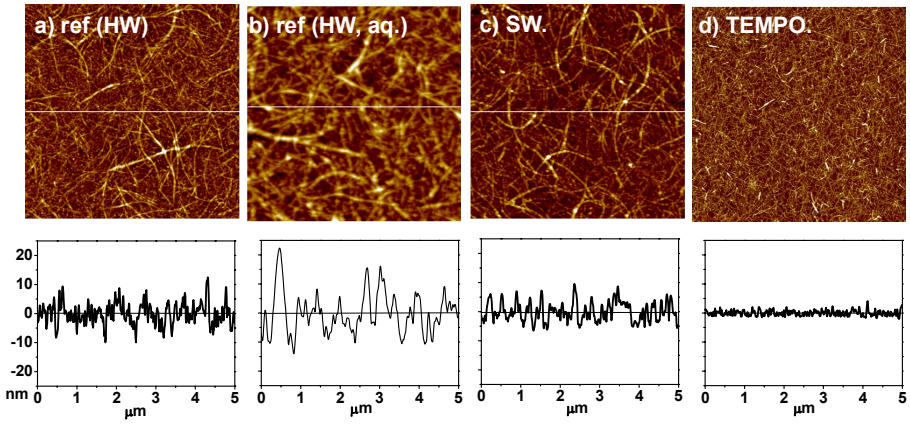

Figure 14. AFM-images of the NFC films used as substrates (5x5 µm). a) unmodified hardwood in air b) similar film imaged in aqueous conditions (after drying) c) unmodified softwood d) TEMPO-oxidized hardwood.

However, to compare, individual TEMPO-oxidized (dried) fibrils were also imaged in water (Fig. 15). The dimensions of these were not as drastically changed, as seen from the comparison to the dried state. The PEI-molecules used to anchor the fibrils are visible in the liquid imaging as swollen granules, but they are small enough to avoid exaggeration of the fibril dimensions. In water, the fibrils are not as tightly attached to the surface, seen from the less straight conformation. In addition, regions of different thickness can be observed in larger fibrils, which could be due to weaker attachment resulting in twisting of the fibrils or could denote the changes between amorphous and crystalline regions of cellulose nanofibers. Again, more measurements are needed to verify these observations.

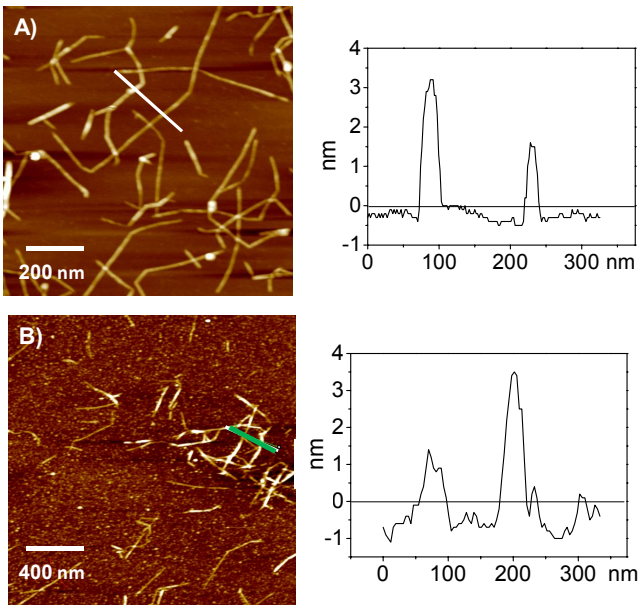

Figure 15. Comparison of individual TEMPO fibrils a) deposited on mica and imaged in air and b) deposited on PEI-coated silica surface and imaged in water. The cross-sections taken from the place indicated by lines are shown in right. (unpublished results).

4.2 Physisorption of polysaccharides on cellulose

The adsorption properties of numerous different polysaccharides known to have interactions with cellulose were studied. The purpose behind this was to find the most suitable ones for the modifications to improve the NFC properties without destroying the fibrillar ultrastructure. The adsorption of both extensively structurally characterized hemicelluloses isolated from currently discarded by-products (Paper II) and commercial polysaccharides used as such was compared (Paper III). In addition, nanofibril substrates prepared from hardwood and softwood were selectively compared (Paper II).

4.2.1 Comparison of structurally characterized hemicelluloses

The established non-ionic interactions between hemicelluloses and cellulose were studied using NFC ultrathin film substrates. Hemicelluloses chosen have potential to be isolated from currently discarded by-products of from either mechanical pulping or agricultural processes. (Willför et al. 2008; Hansen and Plackett, 2008; Ebringerová, 2005). The association of several structurally different hemicelluloses with cellulosic nanofibril substrates was compared. Adsorption was studied in the aqueous state by combining QCM-D and SPR for adsorption studies and AFM for surface morphology characterization. Figures 16 and 17 illustrate the hemicellulose attachment on the NFC substrate as the function of time. Estimations of the aqueous adsorbed mass (Δm) and changes in energy dissipation (ΔD) upon hemicellulose adsorption are shown in a- and b-parts, respectively. As previous studies has established that there are strong interactions between cellulose and xyloglucan (Vincken et al. 1995; Zhou and Rutland 2007), including NFC with dispersing effect (Ahola et al. 2008a), it was used as an internal reference to comparison with other polysaccharides. All hemicellulose samples adsorbed almost irreversibly on unmodified NFC substrates. Spruce galactoglucomannan (GGM) had lower increase in adsorbed mass compared to XG (Fig. 16). However, the corresponding ΔD-values were also lower with GGM compared to XG, indicating a less viscoelastic structure. The cereal arabinoxylans on the other hand were more divergent (Fig. 17). All cereal AXs had a lower increase in adsorbed mass compared to XG. Rye-and wheat AX (RAX and WAX, respectively) increased the adsorbed mass more than GGM, whereas oat spelt arabinoxylan (OAX) had lower Δm-value. Enzymatically hydrolyzed WAXe showed weak attachment and barely adsorbed. The simultaneously detected ΔD-values (Fig. 17b), followed the same relative order as the detected increase in mass. Compared to XG (and GGM), all native AX had higher ΔD-values at comparable adsorbed mass values.

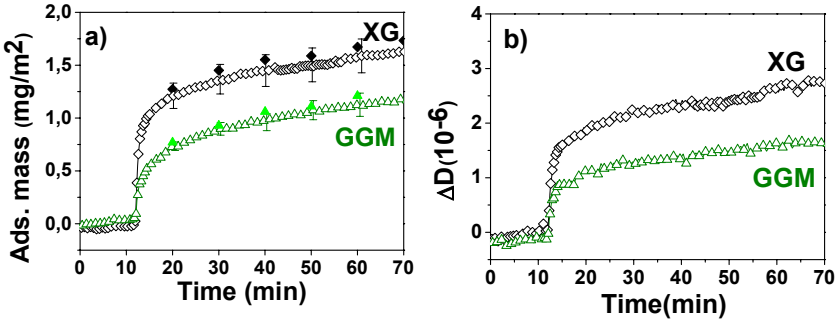

Figure 16. Comparison a) of sensed mass values and b) corresponding energy dissipation values of XG (◇) and GGM (△) adsorption on hardwood NFC film as the function of time (Paper II).

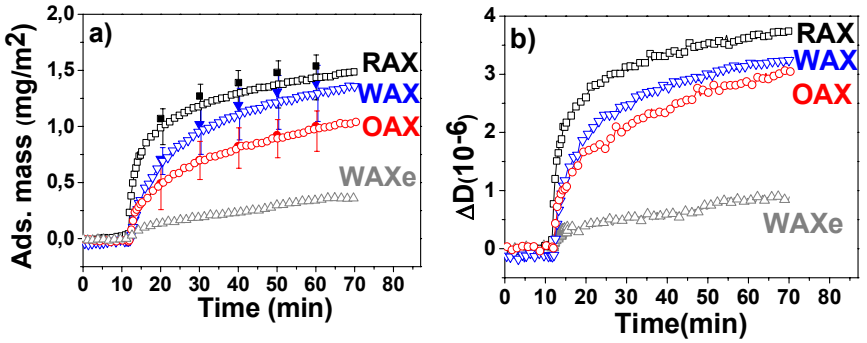

Figure 17. Comparison of a) sensed mass values and b) corresponding energy dissipation values (b) of different and modified cereal arabinoxylan adsorption on hardwood NFC film as the function of time. The cereal AX compared were RAX (□), WAX (▽), OAX (○) and enzymatically modified WAXe (△) (Paper II).

GGM adsorbed in a more rigid conformation, which corresponds well to previous findings by NMR-analysis (Newman and Hemmingson, 1998; Whitney et al. 1998). Of course, the clearly lower M_w of GGM (~20 kDa) compared to XG (~300-470 kDa) could have an effect. Attachment of polysaccharides to various cellulose surfaces has been noticed to increase as the function of M_w (Suurnäkki et al. 2003; Hayashi et al.1994; Vincken et al. 1995; Kabel et al. 2007). Nevertheless, the extent of the side-group substitution of galactomannans affects the adsorbed amount more than just M_w, also observed by Saarinen et al. (2009) when also comparing the structure-M_w relation of different polyelectrolytes adsorbing on cellulose. The ionic strength and pH have a marked effect on the cellulose fibrillar substrate. At higher

pH, dissociation of the adjoined uronic (4-O-methyl-α D-glucuronic) acid residues in the hemicelluloses still present in the NFC substrate promotes swelling of the film via increased electrostatic repulsion between charged cellulose segments (Lindström, 1989; Donnan and Harris; 1911, Katz et al. 1984). Even with planar confined nanofibril substrates, this causes swelling of the fibril substrate yielding to more extended conformation (Ahola et al. 2008b). This most likely affects the available surface area and consequently adsorption sites.

Cereal AX have higher M_w and a more substituted xylose backbone compared to hardwood xylans (Sjöström, 1993; Sun et al. 2004), which is why the highly substituted cereal AXs do not extensively self-associate in solution. The reason for higher adsorbed amounts when M_w increases is the decrease in solubility, i.e. entropical reasons. Also, only one part of the polymer needs to attach in order to drag the rest of the extended molecule with it (Kabel et al. 2007). The markedly lower attachment of the enzymatically modified WAX_e, which still had high M_w of ~ 90 kDa, on NFC, supports this. The side-groups restrict the enzymatic hydrolysis by xylanase more compared to less substituted regions, which are the ones believed to be involved in binding to cellulose. RAX and WAX have very similar arabinose to xylose ratio (Paper II) but RAX has somewhat stiffer and more extended conformation in aqueous solution compared to WAX (Pitkänen et al. 2009). This could explain that RAX adsorbed in a slightly more extended conformation compared to WAX (Fig. 17a and b). The differences between RAX and WAX were nevertheless minor.

4.2.2 Effect of chemical composition of the NFC substrate

In the previous, the role of the hemicellulose structure was found to influence the adsorption. As the NFC contains more hemicelluloses compared to regenerated cellulose model films, the effect of the fibril raw material, i.e. carbohydrate composition was studied. First, an attempt to remove the hemicelluloses enzymatically from the NFC substrate was attempted, but this was found to be ineffective. As an alternative way to study the effect of in-situ hemicelluloses, NFC prepared similarly from soft wood kraft pulp was compared to the hardwood sample

with selected hemicelluloses. Analysis of the NFC gel showed similar carbohydrate composition to those measured from pulps used as raw material. According to the chemical analysis, hardwood NFC contains 26% of xylan and < 2% glucomannan, and softwood NFC contains 10% arabinoxylan and 8% galactoglucomannan. The results were similar to previously reported hardwood and softwood kraft pulp inner layer compositions (Dahlman et al. 2003). The change in energy dissipation is plotted against the change in frequency (Fig 18a). The slope of the ΔD vs. Δf plot correlates with the rigidity of the adsorbed layer. The steeper the slope, the more viscoelastic the layer is. GGM had a similar low ΔD vs. Δf slopes with both hardwood and softwood nanofibrils, indicating good affinity to both cellulose substrates. Experiments with different industrial pulps have also shown that GGM sorption to pulp is not very dependent on the pulp type (Hannuksela et al 2003). With WAX, the layers were more loose and viscoelastic regardless of the nanofibril composition. However, the kinetics of the adsorption (adsorbed amount roughly estimated by Eq. (3.1) during the first minutes of experiment) revealed unusually fast interaction between WAX and softwood NFC (Fig 18b).

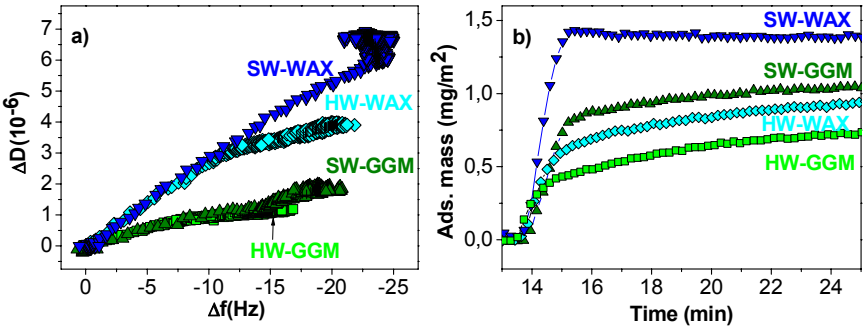

Figure 18. Comparison of hemicellulose adsorption on nanofibril cellulose films prepared either from hard- (HW) or softwood (SW) NFC. a) The change in dissipation (D) is shown as the function of the change in frequency measured at the third overtone of the 5 MHz fundamental frequency. b) The adsorbed amount (Eq.3.1) shown as the function of time.

To verify that the observed slight changes were not due to the different morphology of NFC substrates, AFM imaging was again performed both before and after adsorption studies. Examples of appearance of hardwood and softwood NFC substrates (imaged in air) before adsorption studies is illustrated in Figure 14. The

similarities between fibril surfaces are obvious and the RMS roughness values were also almost identical, about 3.9 nm. The fibrils might have been slightly more aggregated in the softwood NFC films, but the fractionation used in preparation of the NFC substrates ensured the comparability of the NFC substrates. Nevertheless, morphology is not the main contributing factor for the differences in the hemicellulose adsorption between hardwood and softwood NFC. The reason is in the differences in the initial carbohydrate composition of the fibrils. The detailed chemical analysis of the composition of individual nanosized fibrils is challenging or almost impossible to perform with traditional analysis techniques. Therefore this comparison of hardwood and softwood in high-precision interfacial studies can also be considered to indicate how much does the NFC raw material (pulp in this case) affects to the NFC properties. Past studies on pulp fibres have speculated that under mechanical shear, xylans dissolve and redistribute on the opened fibre structure (Roberts and El-Karim, 1983). Some alkali-and DMSO-soluble aggregates were also visualized after beating suspected to originate from xylan (Mora et al. 1986). For softwood kraft fibres enrichment of glucuronoxylan has also been located on the outer fibre wall (Köhnke et al. 2010). For mechanically produced NFCs, these aggregates have not been directly observed, on the contrary, high hemicellulose content has been found to improve fibrillation (Iwamoto et al. 2008). Mechanical treatments of the fibre suspensions have revealed that more organic substances are released from hardwood fibres compared to softwood fibres (Sjöström et al. 2000). In the same study, re-adsorption was evident only at high salt concentrations.

4.2.3 Comparison to commercial water-soluble polysaccharides

Besides the side-stream extracted cereal and process water hemicellulose samples, also adsorption of commercially available polysaccharides with various backbone and charge properties was tested and compared. Measurements were performed in a similar way with QCM-D; the only difference was the lower pH and higher ionic strength (pH 4.5. 10 mM) to ensure solubility of the charged polysaccharides. At these conditions the NFC substrate will be less swollen. The polysaccharides were chosen based on literature study of previous interaction studies with cellulose (Laleg and Pikulik 1991; Laine et al. 2000; Hannuksela et al. 2002;

Christiernin et al. 2003; Westbye et al. 2006; Ren et al. 2009). Molecular weight degradation by simple acid hydrolysis was the only chemical modification applied to the readily available polysaccharides. Adsorption to hardwood NFC substrate was investigated. As an example the adsorption kinetics and corresponding *ΔD*-values for polysaccharides with different charge and backbone but similar molecular weight (about 250-300 kDa) are compared (Fig. 19).

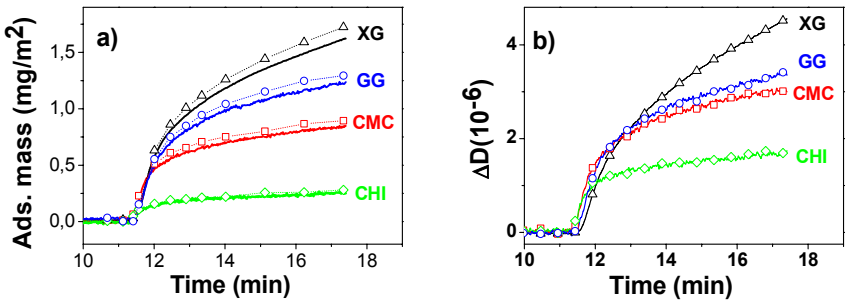

Figure 19. Adsorption of water-soluble polysaccharides during the first 20 minutes of adsorption. In a) increase in sensed mass and b) energy dissipation for water soluble polysaccharides in 10 mM NaAc-acetic acid buffer at pH 4.5 are shown. (Paper III). The dashed line and the open symbols in a) the comparison of the adsorbed amounts calculated by the Johannsmann's equation while the solid line corresponds to Sauerbrey equation.

The comparison of adsorption in the beginning (Fig.19) revealed that XG had fastest attachment rate with highest adsorbed amount. Neutral degraded GG and anionically charged carboxymethyl cellulose (CMC) showed similar change in *ΔD* value but the adsorbed mass was higher for GG indicating that the CMC has more hydrated layer structure. The attachment of CMC was not as strong as for neutral polysaccharides, seen from relatively higher *ΔD* vs. *Δm*-values. Likewise, the lower slope in *Δm/t* plot compared to XG and GG_{deg} indicated slower adsorption. However, the anionic CMC still did adsorb in contrast to previous results, the reason being the lower electrostatic repulsion at pH 4 vs. pH 8 that was used previously (Ahola et al. 2008a). Cationic chitosan adsorbed fast as seen from the leveling off (Fig. 19). The adsorbed amount was lowest of the tested polysaccharides, probably caused by the flat conformation of the relatively high charged cationic polymer. However, the increase in *ΔD*-value was in comparison relatively higher than the *Δm*-value, verifying the attachment.

4.2.4 Estimations of polysaccharide layer properties

The main layer properties of polysaccharides adsorbed on NFC ultrathin films are summarized in Table 3 (Papers II and III). Besides the adsorbed amount at the end of the experiments, also hydrodynamic thicknesses estimated based on the Voigt-model (Voinova et al. 1999) are listed. For selected samples, the adsorbed amount was also measured with SPR to estimate the dry mass of adsorbed polysaccharide. In paper III, an improved equation was derived to better take into account the properties of the different polysaccharides. Based on comparison between results from SPR and QCM-D a rough estimation of bound water in adsorbed polysaccharide layer is presented. It must be pointed out that changes in bound water in the NFC substrate due to adsorption of polysaccharides affect these values.

Table 3. Measured and calculated properties of polysaccharide adsorption on NFC substrates (Papers II and III).

Sample	Ads. mass QCM-D [mg/m^2]	Hydrodynamic thickness (nm)	Ads. mass SPR [mg/m^2]	water content* [%]
XG	2.1[a]/3.0[b]	11.5	0.5[c]/0.8[d]	76[c]/90[d]
GGM[a]	1.5	6	0.6[c]	65[c]
OAX[a]	1.2	-	-	-
RAX[a]	1.5	-	-	-
WAX[a]	1.7	5	0.4[c]	76[c]
WAX_e[a]	0.5	-	-	-
GG[b]	2.6	11	-	-
GG_{deg}[b]	2.9	10	0.3[d]	91[d]
LBG[b]	3.1	12	-	-
CHI[b]	0.7	-	0.1[d]	88[d]
XYL[b]	1.8	5		
CMC[b]	1.7	8		
MC[b]	2.5	34		

* calculated by the comparison of SPR determined dry adsorbed mass with the QCM-D estimated total adsorbed mass

[a)] measured in water without electrolyte addition, Johannsmann estimation (Eq. 3.3).

[b)] measured in 10 mM acetic acid-sodium acetate (pH 4.5), Johannsmann estimation (Eq. 3.3)

[c)] measured in water without electrolyte addition using equation described in Paper II.

[d)] measured in 10 mM acetic acid-sodium acetate (pH 4.5) using equation described in Paper III.

The adsorption of different polysaccharides was surprisingly similar on NFC substrates. Neutral XG and galactomannose gums (GG and LBG) had the highest adsorbed mass, while CHI and the degraded WAX had clearly the lowest. Different xylans both from wood and different cereal sources also adsorbed quite well. When the surfaces were rinsed, there was a higher percentage of desorption with xylans compared to other polysaccharides, which is probably caused by their lower attachment to cellulose. The high water contents were expected based on previous studies (Ahola et al. 2008a, Liu et al. 2011). Low molecular galactomannan from spruce had the lowest water content, which further suggested the tight formation between mannans and cellulose. The hydrodynamic thickness values as estimations from fitting the data to the Voigt-model (Voinova et al. 1999) are best suitable for relative comparison instead of absolute measures of viscosity. Most of the neutral polysaccharides had an estimated hydrodynamic thickness close to 10 nm. The estimated thickness and shear viscosity values of xylan layer are of the same order compared to previous publication by Tammelin et al. (2009).

Interesting properties of adsorbed layers on NFC films from different origin were also revealed. Although the adsorbed amounts were almost similar with hardwood and softwood NFC substrates, Voigt-modeling revealed relative differences in viscoelastic properties of the attached layers. The smallest layer thickness (3 nm) was estimated for similar origin softwood (spruce) fibrils and GGM, (extracted from process waters of spruce thermomechanical pulping). Rather surprisingly, the layer thickness was increased for the hardwood NFC-GGM combination. This could suggest that mannan-mannan interaction is behind the tight interaction for softwood NFC- GGM (Salmén and Olsson 1998). For the cereal WAX, the calculated hydrodynamic layer thickness was similar for both NFC origins, although there were quite notable differences in the kinetics of the adsorption. The presence of galactomannan has been found to affect xylan adsorption (Hansson and Hartler 1969). The adsorption of soluble, highly substituted and high M_w cereal AX to NFC substrate was probably affected more by the formation of extended loops. The drastic reduction in adsorbed amounts when WAX sample was enzymatically hydrolyzed supports this conclusion. The fast interaction of loosely bound WAX layer on softwood NFC could

be influenced by the α-L-arabinofuranosyl substituents present both in WAX and softwood NFC, but not in hardwood NFC (Sjöström 1993).

After adsorption studies for each polysaccharide, the NFC substrates were dried and imaged with AFM. No large aggregates were detected, which is in contrast to previous experiments where slight aggregation has been observed with xylan (Tammelin et al. 2009). Sometimes, the AFM images taken after high M_w galactomannan or cereal AX appeared somehow more dispersed or looser (Fig. 19 c compared to a and b).

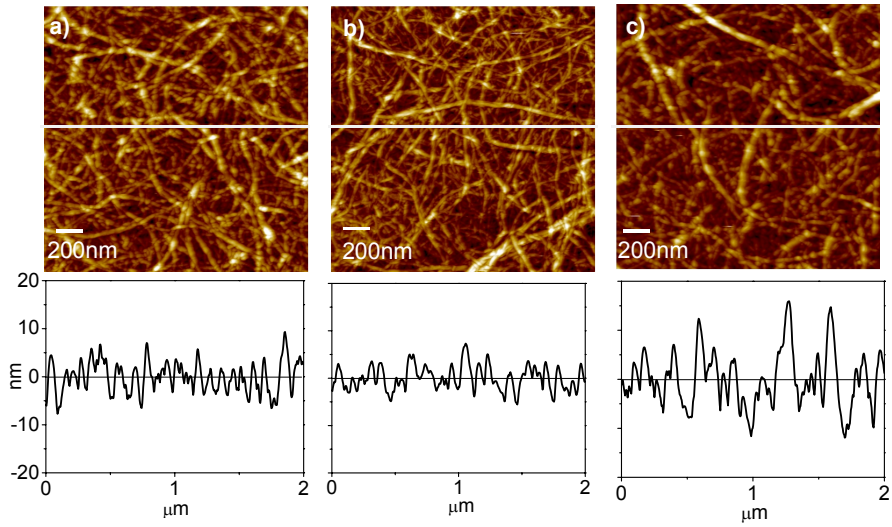

Figure 20. Comparison of NFC films imaged after polysaccharide adsorption by AFM. a) XG, b) GGM and c) WAX-hv. Image size is 2x2 µm².

To further probe this effect and the influence of the polysaccharide layer on the properties of the NFC film DPFM-mode was tested to investigate relative changes in film stiffness and adhesion properties. As an example, the NFC substrates without adsorbed layer and LBG adsorbed layer were compared. First, QCM-D raw data for LBG adsorption and buffer equilibration are shown to compare the Δf and ΔD-values (Fig. 21). The corresponding DPFM-images for reference (above) and LBG-adsorbed films are presented in Figure 22. The topography images for both substrates look very similar, as do the stiffness images. However, in images representing adhesion difference is observed: the adhesion between silicon nitride tip and film surface is lower for the LBG adsorbed NFC compared to reference NFC. This suggests that the

polysaccharide layer uniformly covers the fibrils and it can be detected also from dried films using this technique. Nevertheless, before accurate numbers or more definite conclusions of suitability of this technique are derived, more research should be done. The decrease in apparent adhesion gives an indication how the polysaccharide layer is able to change the surface properties of the NFC fibrils without drastically altering their individual fibrillar morphology.

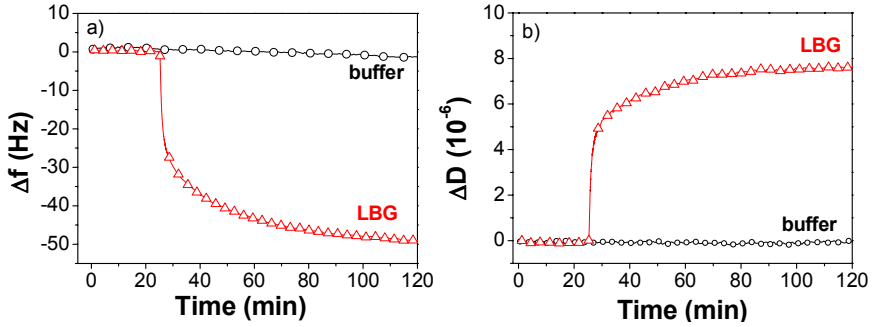

Figure 21. Comparison of QCM-D monitoring of LBG-adsorption and reference sample in 10 mM acetic acid buffer equilibration.

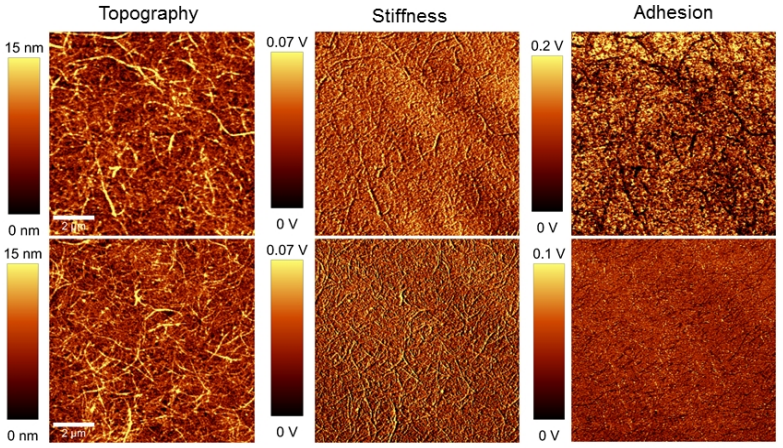

Figure 22. DPFM-mode AFM images of reference NFC substrate (upper row) and LBG-covered NFC substrate. The uniform reduction in adhesive forces verifies that fibrils are covered by a uniform, covering polysaccharide layer (Paper III).

4.3 Chitosan adsorption on cellulose monitored by CPM

4.3.1 Effect on normal forces

The normal surface forces were measured between two cellulose spheres in high (pH 10) and low (pH 3) pH both before and after chitosan adsorption. The chitosan was adsorbed in-situ the AFM-liquid cell for 8h, after which through rinsing was performed. The forces verified the different surface properties of cellulose as the function of pH (Fig. 23). At low pH, the double-layer interaction is almost absent because the cellulose is almost neutral at this pH (due to protonation of carboxylic groups). At higher pH, a double layer force existed at longer range, fitting adequately to the DLVO-theory and previous measurements (Carambassis and Rutland 1999). The estimated surface potential was -12 mV.

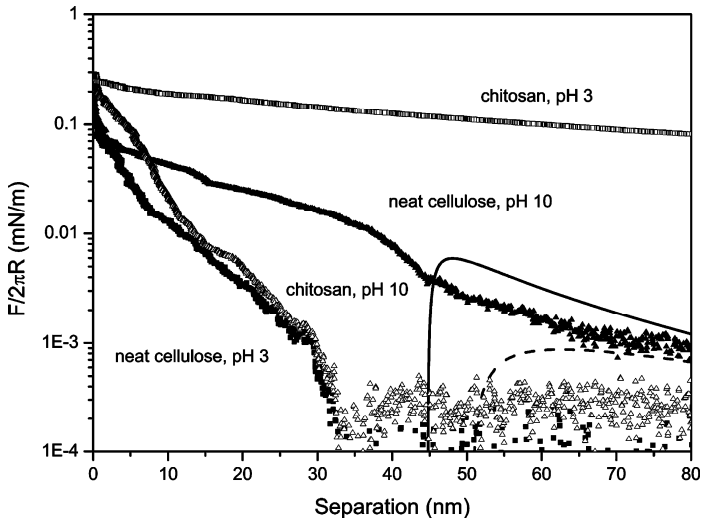

Figure 23. Normalized forces between two spheres in high and low pH before and after 8h chitosan adsorption (Paper IV).

After chitosan adsorption, dramatic differences in the force profiles were seen. At low pH, a long-range force component dominated the interactions, masking completely the electrostatic forces even at very long rang. (30 nm Debye-length is clearly exceeded). The adsorption of relatively large and long (micrometer range) cationic chitosan chains on the cellulose surfaces was verified to occur in the absence of significant electrostatic interactions, as cellulose at pH 3 is low charged due to the

protonation of carboxylic groups. As speculated before, this could be due to the hydrogen bonding between cellulose and chitin backbones, or interaction between carboxylic and amine groups (hydrogen bonding) of cellulose and chitosan, respectively. The high M_w chitosan formed loops and tails extending from the surfaces, (supported by the relatively high dissipation values of chitosan, Fig. 19b, Paper III) which combined with the known high stiffness properties explains the range of repulsive forces. Increase in pH reduces the extent of repulsive forces, and the force profile strongly resembles the one measured between bare cellulose surfaces before chitosan adsorption at lower pH. This indicates how the more charged cellulose surface probably compensates the (now weaker) charges of chitosan, possible in aggregated state (pKa of CHI is ~6, Claesson and Ninham 1992). Comparison to QCM-D results at pH 4.5 verifies the tight attachment of chitosan on NFC fibril substrates (Paper III). Surface forces and QCM-D measurements have also been performed with regenerated cellulose-films and chitosan in different pH (Myllytie et al. 2009). The direct surface force measurements are in good agreement. The non-electrostatic interactions were also observed (at pH 2) and the force profiles had similar, long-ranged repulsive nature. The adhesive forces on separation were found to increase after as the function of contact time after chitosan adsorption, yielding the characteristic saw-tooth pattern with irregular patterns. This is caused by multiple breaking of the interlocked chitosan molecules, which are highly polydisperse accounting for the irregular pull-off distance. The importance of molecular relaxing times became evident, as the adhesive forces increased as the function of contact time. This has also been observed with other biopolymers (XG, Stiernsted et al. 2006) or synthetic polyelectrolytes (Salmi 2007). The QCM-D estimations at low pH are in good accordance when comparing the chitosan adsorption on NFC (0.7 mg/m^2) Paper III) and TMSC (0.6 mg/m^2, Myllytie et al. 2009). The relatively high estimated adsorbed amounts further proves that also other than electrostatic forces influence the chitosan attachment on cellulose.

4.3.1 Effect on friction

The lateral forces between cellulose spheres were determined also in different pH before and after chitosan adsorption. The forces followed the modified Amonton's law (Eq. 2.5). The friction coefficients were determined as the slope of friction vs.

load and they are presented in Figures 24a and b for pH 10 and 3, respectively. The insets show the corresponding normal force curves at specific pH.

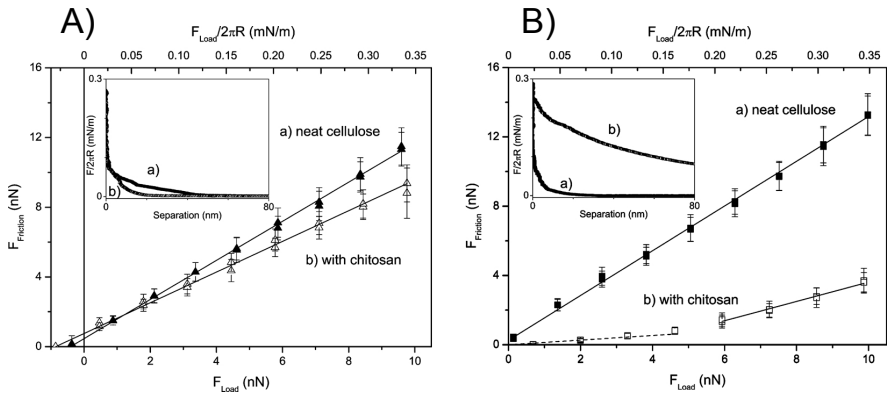

Figure 24. Effect of chitosan adsorption on friction co-efficient at a) pH 10 and b) pH 3.

At higher pH 10 chitosan did not markedly change neither normal nor frictional forces between cellulose. The friction co-efficient was slightly lower after chitosan adsorption. The frictional forces between unmodified cellulose in high and low pH were similar, consistent with macroscopic pulp fibre friction forces, with only slightly increased friction co-efficient in low pH compared to high one. Enormous changes were observed at low pH with adsorbed chitosan layer, as were observed for normal forces. These are related, as two frictional force regimes could be identified depending on the applied load, i.e. constant compliance vs. larger distances. At low applied loads the reduction in friction co-efficient is remarkable, nearly 7 times lower compared to that of unmodified cellulose surfaces. This can be attributed to the high-water swollen gel-like nature of the adsorbed viscous chitosan (Table 3), estimated to contain 88 m-% water. The increased layer solubility of soft layer is able to prevent interlocking of cellulose fibrils by forming a lubricating, cushion-like layer. The (three times) higher friction co-efficient at higher applied loads originates from expelling of the water from the hydrated layer under higher applied load. The interfibril interactions of opposing cellulose spheres are enabled again. The normal forces measured before and after friction measurements indicated how the soft chitosan layer might be partly ruptured after lateral movement, further indicating the

viscoelastic nature of the adsorbed layer. The friction reduction observed with chitosan is comparable to that previously measured with XG (Stiernstedt et al. 2006a), although as XG is neutral polysaccharide the reduction in friction was not as dependent on the pH. The main parameter affecting frictional forces is the surface roughness (Zauscher and Klingenberg 2000c) and as the cellulosic surfaces need to be quite robust to resist the wear in friction experiments, it was not performed in this work for NFC substrates. However, surface force measurements were continued to compare surface interactions of differently prepared NFC with different charge and size properties.

4.4 Comparison of NFC with different charge properties

The purpose of this part of work was to compare the interactions of NFC prepared by different methods from similar raw material. Only mechanical fibrillation without chemical modifications resulted in fibrils with low anionic charge (already used in Papers II and III). Increased negative charge was obtained with chemical pre-treatment. The role of electrostatic interactions was compared with oppositely charged polymers in multilayer build-up using the prominent LbL-technique. Two common papermaking polymers, cationic starch (CS) and poly(diallyldimethyl-ammoniumchloride) (PDADMAC) were chosen. In addition, cellulose nanofibrils, cationized via reaction with epoxytrimethylammonium chloride, in diluted aqueous dispersion were included in the comparison. The cationic counterparts differ in relation to charge density and particle size dimensions as well as origin (synthetic vs. biobased), but are known from previous experiments to have distinct interactions with cellulose surfaces (Kontturi et al. 2008; Ahola et al. 2008a; Aulin et al. 2010b). The interactions were monitored with QCM-D and CPM. Additional AFM-imaging of dried samples was also performed.

4.4.1 Comparison of high-and low charged NFC

Since the properties of underlying layer are important in multilayer formation, the charge, size and interaction of NFC films were characterized. The charge

properties were reported in Table 1, the unmodified fibrils (ref NFC) having in comparison low charge to the highly charged TEMPO-oxidized NFC. The comparison of ultrathin film morphology was shown in Figure 14a and d, but detailed comparison of size properties of individual fibrils is shown in Figure 25. Dilute fibril dispersions were imaged by cryogenic TEM- and AFM-imaging. In this work, the fibril size is about twice as high for the ref compared to TEMPO NFC, but the heterogeneity of the unmodified fibril bundles means that the average size difference could be even bigger. The results were in good accordance with previous characterizations for both ref NFC prepared by mechanical disintegration (Pääkkö et al. 2007, Taipale et al. 2010) and TEMPO-mediated oxidation (Saito et al. 2007, Saito et al. 2009, Li and Renneckar 2009) despite the slight differences in the origin of pulp raw materials used to prepare the fibrils. The physical dimensions of fibrils were greatly influenced by the charge. The ref NFC had clearly larger dimensions, consisting of fibril aggregates. Despite the significant amount of mechanical energy used for disintegrating the pulp fibre structure, the low anionic charge from the uronic acid groups in bound hemicellulose (Sjöström 1993) is not able to prevent the tight association of the liberated fibrils. In comparison, the TEMPO NFC had smaller dimensions, especially the width was reduced to 3-7 nm and the fibrils were not aggregated. The introduction of surface carboxyl groups prevents aggregation by electrostatic repulsion at neutral or alkaline pH. They had straighter conformation in dried state compared to more curled and interlocked ref NFC fibrils. Also the length of TEMPO NFC seemed to be somewhat reduced, however they retained the high aspect ratio.

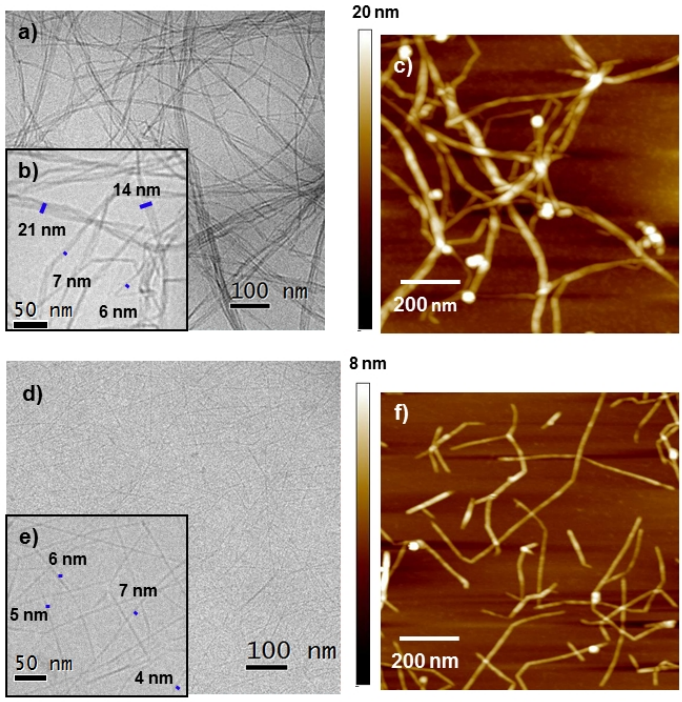

Figure 25. Comparison of TEMPO- and ref NFC by cryo-TEM and AFM-imaging. The upper row shows the ref NFC fibrils and the lower row TEMPO-oxidized fibrils. a) and d)show TEM images of the fibril suspensions. In b) and e) width estimations from the zoomed areas are performed. 1x1 µm² AFM-images support these width estimations.

CPM using colloidal sized amorphous cellulose spheres was applied for ultrathin ref and TEMPO NFC films in order to compare the different fibril grades. The force normalized by probe radius as the function of apparent separation (Fig. 26). The inset graph zooms in the results on logarithmic scale and includes an asymmetrical fit to the DLVO-theory for the ref NFC substrate by nonlinearized Poisson-Boltzmann equation. The line was calculated based on the algorithm for the boundary condition of constant potential (Devereux and de Bruyn, 1963) using the surface charge as the fitting parameter. Both films had monotonically repulsive forces on approach, and the extent of repulsion was as expected higher for the more swollen, highly charged TEMPO- NFC film. The surface potential of the amorphous cellulose spheres was approximated to -20 mV. The corresponding best fit to estimate the surface potential of the ref NFC fibrils was -30 mV (assuming constant surface potential). Fitting of the forces of the TEMPO NFC film to the DLVO theory was not

successful due to the strong presence of non-DLVO contributions. However, for the reference film the magnitude of the repulsion was in good conformation with previous study (Ahola et al. 2008b). Similar effects have also been observed for regenerated cellulose thin films with increased charge (Notley 2008). The inhibiting forces related to cellulose surfaces have been shown to be of steric origin from swollen network and protruding fibrils (Holmberg et al. 1997a) which have been determined to extend further with cellulose nanofibrils in comparison to cellulose spheres or other cellulose surfaces (e.g. Ahola et al. 2008b; Rutland et al. 1997; Notley et al. 2006).

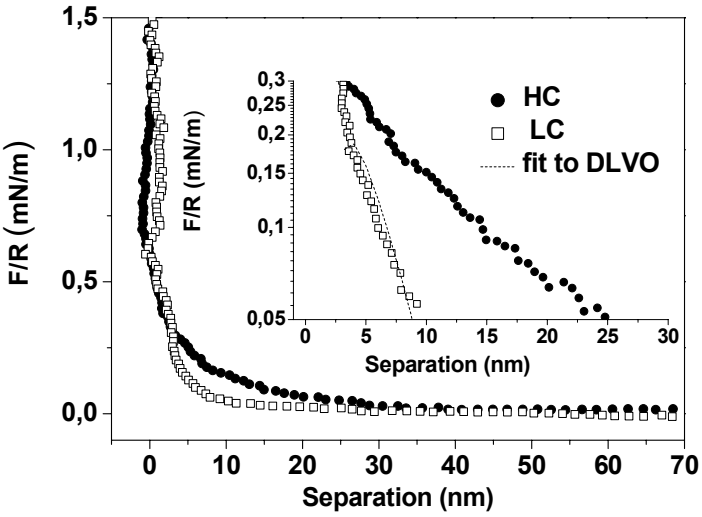

Figure 26. Comparison of surface interactions of NFC grades. The normalized force as the function of apparent separation for ref (□) *and TEMPO NFC films* (●) *in 10 mM NaCl in 1 mM $NaHCO_3$ (pH 8) solution. The inset shows the forces plotted on semilogarithmic scale and a fit to DLVO-theory for the ref NFC assuming constant potential.*

4.4.2 Effect of fibril charge on multilayer build-up

Spincoated nanofibril substrate was used as the starting layer in layer-by-layer build-up monitored by QCM-D. Consecutive layers were formed by feeding oppositely charged, dissolved polymer solutions or dilute NFC dispersions stepwise. Multilayer formation was successful with both NFC samples in all the studied combinations. This is illustrated Figure 27, showing the calculated adsorbed mass

values (Eq. 3.3) as the function of layer number for ref and TEMPO NFC multilayer systems.

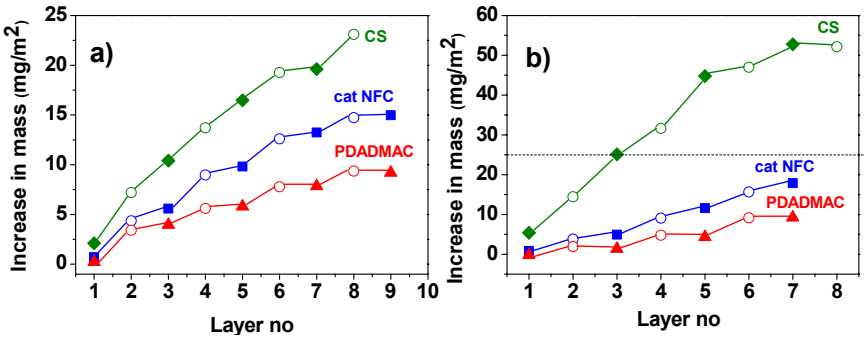

Figure 26. Comparison of multilayer build-up as the function of the layer number for a) mechanically disintegrated, native fibrils and b) TEMPO-oxidized fibrils. The inrease in adsorbed mass was calculated using the Johannsmann estimation (Eq.3.3). The closed symbols illustrate the cationic additive steps, with PDADMAC (▲), cationic cellulose nanofibrils (■) or cationic starch (◆) and the respective open spheres (○) represent the anionic fibril addition steps. The dotted line in b) indicates the scale of a)-part.

The increase in sensed mass after the total 7-9 layer additions were in all of the tested combinations higher with TEMPO compared to ref NFC. The simultaneously recorded energy dissipation values as the function of time are presented in Figure 28a and b for ref and TEMPO NFC, respectively. This comparison supports the more viscoelastic and extended nature of the TEMPO NFC evidenced from the higher energy dissipation values. The adsorbed mass was dependent on the cationic counterpart, and was clearly highest with cationic starch. Otherwise the trends were rather similar for both NFC grades. However, the decrease in adsorbed amounts with PDADMAC and cat NFC between 8th and 9th layer show how the multilayer formation slowed down with ref NFC from approximately 7th layer onwards (Fig. 27a).

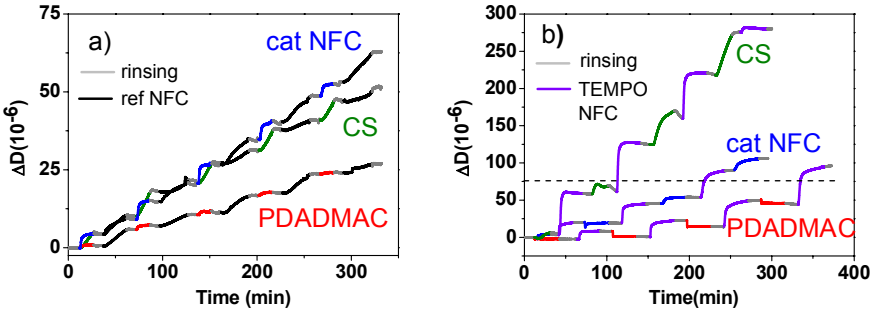

Figure 27. Comparison of dissipation values in multilayer build-up with mechanically disintegrated ref NFC and TEMPO NFC. The dotted line in b) denotes the correspondance between y-axis scales.

Besides the adsorbed amounts and viscoelastic nature, also remarkable differences were observed in adsorption kinetics, highlighting the characteristic inherent properties of ref and TEMPO NFC. With small and highly charged TEMPO NFC, the adsorption was fast and levelled off more quickly compared to the clearly slower kinetics of ref NFC adsorption. However, the extent of adsorption was higher for ref NFC (including the bound aqueous solution) in the first additions step in all studied combinations. The higher the charge, the more pronounced is the polyelectrolyte nature of cellulosic materials, i.e. dependency of pH and ionic strength conditions (Wågberg et al. 2008; Ahola et al. 2008b). According to the basic theory of poly-electrolyte adsorption, higher charge density leads to smaller layer thickness and faster adsorption kinetics (Fleer et al. 1993). This was observed in our experiment as the ref NFC had slower formation and layer stabilization times of the fibril network than TEMPO NFC. With ref NFC, the layer formation also became slower and lower as the function of multilayer steps. Besides the size, also the lower charge probably also contributed to this behavior. As charge reversal is needed for successful PEM formation (Schlenoff 2003), the insufficient charge reversal lead to stronger interpenetration of the layers. This is in contrast with TEMPO NFC, where the adsorption increased with each additional layer. In addition, the adsorption leveled off rather quickly, driven by the electrostatic interaction until charge reversal occurred. The TEMPO NFC probably adopted an extended conformation despite their high charge density, suggested by the very high energy dissipation values (Fig. 28b). In

comparison, ref NFC formed more rigid layers, also between cationic layers, reflecting the underlying NFC ultrathin film properties.

4.4.3 Effect of cationic counterpart

The high CD, linear small M_w polymer PDADMAC had the lowest increase in total adsorbed mass and energy dissipation with both NFC grades, corresponding to formation of more tight layers. This was expected from the basic theory of polyelectrolyte adsorption related to high charge density polyelectrolytes (Fleer et al. 1993). PDADMAC was able to compress the underlying swollen TEMPO NFC layer, seen as the decrease in ΔD-values in Figure 28b. This effect was not clearly seen for ref NFC, one reason could be that the small PDADMAC partly diffused into the voids between ref fibril networks. In QCM-D the two competing processes, de-swelling and adsorption of the polymer cannot be distinguished. However, the values nevertheless reveal differences in the adsorbed amount according to charge properties of NFC. The low charge density and high M_w CS had high adsorbed mass and energy dissipation with both NFC, indicating the formation of coiled, loose, gel-like multilayer structure. The increase in adsorbed amount per layer is also most uniform. Nevertheless, the slope of the increase is of totally different order, resulting in actually the largest deviation between the two anionic fibrils. The adsorbed amount (Eq.3.3) with TEMPO NFC and CS was about 50 mg/m^2 in the 8th added layer, about twice as much compared to ref NFC. By using cationic and anionic starches, comparable thick layers have been achieved (Johansson et al. 2009). Coinciding with the intermediate DS value, cat NFC as colloidal dispersions were in between PDADMAC and CS with both NFC grades when adsorbed amount was monitored. In the first addition step, the underlying fibril layer did not influence the adsorbed amount, which suggests that also nonelectrostatic affinity exits between oppositely charged NFC. The cat NFC adsorbed masses for ref and TEMPO fibrils in the 7th layer were 13 and 18 mg/m², respectively. The value obtained with TEMPO NFC is remarkably similar compared to previous study with carboxymethylated anionic NFC (Aulin et al. 2010b). However, the ΔD-value was higher with cat NFC instead compared to CS with ref NFC. AFM-images taken of the formed multilayers (shown for HC NFC combinations) after careful drying in N_2-flow is shown in Figure 29. The visual

appearance of the films even in their dried form is in good accordance with the detected *Δm*- and *ΔD*-values, although rather surprising was the relatively low small-scale roughness of the TEMPO NFC-CS compared to the very granular visual appearance of the film.

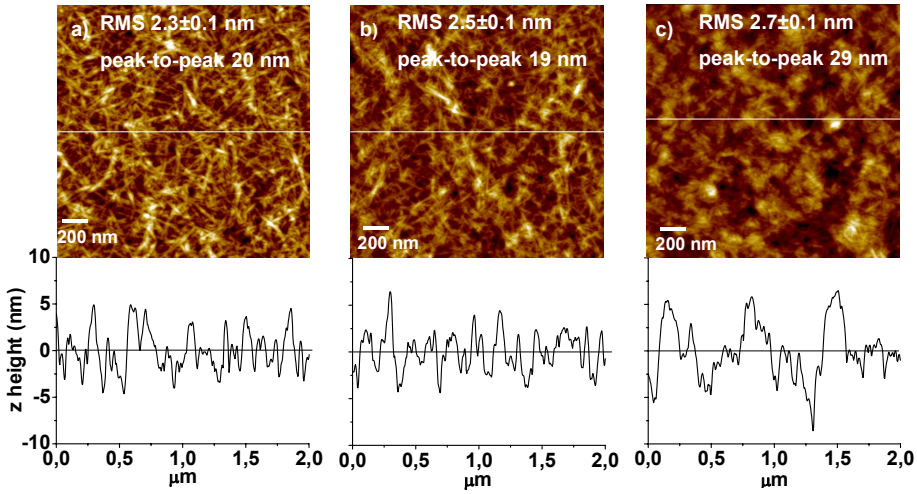

Figure 28. AFM-images of the dried HC NFC multilayers after 8 addition steps for a) PDADMAC, b) cat NFC and c) CS. Image size is 2x2 µm². The corresponding height profiles taken from the place indicated by the white line are shown below images and the calculated roughness properties on upper right corner of the images.

The results from combined QCM-D and AFM-imaging support that other than purely electrostatic contributions influences the interactions, as was the case with chitosan with similar type of reinforcing backbone (Paper IV). However, NFC-NFC or non-ionic polysaccharide multilayers without electrostatic contributions are more difficult to build. Jean et al. (2009) have observed that CNC and xyloglucan form multilayers. These results show that also low charged, mechanical unmodified fibrils from industrial renewable raw material could be utilized in forming multilayers. The interactions were further studied with CPM using selected NFC-cationic counterpart combinations.

4.4.4 Surface force studies on multilayer build-up with TEMPO NFC

The TEMPO NFC system was further used to probe the surface forces during multilayer build-up. PDADMAC and cat NFC was compared as cationic counterpart. As the upper surface, the similar amorphous cellulose spheres as in Paper IV were used. Figures 30 and 31 show the detected surface forces as a function of apparent separation with the multilayer formation for PDADMAC and cat NFC combined with TEMPO NFC, respectively. A schematic drawing clarifying the observed forces is also included. The curves shown were calculated as the averages from representative individual force measurements. The insets in both figures show the adsorbed mass measured with QCM-D (approximate estimation by Eq. 3.1) for corresponding layers. The two techniques support each other in both the studied combinations. Upon adsorption of highly charged PDADMAC on the swollen TEMPO NFC film, there was a reduction in sensed mass (inset in Fig. 30), which has previously been associated with the removal of water from the NFC film (e.g. Ahola et al. 2008a). The observed decrease in magnitude and extension of the repulsion in CPM measurements verified the deswelling of the TEMPO NFC film upon PDADMAC adsorption. Addition of the HC fibrils onto the PDADMAC layer again introduces a long ranged steric repulsion, in analogy with the high increase in mass detected by QCM-D. Further introduction of PDADMAC again decreased the repulsion by compressing the swollen fibril layer.

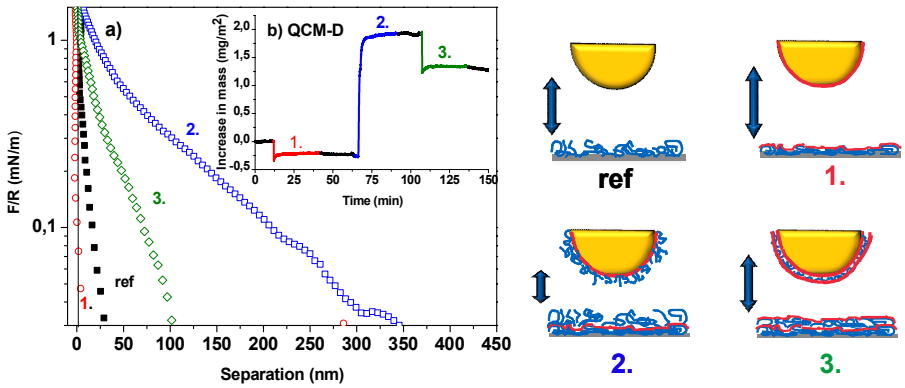

Figure 30. Normalized force vs. separation on approach for high charged TEMPO-NFC and PDADMAC multilayer build-up. The inset shows the corresponding steps from QCM-D measurements. As a reference, spincoated fibril substrate (■) was used, followed by sequential injections of 1. PDADMAC (○), 2. TEMPO NFC (□) and 3.PDADMAC (◇). Between multilayer forming, rinsing with 10 mM NaCl in 1 mM $NaHCO_3$ (pH 8) was done (shown in the QCM-D inset as black lines). A drawing to estimate the changes upon layer formation (not drawn in scale) is shown on the right.

With cat NFC and TEMPO NFC, there was always a stepwise increase in the repulsion as the function of apparent separation (Fig. 31) upon each adsorbed layer. The repulsive forces increased as function of layer number, and no compression of the nanofibril layers was detected. Similarly an increase in detected mass was observed (inset in Fig. 31). The rather low increase in repulsion during the first addition step could originate from the difference between charge densities of cellulose sphere and the anionic TEMPO NFC or the relative stiffness of the fibrils in geometrically restricted sphere-film configuration. As the layer formation by in-situ injection proceeded, the differences between QCM-D and CPM observations diminished. More extended layers were formed, seen from the increase in the range of repulsion. These observations are also in good accordance with the previous study probing the all-cellulosic interactions with (Aulin et al. 2010b). Multilayer formation was tried further, but with both studied combinations the formation of gel-like thick viscous layer prevented the complete detachment of the probe from the network, seen as sudden jump in the baseline. Therefore, those results were not included into comparison of the forces on approach. Forces were also so clearly of steric origin that fitting to the DLVO theory was not attempted.

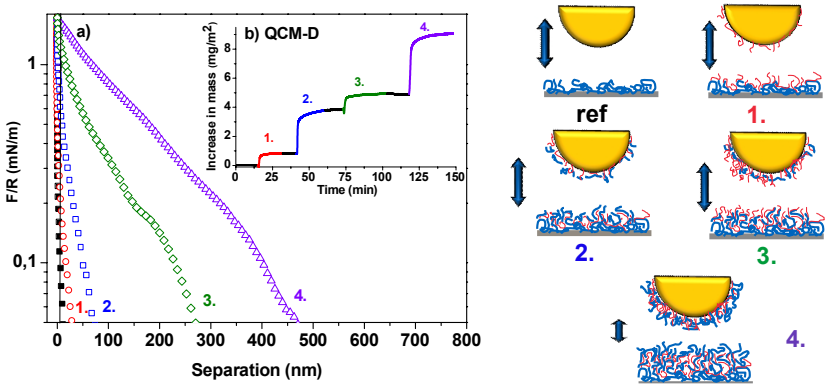

Figure 31. Normalized force vs. separation on approach for TEMPO and cat NFC multilayer build-up. The inset shows the corresponding steps from QCM-D measurements. As a reference, spincoated fibril substrate (■) *was used, followed by sequential injections of cat NFC* (○)*, TEMPO NFC* (□) *,cat NFC* (◇) *and TEMPO NFC* (▽)*. Between multilayer forming, rinsing with 10 mM NaCl in 1 mM* $NaHCO_3$ *(pH 8) was done (shown in the QCM-D inset as black lines). A drawing to estimate the changes upon layer formation (not drawn in scale) is shown on the right.*

4.4.5 Adhesive forces

Information about adhesive forces between surfaces can be obtained by analysing the force curves when separating the surfaces. Figure 32 illustrates the forces on retraction when building the multilayer system, for both PDADMAC (Fig. 32a) and cat NFC (Fig. 32b). Representative, individual force curves are shown. The pull-off forces between a cellulose sphere and the TEMPO NFC surface were very low. The range and magnitude were comparable to previous measurements with either two cellulose spheres (Rutland et al. 1997; Paananen et al. 2004) or a sphere and a flat NFC film (Ahola et al. 2008b; Salmi et al. 2009). Both cationic layers did not increase the adhesion markedly. The addition of further anionic TEMPO NFC increased the adhesion significantly as the function of layer number. The retraction curves also had the characteristic saw-tooth patterns, observed also in previous multilayer studies (Aulin et al., 2010b; Salmi et al. 2009). The notable increase in adhesive forces as the function of TEMPO NFC addition on the other hand can be understood as increased probability to form interlocked fibril-joints. With polymers, the free chain ends are able to increase the adhesion between surfaces to a greater extent compared to loops of polymer chains (Chen et al., 2005) and this can also be

applied with the charged cellulose fibrils with polyelectrolyte nature. The cat NFC-layers did not improve the adhesion as much as did the TEMPO NFC, in agreement with the lower adsorbed amounts seen with QCM-D (Fig. 31 inset) and previous measurements (Aulin et al., 2010b). The detected lower swelling ability (Olszewska et al. 2011) reduces the possibilities for interlocking formation, also suggested by the lower ΔD-values of cat NFC compared to TEMPO NFC (Fig. 28).

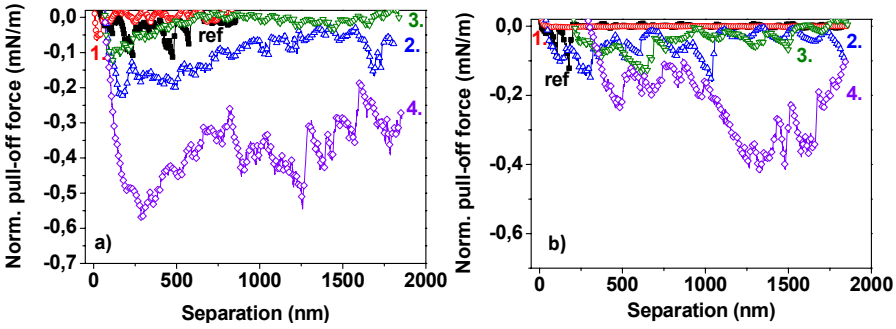

Figure 32. Forces normalized by the probe radius as the function of apparent separation on retraction for high charged TEMPO NFC with a) PDADMAC and b) cationic nanofibril multilayer systems. Different colours and symbols correspond to different steps during the layer build-up. The nanofibril substrate was used as the starting layer (■)*, followed by first cationic addition* (○)*, TEMPO NFC additon* (△)*, second cationic injection* (▽) *and finally the second TEMPO NFC addition* (◇)*.*

The comparison of the separation energy and the apparent zero force position revealed that the zero force position was shifted by the formation of more rigid NFC layers (Fig 32). Despite the large deviations between parallel measurements, a substantial increase in adhesive forces was detected between the entangled TEMPO nanofibrils in multilayer formation irrespective of the nature of the cationic counterpart. These results suggest that NFC fibrils have application potential in both existing applications, such as papermaking or new emerging tailored bionanocomposites. In addition, as the incorporation of unmodified nanofibrils into nanocomposites by mixing or intrusion strategies is rather challenging, the simple LbL-approach might facilitate utilization of this promising biomaterial (Podsialo et al. 2005).

4.5 Example of NFC modification via physisorption

As an example of a more practical application compared to more fundamental studies described in previous papers, functionalization of NFC via nanoparticle attachment was performed (Paper VI). The known adsorption of silver to cellulose yielding antibacterial properties was demonstrated by incorporating fluorescent silver nanoclusters (AgNC) in poly(methacrylic acid) (PMAA), and adsorbing this AgNC-PMAA on NFC. Of special interest was to clarify the interaction mechanism how the AgNC-particles attach onto NFC substrates. This was done by QCM-D monitoring of the attachment and underlying mechanism by comparison of NFC and amorphous regenerated trimethylsilyl cellulose (TMSC) cellulose film prepared by Langmuir-Schäefer (LS)-deposition (Fig. 33). The adsorption was high and fast for both TMSC and NFC substrates, but also PMAA without AgNC adsorbed on both cellulose substrates, although to a lesser extent. This would suggest that binding is favoured between the PMAA and –OH groups of cellulose, although also the carboxylic groups might have been involved, as the adsorbed amount was slightly higher for NFC compared to regenerated cellulose in PMAA adsorption. The opposite was true for the PMAA-AgNC, where more adsorbed on regenerated cellulose compared to NFC. This is probably related to the binding of AgNC on cellulose. The NFC substrates were imaged after adsorption, and no aggregations of silver nanoclusters or PMAA could be detected. This suggests that adsorption does not change the fine morphology of NFC, although functionalization as increased resistivity to E. coli bacteria was observed. Therefore physisorption can also in relatively simple way give additional properties to NFC materials.

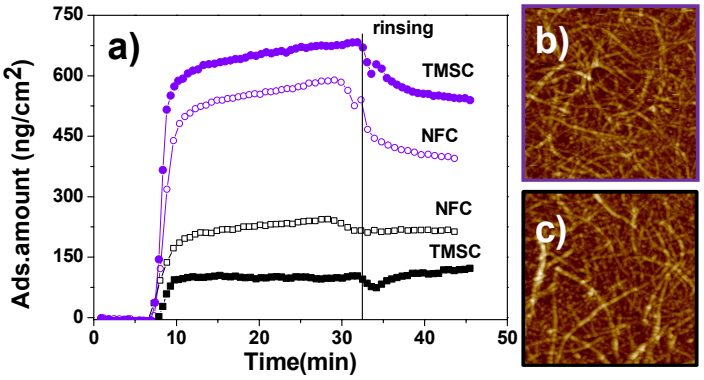

Figure 33. a) Adsorption of AgNC-PMAA (circles) and PMAA (squares) on NFC (open symbols) and TMSC (filled symbols) calculated mass as the function of time. The AFM height images before (b) and after (c) silver nanocluster modification show the non-aggregated substrate morphology, with similar appearance.

5 CONCLUDING REMARKS

In order to better utilize the natural resources in the future, new material applications from renewable cellulose based materials are currently under development. This work focused on determining the fundamental interactions between nanofibrillated cellulose (NFC) substrates and various polymers in aqueous phase. For comparison, also pure and more defined cellulose model substrates were used as reference systems. The knowledge of surface properties of new cellulosic materials is important for the more practical, commercial modifications. Studies were made by using simple physisorption approach in aqueous environment in order to preserve the microfibrillar fine structure beneficial for NFC applications, especially related strength requiring processes.

First, Raman spectroscopy of the different NFC materials verified the effect of chemical pre-treatments. As a preliminary study, Raman and atomic force microscopy (AFM)-imaging techniques were compared for the first time for the same samples to study the effect of mercerization on the cotton cellulose fibres. AFM-imaging revealed how also change in morphology occurred during the well-known alkali-induced conversion from cellulose I to cellulose II. Comparison to these results was useful with NFC. These verified that the cellulose I structure was to great extent maintained. No considerable changes in the crystallinity were detected, in good agreement with previous studies with different techniques.

The main interaction studies to study the surface interactions of nanofibrillated cellulose prepared from industrial pulp were made with ultrathin fibril substrates. A combination of surface sensitive techniques, including quartz crystal microbalance with dissipation monitoring, surface plasmon resonance and atomic force microscopy imaging and colloidal probe microscopy revealed rather uniform behaviour of different NFC grades. Indirect evidence of the surface character of NFC was revealed by systematic comparison of known polymers, of both renewable and synthetic origin with different NFC grades. The high affinity between similar backbone cellulose and hemicelluloses (previously observed with cellulosic fibres) was also verified for NFC substrates. In general, all the studied renewable based polysaccharides showed rather

uniform level of attachment. The properties of adsorbed layers could also be related to their role in native wood-cells. Interesting was also the finding, that tighter association between components from similar wood origin seems to occur. All the studied adsorbed layers contained very high percentage of water, as detected in previous works. A more detailed interaction study related to the biolubrication between one of the studied polysaccharides, chitosan, and cellulose spheres revealed a nonelectrostatic interaction together with reduction in friction at molecular level at low pH. These findings suggest that renewable polysaccharides with natural affinity for cellulose could be utilized as a basis for functional modifications to create new, efficient materials.

Another popular and simple modification method, layer-by-layer (LbL)-technique was in addition applied to compare in a systematic way the properties of high-and low charged fibrils prepared from the same raw material. It was shown that successful multilayer formation was achieved also with lower charged NFC and that properties could be tuned with the choice of polyelectrolyte. Further studies on combinations of oppositely charged NFC revealed that the non-electrostatic interactions were decisive in the initial LbL build-up. Significant increases in adhesion were also achieved with the high charged NFC due to its high compressibility of the multilayer structure. These results suggest advantageous effect of incorporating nanofibrils to various applications, such as papermaking or tailored bionanocomposites. More work however is still required. With the current intensive research, it seems that cellulose nanofibrils, or nanoparticles in general, will have a significant role in future material applications. For example, the incorporation of silver nanoparticles, known for their antibacterial properties, with NFC offers already a quite straightforward physisorption application of this promising new biomaterial.

6 REFERENCES

ABE K., IWAMOTO, S., & YANO, H. (2007). Obtaining cellulose nanofibres with a uniform width of 15 nm from wood. *Biomacromolecules*, 8, 3276-3278

AGARWAL, U. P. (2008). Raman spectroscopic characterization of wood and pulp fibres, In *Chacterization of Lignocellulosic materials*. Hu, T.Q. (Ed.) Blackwell; Oxford., pp. 17-35.

AHOLA, S., MYLLYTIE, P., ÖSTERBERG, M., TEERINEN, T. & LAINE, J. (2008a). Effect of polymer adsorption on cellulose nanofibril water binding capacity and aggregation. *BioResources,* 3**,** 1315-1328.

AHOLA, S., SALMI, J., JOHANSSON, L. S., LAINE, J. & ÖSTERBERG, M. (2008b). Model Films from Native Cellulose Nanofibrils. Preparation, Swelling, and Surface Interactions. *Biomacromolecules,* 9**,** 1273-1282.

AHOLA, S., ÖSTERBERG, M. & LAINE J. (2008c). Cellulose nanofibrils adsorption with poly(amide-amine) epichlorohydrin studied by QCM-D and application as a paper strength additive. *Cellulose*, 15, 303-314.

ALÈN R. (2000). Structure and chemical composition of wood. In *Forest Products Chemistry*, Stenius P. (Ed.) Fapet Oy, Helsinki, pp. 12-57.

ALMOND, A. & SHEEHAN, J. K. (2003). Predicting the molecular shape of polysaccharides from dynamic interactions with water. *Glycobiology, 13*(4), 255-264

ANDRESEN, M, JOHANSSON, L-S., TANEM, B.S. & STENIUS, P. (2006). Properties and characterization of hydrophobized microfibrillated cellulose. *Cellulose*, 13, 665-677.

ANDRESEN, M., STENSTAD, P., MØRETRØ¸, T., LANGSRUD, S., SYVERUD, K., JOHANSSON, L.-S. & STENIUS, P. (2007). Nonleaching antimicrobial films prepared from surface-modified microfibrillated cellulose. *Biomacromolecules,* 8**,** 2149-2155.

ANDRESSON, S.R., NORDSTRAND, T. & RASMUSON, A. (2000). The influence of some fibre and solution properties on pulp fibre friction. *Journal of Pulp and Paper Science*, 26, 67-71.

ASPINALL, GERALD, O. (1982). General Introduction, In *The Polysaccharides, Volume 1*, Aspinall, G.O. (Ed.) Academic Press; New York, pp. 1-18.

ATALLA, R.H. (1976). Raman spectral studies of polymorphy in cellulose. Part 1. Celluloses I and II. *Applied Polymer Symposium*, 28, 659-669.

ATALLA, R.H. (1983). The structure of cellulose: Quantative analysis by Raman spectroscopy. *Journal of Applied Polymer Science: Applied Polymer Symposium*, 37, 295-301.

AULIN, C., AHOLA, S., JOSEFSSON, P., NISHINO, T., HIROSE, Y., ÖSTERBERG, M. & WÅGBERG, L. (2009). Nanoscale cellulose films with different crystallinities and mesostructures:Their surface properties and interaction with water. *Langmuir,* 25**,** 7675-7685.

AULIN, C., GÄLLSTEDT, M. & LINDSTRÖM, T. (2010a). Oxygen and oil barrier properties of microfibrillated cellulose films and coatings. *Cellulose,* 17**,** 559-574.

AULIN, C., JOHANSSON, E., WÅGBERG, L. & LINDSTRÖM, T. (2010b). Self-organized films from cellulose I nanofibrils using the layer-by-layer technique. *Biomacromolecules,* 11**,** 872-882.

AULIN, C., VARGA, I., CLAESSON, P.M., WÅGBERG, L. & LINDSTRÖM, T. (2008). Buildup of polyelectrolyte multilayers of polyethyleneimine and microfibrillated cellulose studied by in situ dual polarization interferometry and quartz crystal microbalance with dissipation. *Langmuir*, 24, 2509-2518.

AZIZI SAMIR, M. A.S., ALLOIN, F. & DUFRESNE, A. (2005) Review of recent research into cellulosic whiskers, their properties and and their application in nanocomposite field. *Biomacromolecules*, 6, 612-626.

BAKER, A.A., HELBERT, W., SUGIYAMA, J. & MILES, M.J. (1997). High-resolution atomic force microscopy of native Valonia cellulose I microcrystals. *Journal of Structural Biology*, 119, 129-138.

BARSBERG, S. & NIELSEN, K. A. (2003). Oxidative quenching of spruce thermomechanical pulp fiber autofluorescence monitored in real time by confocal laser scanning microscopy-implications for lignin autofluorescence. *Biomacromolecules,* 4**,** 64-69.

BERGSTRÖM, L., STEMME, S., DAHLFORS, T., ARWIN, H. & ÖDBERG, L. (1999). Spectroscopic ellipsometry characterisation and estimation of the Hamaker constant of cellulose. *Cellulose,* 6**,** 1-13.

BERMAN, A.D., DUCKER, W. A & ISRAELACHVILI, J.N. (1996). Origin and characterization of different stick-slip friction mechanisms. *Langmuir*, 12, 4559-4563.

BINNIG, G., QUATE, C. F. & GERBER, C. (1986). Atomic force microscope. *Physical Review Letters,* 56**,** 930-934.

BLACKWELL, J. & MARCHESSAULT, R. H. (1971). Structure of cellulose and its derivatives. Infrared spectroscopy. Structure studies. *High Polymers,* 5**,** 1-37.

BLACKWELL, J., VASKO, P.D. & KOENIG, J.L. (1970) Infrared and Raman spectra of the cellulose from the cell wall of Valonia ventricosa. *Journal of Applied Physics,* 41**,** 4375-4379.

BOGDANOVIC G., TIBERG F. & RUTLAND M.W. (2001). Sliding friction between cellulose and silica surfaces. *Langmuir*; 17, 5911-5916

BRAGD, P., VAN BEKKUM H. & BESEMER, A.C. (2004). TEMPO-mediated oxidation of polysaccharides: Survey of methods and applications. *Topics in Catalysis,* 27, 49-66.

BURTON, R. A., GIDLEY, M. J. & FINCHER, G. B. (2010). Heterogeneity in the chemistry, structure and function of plant cell walls. *Nature Chemical Biology,* 6**,** 724-732.

BUTT, H.-J., CAPPELLA, B. & KAPPL, M. (2005). Force measurements with the atomic force microscope: Technique, interpretation and applications. *Surface Science Reports,* 59**,** 1-152.

BUTT, H.-J., BERGER, R., BONACCURSO, E., CHEN, Y. & WANG, J. (2007). Impact of atomic force microscopy on interface and colloid science. *Advances in Colloid and Interface Science,* 133**,** 91-104.

BYGRAVE, G. & ENGLEZOS, P. (1998). Fibre charge from potentiometric titration of kraft pulp and Donnan equilibrium theory. *Nordic Pulp & Paper Research Journal,* 13**,** 220-224.

CAI J., KIMURA S., WADA M. & KUGA, S. (2008). Nanoporous cellulose as metal nanoparticles support. *Biomacromolecules*, 10. 87-94.

CARAMBASSIS A. & RUTLAND, M.W. (1999). Interactions of cellulosic surfaces: Effect of electrolyte. *Langmuir*, 15, 5584-5590.

CARPICK, R.W., AGRAIT, N, OGLETREE, D.F. & SALMERON, M. (1996). Measurement of interfacial shear (friction) with an ultrahigh vacuum force microscope. *Journal of Vacuum Science and Technology B,* 14, 1289-1295.

CARROLL, A. & SOMERVILLE, C. (2009). Cellulosic biofuels. *Annual Review of Plant Biology,* 60**,** 165-182.

CERCLIER, C., COUSIN, F., BIZOT, H. MOREAU, C. & CATHALA, B. (2010). Elaboration of spin-coated cellulose-xyloglucan multilayered thin films. *Langmuir,* 26, 17248-17255.

CHEN, N., MAEDA, N., TIRRELL, M. & ISRAELACHVILI, J. (2005). Adhesion and friction of polymer surfaces: The effect of chain ends. *Macromolecules,* 38**,** 3491-3503.

CHENG, Y., BROWN, K. M. & PRUD'HOMME, R. K. (2002). Preparation and characterization of molecular weight fractions of guar galactomannans using

acid and enzymatic hydrolysis. *International Journal of Biological Macromolecules,* 31**,** 29-35.

CHRISTIERNIN, M., HENRIKSSON,G., LINDSTRÖM, M.E., BRUMER, H., TEERI, T.T., LAINE, J. & LINDSTRÖM, T. (2003). The effects of xyloglucan on the properties of paper made from bleached kraft pulp, *Nordic Pulp & Paper Research Journal,* 18, 182-187.

CLAESSON, P. & NINHAM, B. (1992). pH-dependent interactions between adsorbed chitosan layers. *Langmuir*, 8, 1406-1412.

COSGROVE, D. J. (1997). Assembly and enlargement of the primary cell wall in plants. *Annual Review of Cell and Developmental Biology,* 13**,** 171-201.

CRANSTON, E. & GRAY, D. (2006). Morphological and optical characterization of polyelectrolyte multilayers incorporating nanocrystalline cellulose. *Biomacromolecules*, 7, 2552-2530.

CRANSTON, E, GRAY, D.G. & RUTLAND, M.W. (2010). Direct surface force measurements of polyelectrolyte multilayer films containing nanocrystalline cellulose. *Langmuir*, 26, 17190-17197.

DAHLMAN, O., JACOBS, A. & SJÖBERG, J. (2003). Molecular properties of hemicelluloses located in the surface and inner layers of hardwood and softwood pulps. *Cellulose*, 10, 325-334.

DECHER G., HONG, J.D & SCHMITT J. (1992). Build-up of ultrathin multilayer films by a self-assembly process:III. Consecutively alternating adsorption of anionic and cationic polyelectrolytes on charged surfaces. *Thin solid films,* 210-211, 831-835.

DERJAGUIN, B.V. and LANDAU, L. (1941) Theory of the stability of strongly charged lyophobic sols of the adhesion of strongly charged particles in solution of electrolytes. *Acta Physicochimica URSS* 14, 633-662.

DEVEREUX, O. F. & DE BRUYN, P. L. (1963). *Interaction of plane-parallel double layers*. Massachusetts Institute of Technology Press; Cambridge, MA.

DINAND, E., VIGNON, M., CHANZY, H. & HEUX, L. (2002). Mercerization of primary wall cellulose and its implications for the conversion of cellulose I → cellulose II. *Cellulose*, 9, 7-18.

DONG H., WANG, D., SUN, G. & HINESTROZA, J. (2008). Assembly of metal nanoparticles on electrospun nylon 6 nanofibres by control of interfacial hydrogen-bonding interactions. *Chemistry of Materials*, 20, 6627-6632.

DONNAN, F. & HARRIS, A. (1911). The osmotic pressure and conductivity in aqueous solutions of Congo-red and reversible membrane equilibria. *Journal of The Chemical Society,* 99**,** 1554-1577.

DORRIS, G. M. & GRAY, D. G. (1978a). The surface analysis of paper and wood fibers by ESCA (electron spectroscopy for chemical analysis) I. Application to cellulose and lignin. *Cellulose Chemistry and Technology,* 12**,** 9-23.

DORRIS, G. M. & GRAY, D. G. (1978b). The surface analysis of paper and wood fibres by ESCA. II. Surface composition of mechanical pulps. *Cellulose Chemistry and Technology,* 12**,** 721-734.

DUCHESNE, I., DANIEL, G., VAN LEERDAM, G. C. & BASTA, J. (2003). Surface chemical composition and morphology of ITC kraft fibres as determined by XPS and FE-SEM. *Journal of Pulp and Paper Science,* 29**,** 71-76.

DUCKER, W. A. & SENDEN, T. J. (1992). Measurement of forces in liquids using a force microscope. *Langmuir,* 8**,** 1831-1836.

DUFRESENE, A., CAVAILLE J.Y. & VIGNON, M.R. (1997). Mechanical behaviour of sheets prepared from sugar beet cellulose microfibrils. *Journal of Applied Polymer Science,* 64, 1185-1194.

EBRINGEROVÁ, A. (2005). Structural diversity and application potential of hemicelluloses. *Macromolecular Symposia,* 232**,** 1-12.

EICHHORN, S. (2011). Cellulose nanowhiskers: promising material for advanced applications. *Soft Matter*, 7, 303-315.

EICHHORN, S., DUFRESNE, A., ARANGUREN, M., MARCOVICH, N., CAPADONA, J., ROWAN, S., WEDER, C., THIELEMANS, W., ROMAN, M., RENNECKAR, S., GINDL, W., VEIGEL, S., KECKES, J., YANO, H., ABE, K., NOGI, M., NAKAGAITO, A., MANGALAM, A., SIMONSEN, J., BENIGHT, A., BISMARCK, A., BERGLUND, L. & PEIJS, T. (2010). Review: current international research into cellulose nanofibres and nanocomposites. *Journal of Materials Science,* 45**,** 1-33.

EYEHOLZER, C., BORDEANU, N., LOPEZ-SUEVOS, F., RENTSCH D., ZIMMERMANN, T. & OKSMAN, K. (2010). Preparation and characterization of water-redispersible nanofibrillated cellulose in powder form. *Cellulose*, 17, 19-30.

FARDIM, P. & DURAN, N. (2003). Modification of fibre surfaces during pulping and refining as analysed by SEM, XPS and ToF-SIMS. *Colloids and Surfaces, A: Physicochemical and Engineering Aspects,* 223**,** 263-276.

FARDIM, P., HULTEN HEIJNESSON, A., BOISVERT, J.-P., JOHANSSON, L.-S., ERNSTSSON, M., CAMPBELL, J. M., LEJEUNE, A., HOLMBOM, B., LAINE, J. & GRAY, D. G. (2006). Critical comparison of methods for surface coverage by extractives and lignin in pulps by X-ray photoelectron spectroscopy (XPS). *Holzforschung,* 60**,** 149-155.

FEILER, A., LARSON, I., JENKINS, P. & ATTARD, P. (2000). A quantative study of interaction forces and friction in aqueous colloidal systems. *Langmuir*, 16, 10269-10277.

FENGEL, D., JAKOB, H. & STROBEL, C. (1995). Influence of the alkali concentration on the formation of cellulose II. *Holzforschung*, 49, 505-511.

FENGEL, D. & STROBEL , C. (1994). FTIR spectroscopic studies on the heterogeneous transformation of cellulose I into cellulose II. *Acta Polymerica* 45, 319-324.

FENGEL, D. & WEGENER, G. (1984) *Wood-Chemistry, Ultrastructure, Reactions*, Walter de Gruyter; Berlin.

FLEER, G.J., COHEN STUART, M.A., SCHEUTJENS, J.M.H.M., COSGROVE, T. & VINCENT, B. (1993). *Polymers at interfaces*, Chapman& Hall, University Press, Cambridge.

FUJISAWA, S., OKITA, Y., FUKUZUMI, H., SAITO, T. & ISOGAI, A. (2011). Preparation and characterization of TEMPO-oxidized cellulose nanofibril films with free carboxyl groups. *Carbohydrate Polymers*, 84, 579-583

FÄLT, S., WÅGBERG, L. & VESTERLIND, E.-L. (2003). Swelling of model films of cellulose having different charge densities and comparison to the swelling behavior of corresponding fibers. *Langmuir,* 19**,** 7895-7903.

GANDINI, A. (2011). The irruption of polymers from renewable resources on the scene of macromolecular science and technology. *Green Chemistry,* 13**,** 1061-1083.

GRAY, D. G., WELLER, M., ULKEM, N. & LEJEUNE, A. (2010). Composition of lignocellulosic surfaces: comments on the interpretation of XPS spectra. *Cellulose,* 17**,** 117-124.

GUHADOS, G., WAN, W.K & HUTTER, J.L. (2005). Measurement of the elastic modulus of single bacterial cellulose fibers using atomic force microscopy. *Langmuir*, *21*, 6642-6646.

GUSTAFSSON, J., CIOVICA, L. & PELTONEN, J. (2002). The ultrastructure of spruce kraft pulps studied by atomic force microscopy (AFM) and X-ray photoelectron spectroscopy (XPS). *Polymer,* 44**,** 661-670.

GUSTAFSSON, J. (2004) PhD Thesis: Surface characterization of chemical and mechanical pulp fibres from AFM and XPS. Åbo Akademi, Finland.

HALTTUNEN, M., VYÖRYKKÄ, J., HORTLING, B., TAMMINEN, T., BATCHELDER, D., ZIMMERMANN, A. & VUORINEN, T. (2001). Study of residual lignin in pulp by UV-resonance Raman spectroscopy. *Holzforschung,* 55**,** 631-638.

HAMAKER, H.C. (1937). The London-van der Waals attraction between spherical particles *Physica* 4, 1058-1072.

HANLEY, S.J., GIASSON, J., REVOL, J.F. & GRAY, D.G. (1992). Atomic force microscopy of cellulose microfibrils: comparison with transmission electron microscopy. *Polymer*, 33, 4639-4642.

HANNUKSELA, T., FARDIM, P. & HOLMBOM, B. (2003). Sorption of spruce O-acetylated galactoglucomannans onto different pulp fibres. *Cellulose*, 10, 317-324.

HANNUKSELA, T., TENKANEN, M., & HOLMBOM, B. (2002). Sorption of dissolved galactoglucomannans and galactomannans to bleached kraft pulp *Cellulose,* 9, 251-261.

HANSEN, N. M. L. & PLACKETT, D. (2008). Sustainable films and coatings from hemicelluloses: A review. *Biomacromolecules,* 9**,** 1493-1505.

HANSMA, H. G., KIM, K. J., LANEY, D. E., GARCIA, R. A., ARGAMAN, M., ALLEN, M. J. & PARSONS, S. M. (1997). Properties of biomolecules measured from atomic force microscope images: A review. *Journal of Structural Biology,* 1197**,** 99-108.

HANSSON, J.A. & HARTLER, N. (1969). Sorption of hemicelluloses on cellulose fibers. I. Sorption of xylans. *Svensk Pappertidning*, 72, 521-530.

HAYASHI, T., OGAWA, K. & MITSUISHI, Y. (1994). Characterization of the adsorption of xyloglucan to cellulose. *Plant and Cell Physiology,* 35**,** 1199-1205.

HEIM, L.-O., BLUM, J., PREUSS, M. & BUTT, H.-J. (1999). Adhesion and friction f forces between spherical micrometer-sized particles. *Physical Review Letters*, 83, 3328-3331.

HENRIKSSON, M., BERGLUND, L. A., ISAKSSON, P., LINDSTRÖM, T. & NISHINO, T. (2008). Cellulose Nanopaper Structures of High Toughness. *Biomacromolecules,* 9**,** 1579.

HENRIKSSON, M., HENRIKSSON, G., BERGLUNG; L.A & LINDSTRÖM, T. (2007). An environmentally friendly methos for enzyme-assisted preparation of microfibrillated cellulose (MFC) nanofibres. *European Polymer Journa*l, 43, 3434-3441.

HERRICK, F.W., CASEBIER, R.L., HAMILTON, J. K. & SANDBERG, K.R. (1983). Microfibrillated cellulose:morphology and accessibility. *Journal of applied polymer science: Applied polymer symposium*, 37, 797-813.

HOLMBERG, M., BERG, J., STEMME, S., ÖDBERG, L., RASMUSSON, J & CLAESSON, P. (1997a). Surface force studies of Langmuir-Blodgett cellulose films. *Journal of Colloid and Interface Sciece*, 186, 369-381.

HOLMBERG, M., WIGREN, R., ERLANDSSON R. & CLAESSON, P.M. (1997b). Interactions between cellulose and colloidal silica in the presence of polyelectrolytes. *Colloids and Surfaces A, Physicochemical and Engineering Aspects*, 129-130, 175-183.

HOLMBOM, B. & STENIUS; P. (2000). Analytical methods, In *Forest Products Chemistry*, Stenius, P. (Ed.) Fapet Oy; Helsinki, pp.107-169.

HORVATH, E. & LINDSTRÖM, T. (2007). Indirect polyelectrolyte titration of cellulosic fibres-Surface and bulk charges of cellulosic fibres. *Nordic Pulp & Paper Research Journal,* 22**,** 80-86.

HUANG, F., LI, K. & KULACHENKO, A. (2009). Measurement of interfiber friction force for pulp fibers by atomic force microscopy. *Journal of Materials Science,* 44, 3770-3776.

HUBBE, M. A. & ROJAS, O. J. (2008). Colloidal stability and aggregation of lignocellulosic materials in aqueous suspension: A review. *BioResources,* 3**,** 1419-1491.

HUBBE, M. A., ROJAS, O. J., LUCIA, L. & SAIN, M. (2008). Cellulosic nanocomposites: A review. *BioResources,* 3**,** 929-980.

HUTTER, J. L. & BECHHOEFER, J. (1993). Calibration of atomic force microscope tips. *Review of Scientific Instruments,* 64**,** 1868-1873.

HÖÖK, F., RODAHL, M., BRZEZINSKI, P. & KASEMO, B. (1998). Energy dissipation kinetics for protein and antibody-antigen adsorption under shear oscillation on a quartz crystal microbalance. *Langmuir,* 14**,** 729-734.

IFUKU, S., TSUJI, M., MORIMOTO, M., SAIMOTO, H. & YANO, H. (2009). Synthesis of silver nanoparticles templated by TEMPO-mediated oxidized bacterial cellulose nanofibers. *Biomacromolecules*, 10, 2714-2717.

ISHIMARU, Y. & LINDSTRÖM, T. (1984). Adsorption of water-soluble, nonionic polymers onto cellulosic fibers, *Journal of Applied Polymer Science,* 29, 1675-1691.

ISRAELACHVILI, J. (1992) *Intermolecular and Surface Forces*; 2nd edition, Academic Press; San Diego.

ISRAELACHVILI, J. & WENNERSTRÖM, H. (1996). Role of hydration and water structure in biological and colloidal interactions. *Nature*, 379, 219-225.

IWAMOTO, S., ABE, K., & YANO, H. (2008). The effect of hemicelluloses on wood pulp nanofibrillation and nanofiber network characteristics. *Biomacromolecules,* 9, 1022-1026.

IWAMOTO, S., KAI, W., ISOGAI, A. & IWATA, T. (2009.) Elastic modulus of single cellulose microfibrils from tunicate measured by atomic force microscopy. *Biomacromolecules,* 10, 2571-2576.

JEAN, B., HEUX, L., DUBREUIL, F., CHAMBAT, G. & COUSIN, F. (2009). Non-electrostatic building of biomimetic cellulose-xyloglucan multilayers. *Langmuir*, 25, 3920-3923.

JOHANNSMANN, D., MATHAUER, K., WEGNER, G. & KNOLL, W. (1992). Viscoelastic properties of thin films probed with a quartz-crystal resonator. *Physical Review B,* 46**,** 7808-7815.

JOHANSSON, E., LUNDSTRÖM, L., NORGREN, M. & WÅGBERG, L. (2009). Adsorption behaviour and adhesive properties of biopolyelectrolyte multilayers formed from cationic and anionic starch. *Biomacromolecules*, 10, 1768-1776.

JOSELEAU, J. P., COMTAT, J., & RUEL, K. (1992). Chemical structure of xylans and their interaction in the plant cell walls. In *Progress in biotechnology 7,* Visser, J., Beldman, G., Kusters-van Someron, M.A. and A.Voragen, G.J. (Eds.), Elsevier; Amsterdam, pp.1-15.

JÄHN, A., SCHRÖDER, M., FÜTING, M., SCHENZEL, K. & DIEPENBROCK, W. (2002). Characterization of alkali treated flax fibres by means of FT Raman spectroscopy and environmental scanning electron microscopy. *Spectrochimica Acta: Part A,* 58**,** 2271-2279.

KABEL, M. A., VAN DEN BORNE, H., VINCKEN, J.-P., VORAGEN, A. G. J. & SCHOLS, H. A. (2007). Structural differences of xylans affect their interaction with cellulose. *Carbohydrate Polymers,* 69**,** 94-105.

KATZ, S., BEATSON, R. P. & SCALLAN, A. M. (1984). The determination of strong and weak acidic groups in sulfite pulp. *Svensk Papperstidning,* 87**,** R48-R53.

KIM, D.Y., NISHIYAMA, Y. & KUGA, S. (2002). Surface acetylation of bacterial cellulose. *Cellulose*, 9, 361-367.

KLEEN, M. (2005). Surface lignin and extractives on hardwood RDH kraft pulp chemically characterized by ToF-SIMS. *Holzforschung,* 59**,** 481-487.

KOLJONEN, K., ÖSTERBERG, M., JOHANSSON, L.-S. & STENIUS, P. (2003). Surface chemistry and morphology of different mechanical pulps determined by ESCA and AFM. *Colloids and Surfaces A: Physicochemical and Engineering Aspects,* 228**,** 143-158.

KONG, K. & EICHHORN, S. (2005). The influence of hydrogen bonding on the deformation micromechanics of cellulose fibres. *Journal of Macromolecular Science Part B: Physics,* 44**,** 1123-1136.

KONTTURI, E., TAMMELIN, T. & ÖSTERBERG, M. (2006) .Cellulose-model films and the fundamental approach. *Chemical Society Reviews,* 35**,** 1287-1304.

KONTTURI, E. & VUORINEN, T. (2009). Indirect evidence of supramolecular changes within cellulose microfibrils of chemical pulp upon drying. *Cellulose*, 16, 65-74.

KONTTURI, K. S., TAMMELIN, T, JOHANSSON, L.-S. & STENIUS, P. (2008). Adsorption of cationic starch on cellulose studied by QCM-D. *Langmuir*, 24, 4743-4749.

KUUTTI, L. PELTONEN, J., PERE, J. & TELEMAN, O. (1995). Identification and surface structure of crystalline cellulose studied by atomic force microscopy. *Journal of Microscopy*, 178, 1-6.

KÖHNKE, T., LUND, K., BRELID, H. & WESTMAN, G. (2010). Kraft pulp hornification: A closer look at the preventive effect gained by glucuronoxylan adsorption. *Carbohydrate Polymers*, 81, 226-233.

LAINE, J., LINDSTRÖM, T., GLAD-NORDMARK, G. & RISINGER, G. (2000). Studies on topochemical modification of cellulosic fibres. Part 1. Chemical conditions for the attachement of carboxymethyl cellulose onto fibres. *Nordic Pulp and Paper Research. Journal,* 15, 520-526.

LAINE, J., LÖVGREN, L., STENIUS, P. & SJÖBERG, S. (1994). Potentiometric titration of unbleached kraft cellulose fibre structures. *Colloids and Surfaces A: Physicochemical and Engineering Aspects,* 88**,** 277-287.

LAINE, J. & STENIUS, P. (1994). Surface characterization of unbleached kraft pulps by means of ESCA. *Cellulose,* 1**,** 145-160.

LAINE, J. & STENIUS, P. (1996). The effect of ECF and TCF bleaching on the surface chemical composition of kraft pulp as determined by ESCA. *Nordic Pulp & Paper Research Journal,* 11**,** 201-210.

LALEG, M., & PIKULIK, I. I. (1991). Wet-web strength increase by chitosan. *Nordic Pulp and Paper Research. Journal,* 6, 99-103.

LAWTHER, J.M., SUN, R.C., & BANKS, W.B. (1995). Extraction, fractionation, and characterization of structural polysaccharides from wheat straw. *Journal of Agricultural and Food Chemistry*, 43, 667-675.

LI, Q. & RENNECKAR, S. (2009). Molecularly thin nanoparticles from cellulose: Isolation of sub-microfibrillar structures. *Cellulose*, 16, 1025-1032.

LI, Q. & RENNECKAR, S. (2011). Supramolecular structure characterization of molecularly thin cellulose I nanoparticles. *Biomacromolecules*, 12, 650-659.

LIFSHITZ, E.M. (1956). The theory of molecular attractive forces between solids, *Soviet Physics- JETP* 2, pp. 73-83.

LINDMAN, B., KARLSTRÖM, G. & STIGSSON, L. (2010). On the mechanism of dissolution of cellulose. *Journal of Molecular Liquids*, 156, 76-81.

LINDSTRÖM, T. (1989). Some fundamental chemical aspects on paper forming. In: *Fundamentals of Papermaking*, Baker, C.F. and Punton, V.V. (Eds.) London, Mech. Eng. Pub. Ltd., pp. 311-412.

LINGSTRÖM R., NOTLEY, S.M. & WÅGBERG, L. (2007). Wettability changes in formation of polymeric multilayers on cellulose fibres and their influence on wet adhesion. *Journal of Colloid and Interface Science,* 314, 1-9

LITTUNEN, K., HIPPI, U., JOHANSSON, L.-S., ÖSTERBERG, M., TAMMELIN, T., LAINE, J. & SEPPÄLÄ, J. (2011). Free radical graft copolymerization of nanofibrillated cellulose with acrylic monomers. *Carbohydrate Polymers,* 84**,** 1039-1047.

LIU, Z., CHOI, H., GATENHOLM, P. & ESKER, A. (2011). Quartz crystal microbalance with dissipation monitoring and surface plasmon resonance studies of carboxymethyl cellulose adsorption onto regenerated cellulose surfaces. *Langmuir*, 27, 8718-8728.

LORD, E. (1955). Frictional forces between fringes of fibres. *Journal of the Textile Institute*, 46, 41-58.

LÖNNBERG, H., LARSSON, K., LINDSTRÖM, T., HULT, A. & MALMSTRÖM, E. (2011). Synthesis of polycaprolactone-grafted microfibrillated cellulose for use in novel bionanocomposites: Influence of the graft length on the mechanical properties. *ACS Applied Materials & Interfaces*, 3, 1426-1433.

MAGONOV, S. N. (2000). *Atomic force microscopy in analysis of polymers,* John Wiley & Sons Ltd., Chichester.

MANEERUNG, T., TOKURA, S. & RUJIRAVANIT, R. (2008). Impregnation of silver nanoparticles into bacterial cellulose for antimicrobial wound dressing. *Carbohydrate Polymers*, 72, 43-51.

MAXIMOVA, N., ÖSTERBERG, M., KOLJONEN, K. & STENIUS, P. (2001). Lignin adsorption on cellulose fibre surfaces: effect on surface chemistry, surface morphology and paper strength. *Cellulose,* 8**,** 113-125.

McCANN M.C. & ROBERTS,K. (1991). Architecture of the primary cell wall. In *The Cytoskeletal Basis of Plant Growth and Form*. Lloyd, C.W. (Ed.). Academic Press, London, pp. 109-129.

MIKKONEN, K. S., HEIKKINEN, S., SOOVRE, A., PEURA, M., SERIMAA, R., TALJA, R. A., HELÉN, H., HYVÖNEN, L. & TENKANEN, M. (2009).

Films from oat spelt arabinoxylan plasticized with glycerol and sorbitol. *Journal of Applied Polymer Science,* 114**,** 457-466.

MISHIMA, T., HISAMATSU, M., YORK, W.S., TERANISHI, K. & YAMADA, T. (1998). Adhesion of beta-glucans to cellulose, *Carbohydrates Research*. 308, 389-395.

MIZUNO, H., LUENGO, G.S. & RUTLAND, M.W. (2010). Interactions between crossed hair fibers at the nanoscale. *Langmuir*, 26, 18909-18915.

MOLIN, U. & DANIEL, G. (2004). Effects of refining on the fibre structure of kraft pulps as revealed by FE-SEM and TEM: Influence of alkaline degradation. *Holzforschung,* 58**,** 226-232.

MOON, R. J., MARTINI, A., NAIRN, J., SIMONSEN, J. & YOUNGBLOOD, J. (2011) .Cellulose nanomaterials review: Structure, properties and nanocomposites. *Chemical Society Reviews*. 40, 3941-3994.

MORÁN J.I., ALVAREZ, V.A., CYRAS, V.P. & VÀSQUEZ A. (2008). Extraction of cellulose and preparation of nanocellulose from sisal fibres. *Cellulose*, 15, 149-159.

NAKAGAITO, A. N. & YANO, H. (2005). Novel high-strength biocomposites based on microfibrillated cellulose having nano-order-unit web-like network structure. *Applied Physics A: Materials Science & Processing,* 80**,** 155-159.

NAKAGAITO, A. N., FUJIMURA, A., SAKAI, T., HAMA, Y. & YANO, H. (2009). Production of microfibrillated cellulose (MFC)-reinforced polylactic acid (PLA) nanocomposites from sheets obtained by papermaking-like process. C*omposites Science and Technology,* 69, 1293-1297.

NEUMAN, R.D., BERG, J.M. & CLAESSON, P. (1993). Direct measurement of surface forces in papermaking and paper coating systems. *Nordic Pulp and Paper Research Journal*, 8, 96-104.

NEWMAN, R. H. & HEMMINGSON, J. A. (1998). Interactions between locust bean gum and cellulose characterized by carbon-13C NMR spectroscopy. *Carbohydrate Polymers,* 36**,** 167-172.

NIEMI, H. & PAULAPURO, H. (2002). Review: Application of scanning probe microscopy to wood, fibre and papermaking. *Pap. Puu,* 84**,** 389-406.

NINHAM, B. & PARSEGIAN V.A. (1971). Electrostatic potential between surfaces bearing ionizable groups in ionic equilibrium with physiologic saline solution. *Journal of Theoretical Biology*, 31, 405-428.

NISHIYAMA, Y. (2009). Structure and properties of the cellulose microfibrils. *Journal of Wood Science,* 55**,** 241-249.

NOGI, M., IFUKU, S., ABE, K., HANDA, K., NAKAGAITO, A.N & YANO, H. (2006). Property enhancement of optically transparent bionanofiber composites by acetylation. *Applied Physics Letters*, 89, 233123-1-233123-3.

NOGI, M. & YANO, H. (2008). Transparent nanocomposites based on cellulose produced by bacteria offer potential innovation in the electronics device industry. *Advanced Materials,* 20**,** 1849-1852.

NOTLEY, S.M., PETTERSSON, B. & WÅGBERG, L. (2004). Direct measurement of attractive van der Waals' forces between regenerated cellulose surfaces in an aqueous environment. *Journal of the American Chemical Society,* 126, 13930-13931.

NOTLEY, S. M., ERIKSSON, M., WÅGBERG, L., BECK, S. & GRAY, D. G. (2006). Surface forces measurements of spin-coated cellulose thin films with different crystallinity. *Langmuir,* 22**,** 3154-3160.

NOTLEY, S. M. & WÅGBERG, L. (2005). Morphology of modified regenerated model cellulose II surfaces studied by atomic force microscopy: Effect of carboxymethylation and heat treatment. *Biomacromolecules,* 6**,** 1586-1591.

NOTLEY, S.M. (2008). Effect of introduced charge in cellulose gels on surface interactions and the adsorption of highly charged cationic polyelectrolytes. *Physical Chemistry Chemical Physic*s 10, 1819-1825

OKANO, T. & SARKO, A. (1985). Mercerization of cellulose. II. Alkali-cellulose intermediates and a possible mercerization mechanishm. J*ournal of Applied Polymer Science*, 30, 325-332.

OLSZEWSKA, A., ERONEN, P., JOHANSSON, L.-S., MALHO, J.-M., ANKERFORS, M., LINDSTRÖM, T., RUOKOLAINEN, J., LAINE, J. & ÖSTERBERG, M. (2011). The behaviour of cationic nanofibrillar cellulose in aqueous media. *Cellulose,* 18, 1213-1226.

ORBLIN, E. & FARDIM, P. (2010). Surface chemistry of deinked pulps as analyzed by XPS and ToF-SIMS. *Surface and Interface Analysis,* 42**,** 1712-1722.

PAANANEN, A., ÖSTERBERG, M., RUTLAND, M. W., TAMMELIN, T., SAARINEN, T., TAPPURA, K. & STENIUS, P. (2004). Interactions between cellulose and xylan: An atomic force microscope and quartz crystal microbalance study, In *Hemicelluloses: Science and Technology*. Gatenholm, P. and Tenkanen, M. (Eds.) American Chemical Society; Washington, D.C, pp. 269-290.

PARIKKA, K. LEPPÄNEN, A-S., PITKÄNEN, L., REUNANEN, M., WILLFÖR, S. & TENKANEN, M. (2010). Oxidation of polysaccharides by galactose oxidase. *Journal of Agriculture and Food Chemistry*, 58, 262-271.

PERRY, S.S., SOMORJAI, G. A., MATE, C.M. & WHITE, R.L. (1995). Adhesion and friction properties of hydrogenated amorphous carbon films measured by atomic force microscopy. *Tribology Letters*, 1, 233-246.

PETTERSSON, T., NORDGREN, N. & RUTLAND, M. W. (2007). Comparison of different methods to calibrate torsional spring constants and photodetector for atomic force microscopy friction measurements in air and in liquid. *Review of Scientific Instruments,* 78**,** 093702-1-093702-8.

PHILLIPS, D.L., XING, J., LIU, H., CHONG, C.K. & CORKE H (1999). Raman spectroscopic determination of the degree of cationic modification in waxy maize starches. *Analytical Letters*, 32, 3049-3058.

PIANTANIDA, G., BICCHIERI, M. & COLUZZA, C. (2005). Atomic force microscopy characterization of the ageing of pure cellulose paper. *Polymer*, 46, 12313-12321.

PICOUT, D.R. & ROSS-MURPHY, S.B. (2007). On the Mark-Houwink parameters for galactomannans, *Carbohydrate Polymers*, 70, 145-148.

PICOUT, D. R., ROSS-MURPHY, S. B., ERRINGTON, N., & HARDING, S. E. (2003). Pressure cell assisted solubilization of xyloglucans: Tamarind seed polysaccharide and detarium gum. *Biomacromolecules,* 4, 799-807.

PIGORSCH, E. (2009). Spectroscopic characterization of cationic quaternary ammonium starches. *Starch*, 61, 129-138.

PITKÄNEN, L., VIRKKI, L., TENKANEN, M. & TUOMAINEN, P. (2009). Comprehensive multidetector HPSEC study on solution properties of cereal arabinoxylans in aqueous and DMSO solutions. *Biomacromolecules,* 10**,** 1962-1969.

POPTOSHEV, E. & CLAESSON, P. (2002). Weakly charged polyelectrolyte adsorption to glass and cellulose studied by surface force technique. *Langmuir*, 18, 1184-1189.

PÄÄKKÖ M., ANKERFORS, M., KOSONEN, H., NYKÄNEN, A., AHOLA, S., ÖSTERBERG, M., RUOKOLAINEN, J., LAINE J., LARSSON, P.T., IKKALA, O. & LINDSTRÖM, T. (2007). Enzymatic hydrolysis combined with mechanical shearing and high-pressure homogenization for nanoscale cellulose fibrils and strong gels. *Biomacromolecules*, 8, 1934-1941.

RABINOVICH, Y.I., ADLER, J.J., ATA, A., SINGH, R.K. & MOUDGIL, B.M. (2000). Adhesion between nanoscale rough surfaces. Part I: Role of asperity geometry. *Journal of Colloid and Interface Science*, 232, 10-16.

RAI, M. YADAV, A. & GADE, A. (2009). Silver nanoparticles as a new generation of antimicrobials. *Biotechnology Advances*, 27, 76-83.

RALSTON, J., LARSON, I., RUTLAND, M. W., FEILER, A. A. & KLEIJN, M. (2005). Atomic force microscopy and direct surface force measurements. *Pure and Applied Chemistry,* 77**,** 2149-2170.

REN, J.-L., PENG, F., SUN, R.-C., & KENNEDY, J. F. (2009). Influence of hemicellulosic derivatives on the sulfate kraft pulp strength. *Carbohydrate Polymers,* 75, 338-342.

ROBERTS, J.C. & EL-KARIM S.A. (1983). The behaviour of surface adsorbed xylans during the beating of a bleached kraft pine pulp. *Cellulose Chemistry and Technology*, 17, 379-386.

RODAHL, M., HÖÖK, F., KROZER, A., BRZEZINSKI, P. & KASEMO, B. (1995). Quartz crystal microbalance setup for frequency and Q-factor measurements in gaseous and liquid environments. *Review of Scientific Instruments,* 66**,** 3924-3930.

RUTENBERG, M. W., SOLAREK, D. (1984). Starch derivatives: Production and uses. In *Starch Chemistry and Technology*; Whistler, R. L., Miller, J. N. and Paschall, E. F. (Eds.) Academic Press; Orlando, pp.311−388.

RUTLAND, M. W., CARAMBASSIS, A., WILLING, G. A. & NEUMAN, R. D. (1997). Surface force measurements between cellulose surfaces using scanning probe microscopy. *Colloids and Surfaces A: Physicochemical and Engineering Aspects,* 123-124**,** 369-374.

SAARINEN, T., ÖSTERBERG, M., & LAINE J. (2009). Properties of cationic polyelectrolyte layers adsorbed on silica and cellulose surfaces studied by QCM-D – Effect of polyelectrolyte charge density and molecular weight *Journal of Dispersion Science and Technology* 30(6), 969-979

SADER, J. E., CHON, J.W.M. & MULVANEY, P. (1999). Calibration of rectangular atomic force microscope cantilevers. *Review of Scietificic Instruments*, 70, 3967-3969.

SAID AZIZI SAMIR, M. Y., ALLOIN, F. & DUFRESNE A. (2005). Review of recent research into cellulosic whiskers, their properties and their application in nanocomposite field. *Biomacromolecules*, 6, 612-626.

SAITO, T., HIROTA, M., TAMURA, N., KIMURA, S., FUKUZUMI, H., HEUX, L. & ISOGAI A. (2009). Individualisation of nano-sized plant cellulose fibrils by direct surface carboxylation using TEMPO-catalyst under neutral conditions. *Biomacromolecules*, 10, 1992-1998.

SAITO, T., KIMURA, S., NISHIYAMA, Y. & ISOGAI, A. (2007). Cellulose nanofibers prepared by TEMPO-mediated oxidation of native cellulose. *Biomacromolecules,* 8**,** 2485-2491.

SALMÈN, L. & OLSSON, A.-M. (1998). Interaction between hemicelluloses, lignin and cellulose: Structure-property relationships. *Journal of Pulp and Paper Science*, 24, 99-103.

SALMI, J., NYPELÖ, T., ÖSTERBERG, M. & LAINE, J. (2009). Layer structures formed by silica nanoparticles and cellulose nanofibrils with cationic polyacrylamide (C-PAM) on cellulose surface and their influence on interactions. *BioResources,* 4**,** 602-625.

SALMI, J., ÖSTERBERG, M. STENIUS; P. & LAINE J. (2007). Surface forces between cellulose surfaces in cationic polyelectrolyte solutions: The effect of polymer molecular weight and charge density. *Nordic Pulp and Paper Research Journal*, 22, 249-257.

SCHELLER, H. V. & ULVSKOV, P. (2010). Hemicelluloses. *Annual Review of Plant Biology,* 61**,** 263-289.

SCHENZEL, K. & FISHCHER, S. (2001). NIR FT Raman spectroscopy- A rapid analytical tool for detecting the transformation of cellulose polymorphs. *Cellulose*, 8, 49-57.

SCHENZEL, K., FISHCHER, S. & BRENDLER, E. (2005). New method for determining the degree of cellulose I crystallinity by means of FT Raman microscopy. *Cellulose*, 12, 223-231.

SCHLENOFF, J.B. (2003). Charge balance and transport in polyelectrolyte multilayers. In *Multilayer Thin Films*, G. Decher and J.B. Schlenoff (Eds.). Wiley-VCH; Weinham, pp. 99-132.

SCHMIDT, U., HILD, S., IBACH, W. & HOLLRICHER, O. (2005). Characterization of thin polymer films on the nanometer scale with confocal Raman AFM. *Macromolecular Symposia,* 230**,** 133-143.

SEHAQUI, H., LIU, A., ZHOU, Q. & BERGLUND, L.A. (2010). Fast preparation procedure for large, flat cellulose and cellulose/inorganic nanopaper structures. *Biomacromolecules* 11, 2195-2198.

SIRÓ, I. & PLACKETT, D. (2010). Microfibrillated cellulose and new nanocomposite materials: A review. *Cellulose,* 17**,** 459-494.

SJÖSTRÖM, E. (1993) *Wood Chemistry: Fundamentals and applications, 2nd edition* Academic Press; San Diego.

SJÖSTRÖM, E., JANSON, J., HAGLUND, P. & ENSTRÖM, B. (1965). Acidic groups in wood and pulp as measured by ion exchange. *Journal of Polymer Science, Part C: Polymer Symposia***,** 221-241.

SJÖSTRÖM, L., LAINE, J., & BLADEMO, Å. (2000). Release of organic substances from bleached sulphate pulps during slushing and refining. *Nordic Pulp and Paper Research Journal,* 15, 469-475.

SPENCE, K. L., VENDITTI, R.A., ROJAS, O. J., HABIBI, Y. & PAWLAK, J. (2010). The effect of chemical composition on microfibrillar cellulose films from wood pulps: Water interactions and physical properties for packaging applications. *Cellulose,* 17, 835-848

STANA-KLEINSCHECK, STRNAD, S. & RIBITSCH, V. (1999). Surface characterization and adsorption abilities of cellulose fibers. *Polymer Engineering and Science*, 39, 1412-1424.

STELTE, W. & SANADI, A. R. (2009). Preparation and characterization of cellulose nanofibers from two commercial hardwood and softwood Pulps. *Industrial & Engineering Chemistry Research,* 48**,** 11211-11219.

STENSTAD, P., ANDRESEN, M., TANEM, B. & STENIUS, P. (2008). Chemical surface modifications of microfibrillated cellulose. *Cellulose,* 15**,** 35-45.

STIERNSTEDT, J., BRUMER, H., ZHOU, Q., TEERI, T. T. & RUTLAND, M. W. (2006a). Friction between cellulose surfaces and effect of xyloglucan adsorption. *Biomacromolecules,* 7**,** 2147-2153.

STIERNSTEDT, J., NORDGREN, N., WÅGBERG, L., BRUMER III, H., GRAY, D. G. & RUTLAND, M. W. (2006b). Friction and forces between cellulose model surfaces: A comparison. *Journal of Colloid and Interface Science,* 303**,** 117-123.

SUN, R., SUN, X.F. & TOMKINSON, J. (2004). Hemicelluloses and their derivatives. In *Hemicelluloses:Science and Technology*, P. Gatenholm and M. Tenkanen (Eds.) American Chemical Society, Washington, D.C, pp. 2-22.

SUREHSKUMAR, M. SISWANTO, D. Y. & LEE, C-K. (2010). Magnetic antimicrobial nanocomposite based on bacterial cellulose and silver nanoparticles. *Journal of Materials Chemistry*, 20, 6948-6955.

SURYANEGARA, L., NAKAGAITO, A. N. & YANO, H. (2010). Thermo-mechanical properties of microfibrillated cellulose-reinforced partially crystallized PLA composites. *Cellulose,* 17**,** 771-778.

SUURNÄKKI, A., OKSANEN, A. T., KETTUNEN, H. & BUCHERT, J. (2003) The effect of mannan on physical properties of EGF bleached softwood kraft fibre handsheets. *Nordic Pulp and Paper Research Journal,* 18**,** 429-435.

SWANSON, J.W. (1950). The effects of natural beater additives on papermaking fibers, *Tappi* 33, 451-462.

SWERIN, A., ÖDBERG, L. & LINDSTRÖM, T. (1990). Deswelling of hardwood kraft pulp fibers by cationic polymers: the effect on wet pressing and sheet properties. *Nordic Pulp and Paper Research Journal,* 5**,** 188-196.

SYVERUD, K., CHINGA-CARRASCO, G., TOLEDI, J. & TOLEDO, P.G (2011). A comparative study of Eucalyptus and Pinus radiata pulp fibres as raw materials for production of cellulose nanofibrils**.** *Carbohydrate Polymers*, 84, 1033-1038.

SYVERUD, K. & STENIUS, P. (2009). Strength and barrier properties of MFC films. *Cellulose,* 16**,** 75-85.

TAIPALE, T., ÖSTERBERG, M., NYKÄNEN, A., RUOKOLAINEN, J. & LAINE, J. (2010). Effect of microfibrillated cellulose and fines on the drainage of kraft pulp suspension and paper strength. *Cellulose,* 17**,** 1005-1020.

TAMMELIN, T., PAANANEN, A. & ÖSTERBERG, M. (2009). Hemicelluloses at interfaces: Some aspects of the interactions, In *The Nanoscience and Technology of Renewable Materials*, Lucia, L.A. and Rojas, O.J. (Eds.) Wiley-Blackwell Publishing Ltd., Chichester, pp. 149-172.

TAMMELIN, T., SAARINEN, T., ÖSTERBERG, M. & LAINE, J. (2006). Preparation of Langmuir/Blodgett-cellulose surfaces by using horizontal dipping procedure. Application for polyelectrolyte adsorption studies performed with QCM-D. *Cellulose,* 13**,** 519-535.

TEERI, T. T., BRUMER III, H., DANIEL, G. & GATENHOLM, P. (2007). Biomimetic engineering of cellulose-based materials, *Trends in Biotechology* 25, 299-306.

TENKANEN, M., GELLERSTEDT, G., VUORINEN, T., TELEMAN, A., PERTTULA, M., LI, J. & BUCHERT, J. (1999). Determination of hexenuronic acid in softwood kraft pulps by three different methods. *Journal of Pulp and Paper Science,* 25**,** 305-311.

TINGAUT, P., ZIMMERMANN, T. & LOPEZ-SUEVOS, F. (2009). Synthesis and characterization of bionanocomposites with tunable properties from Poly(lactic acid) and acetylated microfibrillated cellulose. *Biomacromolecules,* 11**,** 454-464.

TREIMANIS, A. (1996). Wood pulp fibre structure and chemical composition, their influence on technological processes. *Nordic Pulp and Paper Research Journal*, 11, 146-151.

TURBAK, A. F., SNYDER, F. W. & SANDBERG, K. R. (1983). Microfibrillated cellulose, a new cellulose product:properties, uses, and commercial potential. *Journal of Applied Polymer Science, Applied Polymer Symposium,* 37**,** 815-827.

UTSEL, S., MALMSTRÖM, E.E., CARLMARK, A. & WÅGBERG, L. (2010). Thermoresponsive nanocomposites from multilayers of nanofibrillated celluloe and specially designed N-isopropylacrylamide based polymers. *Soft Matter*, 6, 342-352.

WANG, M., OLSZEWSKA, A., WALTHER, A., MALHO, J.-M., SCHACHER, F.H., RUOKOLAINEN, J., ANKERFORS, M., LAINE, J. BERGLUND, L.A., ÖSTERBERG, M. & IKKALA, O. (2011) Colloidal Ionic Assembly between Anionic Native Cellulose Nanofibrils and Cationic Block Copolymer Micelles into Biomimetic Nanocomposites. *Biomacromolecules*, 12, 2074-2081.

VAN DER VEN, T.G.M. (2000). A model for the adsorption of polyelectrolytes on pulp fibers:relation between fiber structure and polyelectrolyte properties. *Nordic Pulp & Paper Research Journal,* 15**,** 494-501.

WALECKA, J.A. (1956). Low degree of substitution of carboxymethylcelluloses. *Tappi*, 39, 458-463.

VERWEY, E. J. W. and OVERBEEK, J. Th. G. (1948). *Theory and Stability of Lyophobic Colloids: the interactions of sol particles having an electric double layer*, Elsevier, New York.

WESTBYE, P., SVANBERG, C. & GATENHOLM, P. (2006). The effect of molecular composition of xylan extracted from birch on its assembly onto bleached softwood kraft pulp, *Holzforschung,* 60, 143-148.

WHITNEY, S. E. C., BRIGHAM, J. E., DARKE, A. H., REID, J. S. G. & GIDLEY, M. J. (1998). Structural aspects of the interaction of mannan-based polysaccharides with bacterial cellulose. *Carbohydrate Research,* 307**,** 299-309.

WILLFÖR, S., SUNDBERG, K., TENKANEN, M. & HOLMBOM, B. (2008). Spruce-derived mannans - A potential raw material for hydrocolloids and novel advanced natural materials. *Carbohydrate Polymers,* 72**,** 197-210.

VINCKEN, J.-P., DE KEIZER, A., BELDMAN, G. & VORAGEN, A. G. J. (1995). Fractionation of xyloglucan fragments and their interaction with cellulose. *Plant Physiology,* 108**,** 1579-1585.

VIRKKI, L., MAINA, H. N., JOHANSSON, L. & TENKANEN, M. (2008). New enzyme-based method for analysis of water-soluble wheat arabinoxylans. *Carbohydrate Research,* 343**,** 521-529.

VOINOVA, M. V., RODAHL, M., JONSON, M. & KASEMO, B. (1999). Viscoelastic acoustic response of layered polymer films at fluid-solid interfaces: Continuum mechanics approach *Physica Scripta,* 59**,** 391-396.

WÅGBERG, L. (2000). Polyelectrolyte adsorption onto cellulose fibres-A review. *Nordic Pulp & Paper Research Journal,* 15**,** 586-597.

WÅGBERG, L., ÖDBERG, L. & GLAD-NORDMARK, G. (1989). Charge determination of porous substrates by polyelectrolyte adsorption. Part 1. Carboxymethylated, bleached cellulosic fibres. *Nordic Pulp & Paper Research Journal,* 4**,** 71-76.

WÅGBERG, L., DECHER, G., NORGREN, M., LINDSTRÖM, T., ANKERFORS, M. & AXNÄS, K. (2008). The build-up of polyelectrolyte multilayers of microfibrillated cellulose and cationic polyelectrolytes. *Langmuir*, 24, 784-795.

WÅGBERG, L., ÖSTERBERG, M. & ENARSSON, L-E. (2010). Interactions at cellulose model surfaces. In *Encyclopedia of surface and colloid sciece 2nd ed*. Somasundran, P. & Hubbard, A. (Eds.) Taylor & Francis, New York, pp. 1-19.

VUORINEN, T. & ALÉN, R. (1999). Carbohydrates, In *Analytical Methods in Wood Chemistry, Pulping and Papermaking*, Sjöström, E. and Alén R. (Eds.) Springer, Berlin-Heidelberg. pp. 37-75.

XHANARI, K., SYVERUD, K., CHINGA-CARRASCO, G., PASO K. & STENIUS, P. (2011). Reduction of water wettability of nanofibrillated cellulose by adsorption of cationic surfactants. *Cellulose*, 18, 257-270.

XU, C., WILLFÖR, S., SUNDBERG, K., PETTERSON, C., & HOLMBOM, B. (2007). Physico-chemical characterization of spruce galactoglucomannan solutions: stability, surface activity and rheology. *Cellulose Chemistry and Technology,* 41, 51-62.

ZAUSCHER, S. & KLINGENBERG, D. J. (2000a). Normal forces between cellulose surfaces measured with colloidal probe microscopy**.** *Journal of Colloid and Interface Science,* 229, 97-510.

ZAUSCHER, S. & KLINGENBERG, D. J. (2000b). Surface and friction forces between cellulose surfaces measured with colloidal probe microscopy. *Nordic Pulp & Paper Research Journal*, 15, 459-468.

ZAUSCHER, S. & KLINGENBERG, D. J. (2000c). Friction between cellulose surfaces measured with colloidal probe microscopy. *Colloids and Surfaces A. Physicochemical and Engineering Aspects*, 178, 213-229.

ZHONG, Q., INNISS, D., KJOLLER, K. & ELINGS, V.B. (1993) Fractured polymer/silica fiber surface studied by tapping mode atomic force microscopy. *Surface Science*, 290, L688-L692.

ZHOU, Q., RUTLAND, M.W., TEERI, T.T. & BRUMER, H. (2007). Xyloglucan in cellulose modification. *Cellulose*, 14, 625-641.

ZHU, J. Y., SABO, R. & LUO, X. (2011). Integrated production of nano-fibrillar cellulose and cellulosic biofuel (ethanol) by enzymatic fractionation of wood fibers. *Green Chemistry*, 13, 1339-1344.

ZIMMERMANN, T., BORDEANU, N. & STRUB, E. (2010). Properties of nanofibrillated cellulose from different raw materials and its reinforcement potential. *Carbohydrate Polymers,* 79**,** 1086-1093.

ZULUAGA, R., PUTAUX, J. L. RESTREPO, A.MONDRAGÒN, I. & GANAN, P. (2007). Cellulose microfibrils from banana farming residues: isolation and characterization. *Cellulose*, 14, 585-592.

Aalto-DD 108/2011

ISBN 978-952-60-4341-8 (pdf)
ISBN 978-952-60-4340-1
ISSN-L 1799-4934
ISSN 1799-4942 (pdf)
ISSN 1799-4934

Aalto University
School of Chemical Technology
Department of Forest Products Technology
www.aalto.fi

BUSINESS + ECONOMY

ART + DESIGN + ARCHITECTURE

SCIENCE + TECHNOLOGY

CROSSOVER

DOCTORAL DISSERTATIONS